PERFORMANCE PREDICTION OF HORIZONTAL AXIS WIND TURBINES USING VORTEX THEORY

A THESIS SUBMITTED TO
THE GRADUATE SCHOOL OF NATURAL AND APPLIED SCIENCES
OF
MIDDLE EAST TECHNICAL UNIVERSITY

BY

BURAK YÜCEL

IN PARTIAL FULFILLMENT OF THE REQUIREMENTS
FOR
THE DEGREE OF MASTER OF SCIENCE
IN
MECHANICAL ENGINEERING

DECEMBER 2004

Approval of the Graduate School of Natural and Applied Sciences

_____

Prof. Dr. Canan ÖZGEN
Director

I certify that this thesis satisfies all the requirements as a thesis for the degree of Master of Science

_____

Prof. Dr. Kemal İDER
Head of the Department

This is to certify that we have read this thesis and that in our opinion it is fully adequate, in scope and quality, as a thesis for the degree of Master of Science.

_____	_____
Prof. Dr. Kahraman ALBAYRAK Co-Supervisor	Asst. Prof. Dr. Tahsin A. ÇETİNKAYA Supervisor

Examining Committee Members

Prof. Dr. M. Haluk AKSEL	(METU, ME)	_____
Asst. Prof. Dr. Tahsin A. ÇETİNKAYA	(METU,ME)	_____
Prof. Dr. Kahraman ALBAYRAK	(METU,ME)	_____
Prof. Dr. İ. Sinan AKMANDOR	(METU,AEE)	_____
Asst. Prof. Dr. İlker TARI	(METU, ME)	_____

I hereby declare that all information in this document has been obtained and presented in accordance with academic rules and ethical conduct. I also declare that, as required by these rules and conduct, I have fully cited and referenced all material and results that are not original to this work.

Name, Last name : Burak YÜCEL

Signature :

ABSTRACT

PERFORMANCE PREDICTION OF HORIZONTAL AXIS WIND TURBINES USING VORTEX THEORY

YÜCEL, Burak

M.S., Department of Mechanical Engineering

Supervisor: Asst. Prof. Dr. Tahsin A. ÇETİNKAYA

Co-Supervisor: Prof. Dr. Kahraman ALBAYRAK

December 2004, 115 pages

Performance prediction of HAWTs is important because it gives an idea about the power production of a HAWT in out of design conditions without making any experiments. Since the experiments of fluid mechanics are difficult to afford, developing some models is very beneficial.

There are some models developed about this subject using miscellaneous methods. In this study, one can find "Vortex Theory" among one of these theories.

Some basic 3D aerodynamics was discussed in order to make the reader to understand the main subject of this study. Just after that, performance prediction of constant speed, stall controlled HAWTs was discussed.

In order to understand the closeness of this theory to experiments, as a sample, NREL "Combined Experiment Rotor" was considered. Performances

obtained by AEROPOWER, written in Visual Basic 6.0 and Excel combination, and experimental results were compared for different wind velocities. Acceptable results were obtained for wind speeds not much different than the design wind speed. For relatively lower wind speeds, due to “turbulence”, and for relatively higher wind speeds, due to “stall”, the program did not give good results. In the first case it has not given any numerical result.

Power curves were obtained by only changing the settling angle, and only changing the rotor angular speed using AEROPOWER. It was seen that, both settling angle and rotor rpm values influence the turbine power output significantly.

Keywords: Vortex Theory, Wind Turbine, Helicoidal Wake, Lifting Surface Methods.

ÖZ

GİRDAP TEORİSİNİ KULLANARAK
YATAY EKSENLİ RÜZGAR TÜRBİNLERİNİN PERFORMANS TAHMİNİ

YÜCEL, Burak
Yüksek Lisans, Makine Mühendisliği Bölümü
Tez Yöneticisi : Yrd. Doç. Dr. Tahsin A. ÇETİNKAYA
Ortak Tez Yöneticisi: Prof. Dr. Kahraman ALBAYRAK

Aralık 2004, 115 sayfa

Yatay eksenli rüzgar türbinlerinin performanslarını önceden tahmin edebilmek önemlidir çünkü herhangi bir deney yapmadan güç üretimi hakkında fikir verirler. Akışkanlar mekaniği deneyleri oldukça pahalıya mal olduğundan, bazı modeller geliştirmek oldukça faydalıdır.

Bu konuyla ilgili, çeşitli metotlar kullanarak birçok model geliştirilmiştir. Bu çalışmada, bunlardan biri olan "Girdap Teorisi" nden bahsedilmiştir.

Okuyucuya bu çalışmanın ana konusunu anlatabilmek için temel üç boyutlu aerodinamiden bahsedilmiştir. Sabit hızlı, "stall" kontrollü rüzgar türbinlerinin güç tahminleri anlatılmıştır.

Bu teorinin deneylere yakınlığını anlamak için, örnek olarak, "Ulusal Yenilenebilir Enerji Laboratuarı" (NREL) rotoru alınmıştır. Visual Basic 6.0 ve

Excel kombinasyonu ile yazılan AEROPOWER ile ve deneylerden elde edilen sonuçlar değişik rüzgar hızlarında karşılaştırılmıştır. Dizayn rüzgar hızına çok uzak olmayan hızlarda kabul edilebilir sonuçlar elde edilmiştir. Nispeten düşük rüzgar hızlarında, "türbülans"tan dolayı, ve nispeten yüksek rüzgar hızlarında "stall"dan dolayı, programın iyi sonuçlar vermediği görülmüştür. Birinci durumda hiçbir nümerik sonuç alınamamıştır.

Sadece kanat oturma açılarını değiştirerek, ve sadece rotor açısal hızlarını değiştirerek güç değerleri elde edilmiştir. Hem oturma açısının hem de rotor hızının çıkış gücünde oldukça etkili oldukları görülmüştür.

Anahtar Kelimeler: Girdap Teorisi, Rüzgar Türbini, Helisel İz, Kaldıran Yüzey Metotları

ACKNOWLEDGEMENTS

I express sincere appreciation to Asst. Prof. Dr. Tahsin Çetinkaya for his guidance and insight throughout the research.

Thanks go to the other one of the faculty members Prof. Dr. Kahraman Albayrak for his suggestions and comments.

I am also grateful to Mr. Jean Jacques Chattot from University of California and Mr. Nord-Jan Vermeer from Delft University of Technology, The Netherlands, for their contribution to my study.

I also send my respects to my family for their patience and helps during this study.

TABLE OF CONTENTS

LIST OF TABLES

TABLES

LIST OF FIGURES

FIGURES

LIST OF SYMBOLS AND ABBREVIATIONS

A_P : Projection area (same as A)…….(m^2)

a : Axial induction factor…….....( )

a' : Angular induction factor……( )

$a_{j,k}$: Influence coefficient for the downwash induced velocity……...( )

$b_{j,k}$: Influence coefficient for the backwash induced velocity…….....( )

B : Number of blades……...(#)

B : Magnetic field……...(Wb)

c : Chord length……...(m)

C_d : Two-dimensional drag coefficient……..……..( )

C_l : Two-dimensional lift coefficient……...( )

C_D : Three-dimensional drag coefficient……..( )

C_L : Three-dimensional lift coefficient……( )

C_P : Rotor power coefficient……( )

C_{P_D} : Device power coefficient…….....( )

C_T : Thrust coefficient……..( )

C_τ : Torque coefficient…….....( )

c_{lp} : Chord length of the low-pressure aerodynamic control surface……..(m)

dV : Induced velocity at point C, due to the vortex filament AB...……(m/s)

dF_l : Differential lift force at that section (same as dL)……...(N)

dF_d : Differential drag force at that section (same as dD)…….....(N)

dR : Differential aerodynamic resultant force at that section……(N)

dF_N : Incremental aerodynamic normal (thrust) force by the section……...(N)

dF_T : Incremental aerodynamic tangential force by the section……(N)

d_v : Vortex drag…….....(N)

dx_0 : Initial mesh step……...( )

F_d : Drag force per unit span…….....(N/m)

F_l : Lift force per unit span……...(N/m)

F_R : Resultant aerodynamic force per unit span…….....(N/m)

g : Gravitational acceleration……..……..(m/s^2)

H_{TUR} : Head of the turbine……...(m)

H_{th} : Theoretical head of the turbine……...(m)

ix : Number of points on the vortex filaments in the flow direction……(#)

jx : Number of points along the blades…….……...(#)

L : Distance to the Trefftz Plane……..(m)

P_τ : Rotor speed power coefficient…….....( )

P_{NET} : Net rotor power production (generally electrical power obtained)……(W)

P_R : Rotor power output (same as P)……..……(W)

P_2 : Static pressure just upstream of the rotor……..(Pa)

P_3 : Static pressure just downstream of the rotor…….(Pa)

q : Dimensionless local incoming velocity…….....( )

R : Rotor radii…….....(m)

R : Degree of reaction of a HAWT……..( )

s : Stretching parameter……...( )

s : Unit length in the spanwise direction…….....(m)

T : Thrust force on the rotor……(N)

U : Translating velocity of the blade at the section of interest……..(m/s)

U_∞ : Steady, uniform free-stream wind velocity (same as V_1)……..…….....(m/s)

u_a : Induced velocity in the axial direction w.r.t. ADT theory……...(m/s)

u : Induced velocity in the axial direction (backwash) for VT…….(m/s)

w: Induced velocity in the tangential direction (downwash) for VT……....(m/s)

V_2: Absolute velocity at the inlet of the blade element……..(m/s)

V_3: Absolute velocity at the outlet of the blade element……(m/s)

W_2: Relative velocity at the inlet of the blade element……..(m/s)

W_3: Relative velocity at the outlet of the blade element……(m/s)

W_∞ : Incoming velocity……...……(m/s)

$W_{\theta\infty}$: Tangential component of the incoming velocity at that section……..……..(m/s)

x, y, z : Cartesian frame of reference attached to the rotor.

x_0: Dimensionless blade location relative to the frame of reference……...( )

y_0: Dimensionless root chord location relative to the reference frame……...( )

Greek Letters

α : Angle of attack……...(°)

α_G : Geometric angle of attack…….....(°)

α_{0l} : Zero-lift angle of attack……(°)

ξ: Angle between incoming flow and free-stream flow……..(°)

ρ_∞ : Density of the air in the far upstream…….....(kg/m^3)

θ_P: Section pitch angle…….....(°)

θ_{P0}: Blade pitch angle at the tip (or tip angle)……..….....(°)

θ_T: Section twist angle…….....(°)

φ : Angle of relative wind (or angle of incoming flow)…….....(°)

ϕ : Angle for parametric representation of blade point distribution……(°)

λ : Tip-speed-ratio…….....( )

λ_r : Local-speed-ratio……...( )

τ : Torque exerted on the rotor……..(Nm)

γ : Density x gravitational acceleration……...(kg/m^{2}s^2)

Γ : Dimensionless bound circulation around theblade at the section of interest…..( )

Ω : Angular velocity of the rotor……..(rad/s)

η_h : Hydraulic efficiency……..( )

η_{mech} : Mechanical efficiency……( )

η_v : Volumetric efficiency……( )

$\eta_{overall}$: Overall efficiency……...…….( )

INDICES:

i : Index for discrete variables in x-direction

j & k : Indices for discrete variables in y-direction

v : For viscous & vortex

: Average value

ABBREVIATIONS:

ACS: Aerodynamic Control Surface

ADT: Actuator Disk Theory

AIAA: American Institute of Aeronautics & Astronautics

AOR: Axis of Rotation

AR: Aspect Ratio

ASME: American Society of Mechanical Engineers

AWEA: American Wind Energy Association

BEM: Blade Element Momentum Theory

CER: Combined Experiment Rotor.

CP: Control Point

DOT: Direction of Travel

HAWT: Horizontal Axis Wind Turbine

IP: Integration Point

NREL: National Renewable Energy Laboratory

Re: Reynolds Number

SERI: Solar Energy Research Institute

TSR: Tip Speed Ratio

VAWT: Vertical Axis Wind Turbine

VT: Vortex Theory (same as HVT: Helicoidal Vortex Theory)

w.r.t: With respect to

WT: Wind Turbine

1D: One Dimensional

2D: Two Dimensional

3D: Three Dimensional

CHAPTER I

INTRODUCTION

1.1 HISTORY OF WIND MACHINES:

It should be noted that, human being has managed to benefit from the nature since their creation. As the time passed they have improved their abilities parallel to their intelligences. They found fire, wheel etc… then they established some primitive water tanks (early dams, artificial ponds etc…) and while carrying out those they felt something; WIND. They decided to benefit from wind because it is a powerful and a permanent type of energy of the nature given them.

Let's consider how people have accomplished these wind related tasks from the early ages to modern times.

The Persians built the first windmills on record in approximately 900 AD. It is of note that these windmills had vertical axes and were drag type devices. As such they were inherently inefficient, and particularly susceptible to damage in high winds.

Wind energy made its appearance in Europe during the middle ages. These windmills all had horizontal axes. They were used for almost every mechanical task, including water pumping, grinding grain, sawing wood, and powering various tools.

The early mills were built on posts, so that the entire mill could be turned to face the wind (or yaw) when its direction changed. These mills normally had four blades (ref [1, 2]).

The wind continued to be a major source of energy in Europe through the period just prior to the Industrial Revolution, but began to recede in importance after that time. The reason that wind energy began to disappear is primarily attributable to its non-transportability. This means that wind energy only can be facilitated where it blows. It cannot be stored or conveyed to another place.

One significant development in the eighteenth century was the introduction of scientific testing and evaluation of windmills. The Englishman John Smeaton discovered three basic rules that are still applicable for wind turbines.

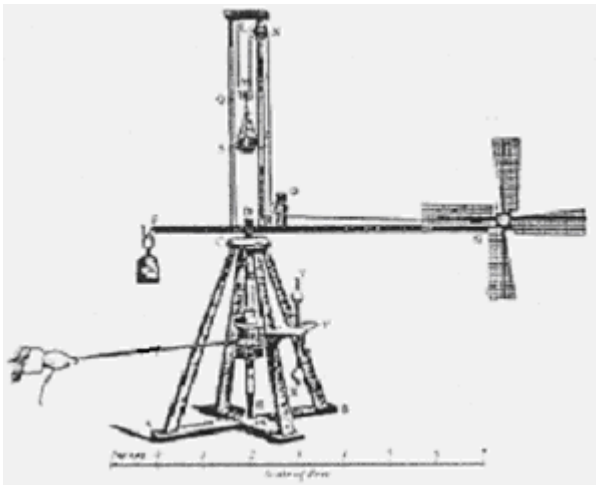

Figure 1.1 Smeaton Apparatus (Illustration from ref [1]).

According to Smeaton apparatus:

- The speed of the blade tips is ideally proportional to the speed of the wind.
- The maximum torque is proportional to the speed of the wind squared.
- The maximum power is proportional to the speed of the wind cubed.

The eighteenth century European windmills represented the culmination of one approach to using wind for mechanical power and included a number of

features, which were later incorporated into some early electricity generating wind turbines.

As the European windmills were entering their final years, another variant of windmill came into widespread use in the United States. This type of windmill was most notably used for pumping water, particularly in the West. These windmills were distinctive for their multiple blades and are often referred to as “fan mills” (ref [1, 2]).

1.2 WHAT IS A WIND TURBINE? :

One should know the difference between terms called “windmill” and “wind turbine”. If one uses it’s early name (the first one), at that time she/he is talking about wind machines used for water pumping, grinding grain etc… businesses, which were fulfilled mostly in the early ages. The term “turbine” is a modern word that is used for the machines, especially “electric generators”, but one should also consider that modern wind turbines are also used for water pumping directly or indirectly with the help of an electric motor or by a mechanical pump.

A wind turbine is a kind of turbomachine that operates externally (without casing) and generally considered to be incompressible, but sometimes the blade velocity at the tip may exceed 0.3 Mach and it may be considered as compressible at that region. Therefore the air density in the compressible region should be calculated separately from the incompressible region. In the incompressible region one should consider the freestream density of the air.

The abbreviation “HAWT” is used to indicate “Horizontal Axis Wind Turbine” and the term “VAWT” is used for its vertical case. One will consider HAWT systems in this study rather than VAWTs. The axis “horizontal” implies that the rotor main shaft of the machine is parallel to the ground; on the contrary “vertical” implies the rotor main shaft is perpendicular to the ground.

HAWT rotors decelerate the air rather than accelerating, and their tip speeds are much lower than those of aircraft propellers.

More information about vertical axis types can be found in references [1, 2].

Figure 1.2 indicates the principal subsystems of a HAWT.

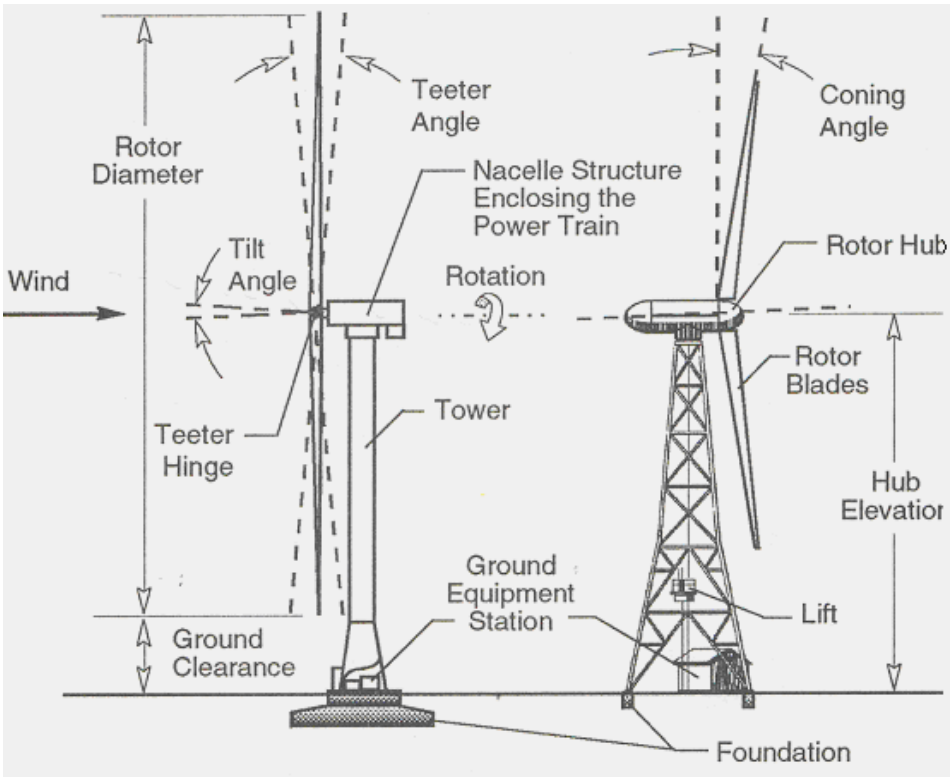

Figure 1.2 Principal subsystems of a HAWT. (Illustration from ref [2])

1.3 MODERN WIND TURBINES:

As long as the technology develops, wind turbines were also improved as well like the other technologies until recent times and they are continously developing. As it was mentioned earlier there are also VAWTs which are geometrically differ from HAWTs. They can be analyzed completely and detailed in

another unique study, but one will deal with HAWTs in this study.

The world's largest horizontal axis wind turbine built on Hawaii Island, manufactured by Boeing Aerospace Industry. This turbine has a rotor diameter of 97.5m and has a rotor swept area of 7,470m^2. It's rated power is 3.2 MW (ref [2]).

HAWTs are most preferrable wind power machines due to their effectiveness when compared with VAWTs, but VAWTs have some superiorities upon HAWTs. One of them is they do not need any yaw mechanism and their installation is more easy, so their maintenance as well.

1.4 STUDIES ON PERFORMANCE PREDICTIONS:

Developing a model, without manufacturing a wind turbine rotor is very important. By looking at this model one can predict a power production of a HAWT in out of design conditions or off-design conditions. The difference between the "out of design" and "off-design" here is, when one considers out of design conditions, it means that the turbine is operating in the conditions that is not extreme. As it will be seen in the later parts the turbine flow state would be in the "windmill" state. The term "off-design" used in this study is to refer the extreme conditions, "stall" and "turbulent wake state" conditions.

In relatively low and relatively high wind speeds almost all theories developed, give further results than the experimental ones. They may overpredict or lower-predict the power values.

Actuator Disc Theory (or Rankine-Fraud Theory) is the starting point of all these theories for wind turbines, but it is the most imaginary theory of them all, because it has not any physical correspondence due to one should consider an infinite number of blades with zero thickness. The basis of this theory is to consider the whole rotor as a blackbox (i.e, one cannot observe the shape of the blades). Only the maximum power that can be extracted from the wind and the maximum thrust force on the rotor due to wind can be concluded (for more information see references [1,2,]).

Blade Element Momentum Theory (BEM) is the combination of ADT and Blade Element Theory. This theory (BEM) is widely used to predict the performance of a HAWT nowadays widespreadly. With the help of "Blade Element Theory" part, one can define the blade shapes of the blades since it is possible to make a blade differential section (or airfoil) analyze.

Some computer codes were developed, such as WT_PERF and PROPID'93 using this theory (ref [3]). Those computer programs still rely on ADT (i.e., 1D Momentum Theory). When ADT does not valid in a condition, then BEM does not valid in the same condition as well, due to the dependence on ADT. A lot of limitations are made in order to establish a performance prediction model. Some experimental results are benefited to get closer results to the experiments (ref [4]).

Glauert has developed a model using a streamtube analysis with the help of 1D Momentum Theory and BEM Theory (ref [5]).

The mentioned theories above upmost make 2D flow analysis, but one should consider that in reality, every flow is 3D in nature. It is beneficial to develop new theories for this reason.

Prandtl has found "Lifting Line Theory" for wings (i.e., translating airfoils). This simple model became the starting point of the performance prediction of HAWTs from another view (ref [6]). Scientists have started to think in a different way, a different approach to make the analyze of HAWTs. A name "Prescribed Wake Approach" was given to the extension of Prandtl's theory. The Lifting Line Method is a classical method to calculate the lift distribution over the wing span (translating body). The Lifting Surface Method is useful to calculate complex wing shapes (for ex. rotating blades).

Another approach for analyzing the aerodynamics of HAWTs is "Panel Methods". This gives pressure distributions around a body (ref. [7]). Potential flow models have long been used in aerodynamics in a more or less sophisticated form. In the past decade the progress in computer technology has stimulated the use of the panel methods to an increasing scale of complexity.

For most of the methods currently in use the governing equation is based on

Green's second identity, and is solved with the requirement of zero normal flow at the solid boundaries. The notes in this method are restricted to incompressible flows. Formulations for compressible flows have also been formulated, but they are far less advanced from the application point of view.

Meanwhile the formulation of the problem has undergone very little refinement, whereas it was becoming evident that the step from the formulation to the numerical solution of the equations was not a simple one. This step involves approximations of various sorts, among which two are easily identified.

While most methods work, some work better with thick bodies, and others work better with thin bodies. Among the latter ones the velocity potential method is probably the most accurate. Methods that use potential, source and doublet distributions are one order less singular than the corresponding influence coefficients of a velocity (or vorticity) method. Therefore, potential methods tend to be less sensitive to the paneling details. The computation of the influence coefficients (a major requirement in terms of CPU) is faster for potential based methods than for corresponding velocity methods. The storage requirement is reduced to one third. A low order potential method is substantially more accurate than a velocity (or vorticity) method at given number of panels.

There is a number of boundary conditions that must be satisfied: boundary conditions on the body; Kutta condition at the trailing edge; conditions on the vortex wake.

The presented method (Prescribed wake) uses a lifting line to calculate the velocities and angle of attack for each blade section. So the forces can be calculated with profile data (wind tunnel measurements) like with the blade element method. A wake model is necessary. For rotating blades the wake must be in a helical form. The actual application of the vortex theory has led to more and more sophisticated models. Models based on linearized theory and empirical evidence assume rigid wakes, moving uniformly according to the free stream. There are models incorporating corrections that account for the deformation of the wake caused by contraction (propellers, helicopter rotors) (ref [8]) or relaxation (wind turbines).

These models are called quasi-linearized. The last step in this development is the fully-non linear model, based on the concept of mutual interaction among vortices. The free wake concept allows the vorticity to evolve in a free motion, and represents the physically correct approach to the unsteady aerodynamics.

In 80's and 90's there were so many studies carried out using this theory especially in the US and Denmark.

Most of the scientists preferred to model the wake behind a rotor as an organized collection of discrete vortex elements. These elements may contain straight line segments, curved line segments, particles or vortex sheets. More detailed information can be found in reference [9].

Reference [9] belongs to Fisichella who has fulfilled some experiments and analytical methods in his study. He has made some experiments in order to obtain a performance prediction model for HAWTs. This experiments helps him to correlate the analysis method.

Free wake models; It is an iterative process to get the shape of a free wake of a wind turbine for steady conditions. There are two ways to start this procedure. One can start at "zero" at the beginning of the rotation of the rotor. The result is the history of the wake.

Velocity potential methods, Acceleration Potential Method and CFD Methods can be considered except the above mentioned models. The CFD methods developed for HAWT rotors are the most cumbersome ones of them all, because a lot of time and effort are consumed to write the codes. Full potential, Euler and Navier-Stokes methods have been exploding in the last decade, thanks also to the progress in computer hardware. Virtually all problems have been attempted. Full potential methods have been left behind due to the difficulty of modeling the wake; Euler methods are limited by the lack of viscosity. Additional wake modeling is needed is the grid has not enough resolution, but this problem is just contingent, because limited by the current computer power.

The development of accurate CFD codes for a rotating blade is in itself a difficult task, that requires lengthy computer programming and debugging sessions.

In recent times the “Prescribed Wake Approach” is improved by Chattot J. J., [ref 10] and Afjeh A. [ref 11]. They try to obtain a performance prediction model of a HAWT using the wake behind the rotor. Chattot has established “Helicoidal Vortex Theory” for power prediction.

A number of experiments also carried out in the Netherlands, at Delft University of Technology, to understand the shape of the wake behind a HAWT rotor in order to develop a performance prediction model (ref [12]). A “WT aerodynamics simulation module” was developed in the Netherlands also related to vortex model (ref. [13]).

In Chattot’s approach the wake geometry is prescribed before the solution is carried out and then the calculations are made selecting a cosine distribution of control points on the blades, but one can not apply the formulations on this control points directly. A number of integration points is selected among those control points and the necessary parameters are calculated. As the number of control points increase on the blades he used some advanced mathematical techniques to solve the problem, for example he used “relaxation methods” (ref. [14]).

In this study one will try to obtain a power curve for different steady free stream wind velocities using “Vortex Theory”. A computer program AEROPOWER will be introduced for this purpose. A comparison will be done using the NREL “combined experiment rotor” (CER) experimental data.

Besides the change of the wind velocity one can find the performance prediction of a HAWT by changing the rotor angular speed, tip settling angle and the root location, which is the starting of the first chord on the blade span closest to the hub center (or axis of rotation).

1.5 AIRFOIL TERMINOLOGY & DEFINITION OF SETTLING ANGLE:

As long as HAWT blades are constructed by the association of the small lifting surfaces -airfoils- like the other surfaces moving in the fluid stream, “airfoil terminology” should be recalled.

Figure 1.3 indicates the airfoil terminology that will be used during this study. Because there could be some different notations, for example determination of the angle of attack may be taken relative to zero lift line, or different angle of attack definitions from different datum may be encountered.

Zero-lift-line can be taken as the line that connects the trailing edge to the point of maximum camber on the mean camberline. For symmetric airfoils this line coincides with the chordline.

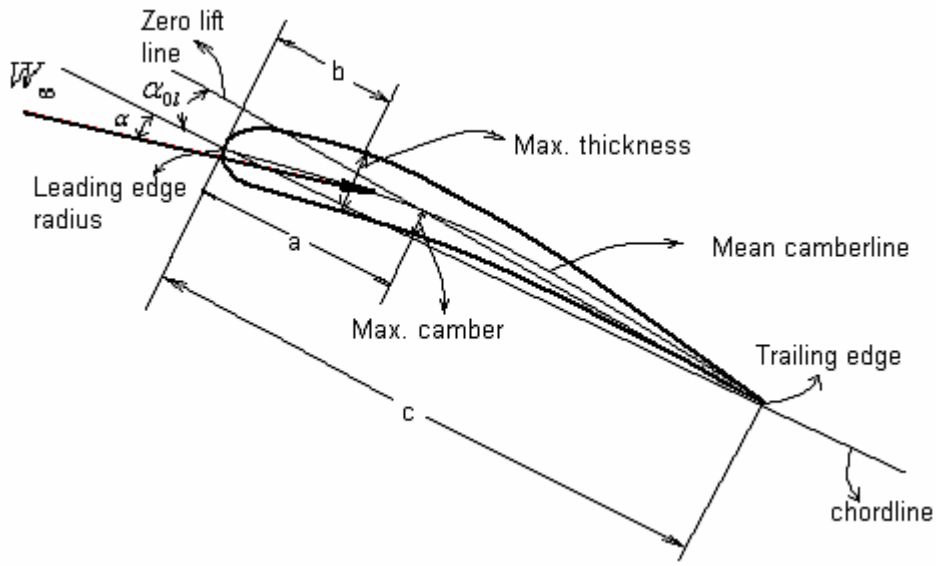

Figure 1.3 Airfoil terminology.

Settling angle of a HAWT defined in Figure 1.4 as,

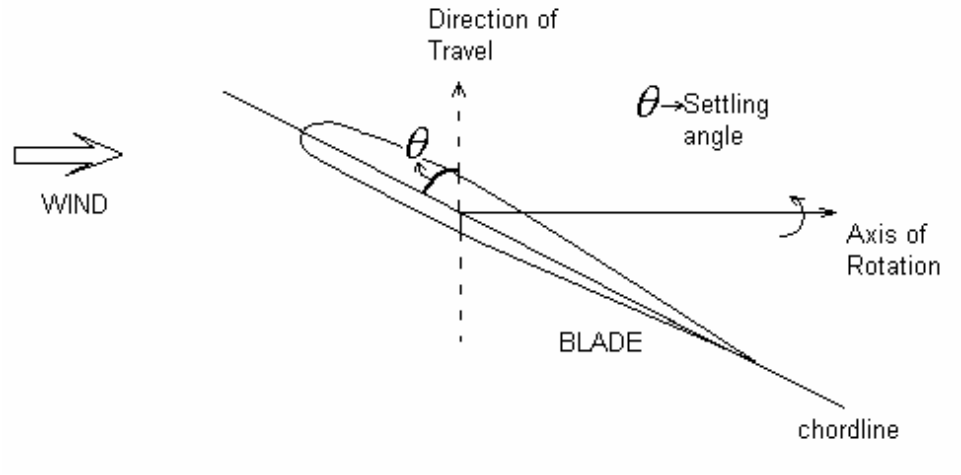

Figure 1.4 Definition of settling angle

In Figure 1.4 the settling angle is considered to be "positive" relative to the sign convention taken. In Figure 1.5 the tip-angle (or tip-settling angle) is negative w.r.t the same sign convention.

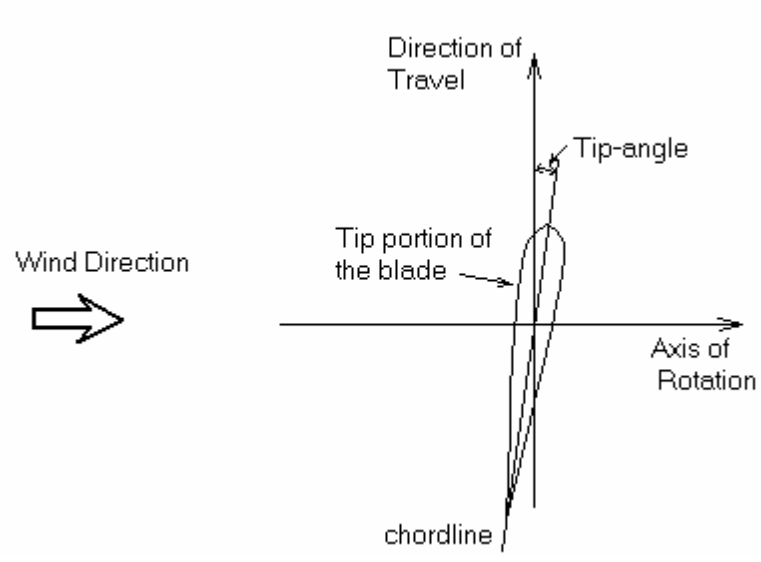

Figure 1.5 Definition of tip-angle

1.6 TORQUE & THRUST EXERTED ON A HAWT BLADE:

When the incoming flow interacts with a HAWT blade, it tries to turn the blade around its axis of rotation, and tries to push the blade in the axial direction. These two main forces “lift” and “drag” do so. The forces acting on a (2D airfoil) HAWT blade section are,

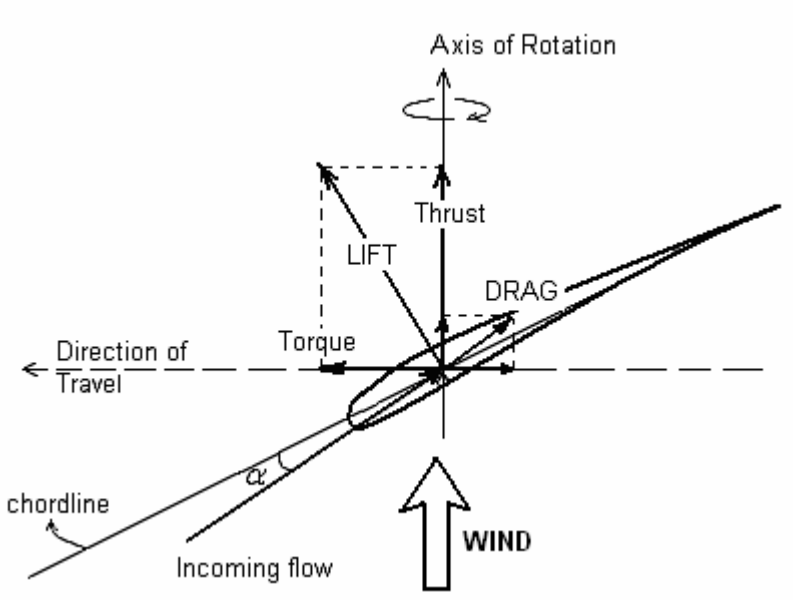

Figure 1.6 Torque & thrust exerted on a HAWT blade section

The torque exerted on a blade section comes from both lift and drag, and they are opposite in direction, but thrust components are both same in direction (towards the axial direction).

1.7 HAWT EFFICIENCY DEFINITION:

The term efficiency and availability are similar, but not as same as each other, since the input and output conditions are important for these phenomenons.

These terms should be considered relatively. For HAWTs the latter one, availability, is more appropriate for aerodynamic analysis, but the term “availability” is going to be included into the efficiency as one will see in the preceeding pharagraphs.

Wind turbine blades try to catch some amount of wind power by retarding it down to a certain value. There is no doubt that retardation occurs at the rotor.

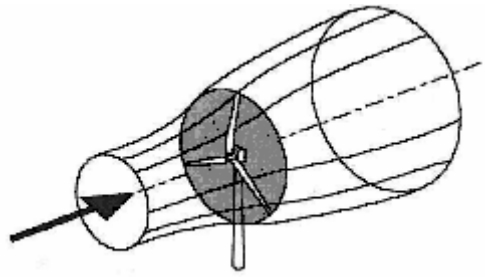

Figure 1.7 Streamtube formation for HAWTs

In Figure 1.7 the streamtube shape forms in that way due to the conservation of the continuity equation. The axial velocity of the air stream interacting with the blades is smaller than the steady freestream wind velocity. Due to the conservation of mass the bunch of streamlines just upstream of the rotor, affecting the rotor, needs to have a smaller area than the rotor swept area, since the air density is considered to be constant. The indicated streamtube shape exists naturally.

The power in the bunch of streamlines that the rotor is exposed to defined as,

$$\mathrm{P} = 0.5\rho_{\infty} U_{\infty}^{3} A \tag{1.1}$$

The area in the above equation indicates the rotor swept area, defined as,

$$A = \pi R^{2} \tag{1.2}$$

As it was said earlier the definitions are important for availability and efficiency. Hence if one considers the availability as the ratio of the rotor power

delivered to the power in the wind, defined in equation (1.1). This term is named as POWER COEFFICIENT, which is an important parameter defining the relative power production of a wind turbine and defined as,

$$C_p = \frac{\mathrm{P}_R}{0.5\rho_\infty U_\infty^3 A} \tag{1.3}$$

From the definition, it is thought that a wind turbine rotor should benefit from an amount of airflow area equal to the rotor swept area, but it is impossible due to the "smaller area" definition which discussed above. The air molecules in the ring between the rotor swept area and the smaller upstream area is considered to be a leakage loss.

1.8 VELOCITY VECTORS AT THE INLET AND OUTLET OF THE BLADE ELEMENT:

There is a 1D flow of air in the wind blowing direction and turbine blades turn in the tangential direction, so the flow stream has to change its direction after interacting with the blades.

The flow at the inlet of the horizontal axis wind turbine blades is considered to be 1D (purely axial flow).

The schematic view of this interaction is shown in Figure 1.8. In that figure, the flow at the inlet of the blade is considered to be 1D-even it is not the actual case in nature-as the fluid gains a tangential component due to the reaction of the blade. This causes a free wake structure emanating from the rotor and heading in the direction away from the wind turbine.

Due to the conservation of mass, the outlet axial flow has to be equal to the one at the inlet. In Figure 1.8, a 2D flow is considered. An inner section of the wind turbine blade is taken as a sample and the velocity diagrams have been drawn. Note that the relative velocity at the outlet is larger than its counterpart at the inlet.

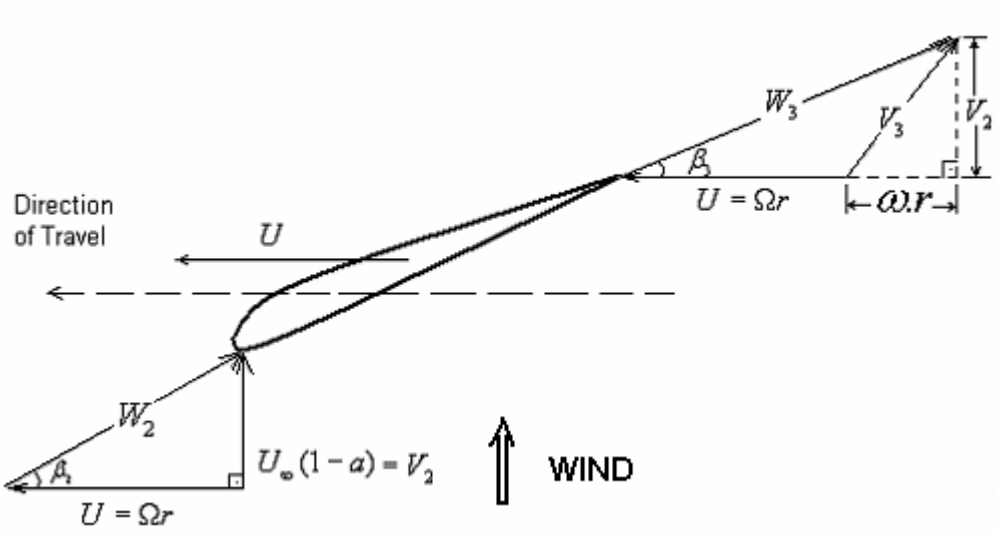

Figure 1.8 Velocity vectors at the inlet and outlet of the blade section

As one can see in Figure 1.8, the tangential component of the velocity, which is an absolute velocity at the outlet of the blade element (i.e., relative to the stationary frame of reference), creates the TURBINE HEAD.

1.9 WIND TURBINE HEAD:

The following calculations leads to the wind turbine head as,
The apex velocity triangles is drawn in Figure 1.9,

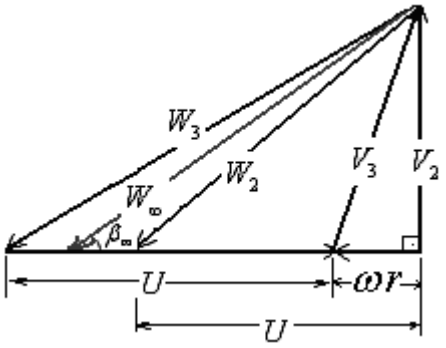

Figure 1.9 Apex velocity triangles indicating the incoming velocity.

$$W_{\theta\infty} = \frac{W_{\theta 2} + W_{\theta 3}}{2} = \frac{\Omega r + (\Omega r + a r)}{2} = r(\Omega + \omega/2) \tag{1.4}$$

$$W_{\infty} = [V_2^2 + (\frac{W_{\theta 2} + W_{\theta 3}}{2})^2]^{1/2} \tag{1.5}$$

where W_{∞} is the local incoming velocity applies on the aerodynamic center of that blade section at which quarter chord length of the symmetric airfoils. For cambered airfoils the point if application (i.e., the aerodynamic center) is close to quarter chord and the exact point of the center can be found by using the Fourier coefficients (see ref [6]).

a is the angular velocity imparted to the flow stream, is small compared to Ω. Since Ω is very large w.r.t a, then it can also be assumed that the pressure in the far wake is equal to the pressure in the free-stream.

If one defines a' (angular induction factor) as,

$$a' = a / 2\Omega \tag{1.6}$$

then,

$$W_{\theta\infty} = \Omega r(1 + a') \tag{1.7}$$

and, from continuity we know that axial velocity does not change across the blade, since the flow is incompressible and the flow area is constant due to the axial flow assumption,

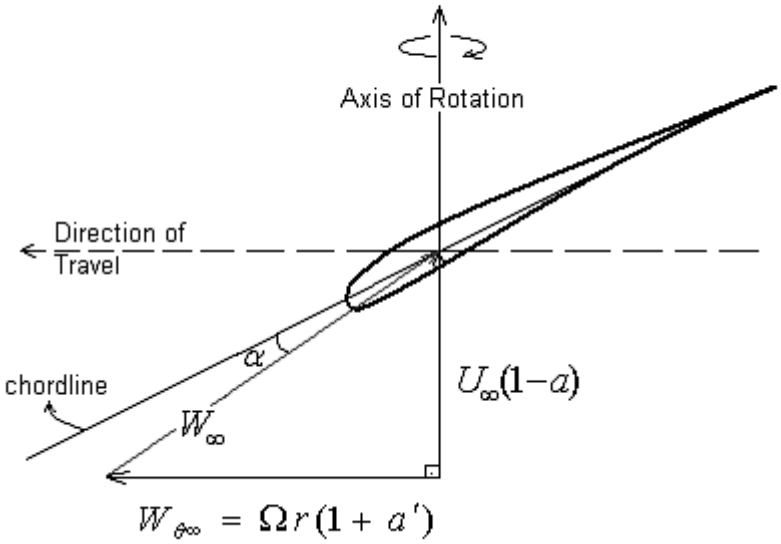

Figure 1.10 Incoming (effective) velocity.

Bernoulli equation between inlet and outlet of the blade,

$$\frac{P_2}{\gamma}+\frac{V_2^2}{2g}=\frac{P_3}{\gamma}+\frac{V_3^2}{2g}+H_{TUR} \tag{1.8}$$

assume that hydraulic efficiency is 100 % for this inviscid consideration, since HAWT has no casing.

$$\eta_h=\frac{H_{th}}{H_{TUR}} \tag{1.9}$$

from the above equation we find that the theoretical head is equal to the turbine head. Then, from "Euler's Turbine Equation",

$$H_{th}=\frac{u}{g}(V_{\theta 2}-V_{\theta 3}) \tag{1.10}$$

this can be written for axial flow machines. Equating the above equation to turbine head we obtain,

$$H_{TUR}=\frac{u}{g}(V_{\theta 2}-V_{\theta 3}) \tag{1.11}$$

Since the flow is assumed to be purely axial at the inlet, then the above equation reduces to,

$$H_{TUR} = \frac{- uV_{\theta 3}}{g} \tag{1.12}$$

One should note that in this turbine, inlet velocity is purely axial in contrast to the other most of the turbine applications which have guide vanes at the entrance. One desires to obtain an outlet whirl, again which is an undesired situation for most of the usual turbines (gas turbines, hydraulic turbines, etc…). The Bernoulli Equation for the absolute streamline between 2 & 3 can be written in the form,

$$\frac{P_3 - P_2}{\gamma} = \frac{V_2^2 - V_3^2}{2g} - H_{TUR} \tag{1.13}$$

after replacing absolute fluid velocity at the outlet of the blade by substituting its another equivalence with the help of Pythagoras Theorem in terms of the absolute fluid velocity at the inlet and the angular velocity imparted to the flow stream becomes,

$$P_2 - P_3 = \rho(\frac{a}{2} + \Omega)\omega r^2 \tag{1.14}$$

Note that, since counter-clockwise rotation of the blades is taken as positive as indicated Figure 1.11,

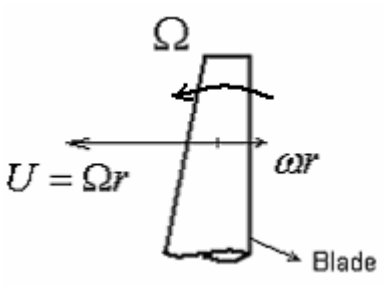

Figure 1.11 Interaction of the fluid with the blade causes the wake to rotate in the opposite direction relative to rotor blade.

from the above relations one can easily conclude that,

$$H_{TUR} = \frac{\Omega \omega r^2}{g} \tag{1.15}$$

and lastly, since one has assumed infinite number of blades, fluid angles and the blade angles at the inlet and outlet are equal.

1.10 DEGREE OF REACTION OF A HAWT:

Degree of reaction is defined as the ratio of the static pressure rise across the runner (or rotor) to the total pressure rise across the runner.

$$R = \frac{\Delta P}{\Delta P_t} \tag{1.16}$$

or in another form,

$$R = \frac{\frac{1}{2g}(W_2^2 - W_3^2)}{\frac{1}{2g}[(V_3^2 - V_2^2) + (W_2^2 - W_3^2)]} \tag{1.17}$$

since blade velocity is constant across the rotor. Note that the inlet and exit conditions should be calculated at the mean radius of the runner. Degree of reaction of a HAWT is,

$$R = 1 + a' \tag{1.18}$$

after substituting the values of the velocities, from the velocity triangles into equation (1.17). The above equation, (1.18), is valid for axial, frictionless, steady and incompressible flow with no-inlet whirl and infinite number of blades for a HAWT.

1.11 HAWT EFFICIENCY DEFINITION:

Benefiting from the basic turbomachinery formulations and adapting the HAWTs to these definitions one can make the definiton of efficiency of a HAWT as,

$$\eta_{overall} = \eta_{mech}.\eta_{v}.\eta_{h} \tag{1.19}$$

The overall efficiency is defined in turbomachinery using equation (1.19).

It should be noted that the hydraulic efficiency is equal to the multiplication of impeller and casing efficiencies. Since we do not have any casing, casing efficiency is equal to unity, and the impeller efficiency is taken into account implicitly by considering drag. Volumetric efficiency is some kind of leakage indicator that is also implicitly included in the formulas by the help of the power coefficient definition.

The area of the bunch of streamlines at the far downstream corresponding to the rotor swept area has a less area than the rotor swept area. This means some air is escaping from the rotor without interacting with the blades. The escaped air (this is the mentioned leakage) implicitly exists in the power coefficient (from definition). That implied smaller area far upstream of the rotor occurs naturally -because of continuity equation- due to the axial retardation of the air molecules at the rotor.

For HAWTs, the mechanical efficiency includes the electrical efficiency as well. The impeller and volumetric efficiencies are both inside the power coefficient. This means considering only the power coefficient and the mechanical efficiency yields the overall efficiency (ref [1]). This means the following equation gives the relation between the power in the wind and the net power output,

$$P_{NET} = P_{WIND}.C_{p}.\eta_{mech} \tag{1.20}$$

The mechanical efficiency includes the gearbox, bearing, belt (if available), generator efficiencies (etc…).

1.12 DEFINITION OF TIP-SPEED-RATIO (TSR):

As it was mentioned earlier the speed of the blade tips is ideally proportional to the speed of the wind. The ratio of the translational velocity of the blade tip in the tangential direction to the steady freestream wind velocity is defined as the tip-speed-ratio and abbreviated as TSR. This is a non-dimensional parameter and it is a kind of flow coefficient. For high speed rotors this parameter is relatively large, but this does not mean that for low speed rotors this parameter is small. For a large radius wind power machine-even turning at lower rpm-this coefficient becomes relatively large. Modern wind turbines are designed to have large TSR values.

$$\lambda = \Omega R / U_{\infty} \tag{1.21}$$

Every wind turbine has its own power coefficient vs. TSR curve. A sample curve is illustrated in Figure 1.12.

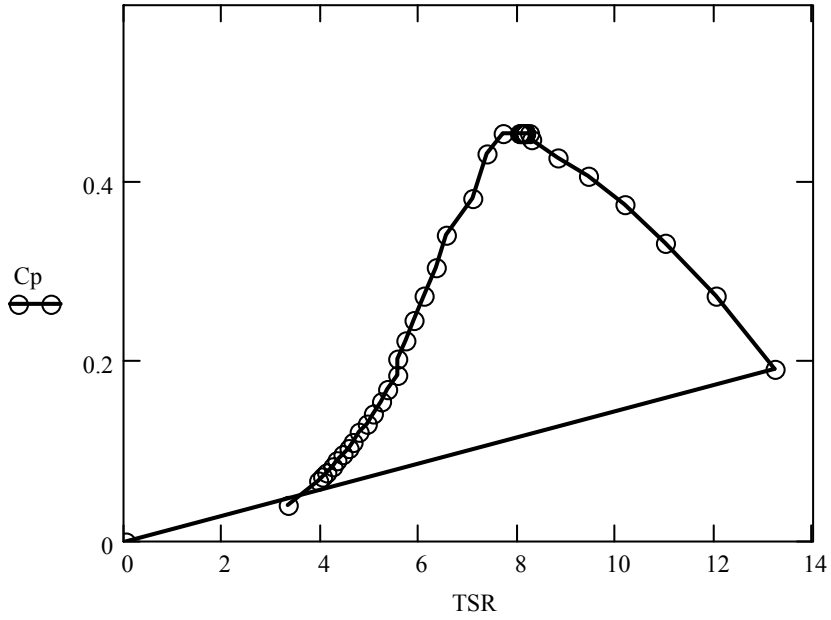

Figure 1.12 Power coefficient vs. TSR curve of a large scale HAWT
(Belongs to Mod-5 HAWT, manufactured by Boeing Aerospace Industry)

The power coefficient vs. TSR curves of HAWTs give an idea about the relative power production of a HAWT at a first glance. They can be obtained from the manufacturer company.

CHAPTER II

PERFORMANCE PREDICTION OF HORIZONTAL AXIS WIND TURBINES USING VORTEX THEORY

2.1 THREE DIMENSIONAL FLOW ANALYSIS:

It is worthwhile to discuss the basic 3D flow aerodynamics before starting the analysis of HAWTs.

In reality, every flow is three dimensional. One makes some assumptions so as to simplify the problems. By doing so, one moves far away from the real case as the limitation level increases.

It will be recalled briefly the basic 3D flow aerodynamics in order to make the reader, ready to understand the HAWT performance prediction by using a theory called “Helicoidal Vortex Theory (or Vortex Theory)”. First of all it is beneficial to start with a 3D airfoil analysis that making translational motion (for ex. wing), and then this guides the reader to understand the 3D flow around the airfoils making both rotational and translational motion (HAWT blades).

In the BEM Theory, 2D analysis is carried out and then due to the 3D effects, this 2D assumption was correlated by considering the tip losses by using, for example, Prandtl’s tip loss formula. In this section the spanwise distribution of the pressure, circulation etc… will not be considered as uniform due to 3D effects. This means the tip losses will be included implicitly into the calculations during the whole process.

When the span of an airfoil is infinite, the flow is identical for each spanwise station. The lift produced by the pressure differences between the lower surface (i.e., pressure side) and the upper surface (i.e., suction side) of the wing, and therefore the circulation, integrated along the chord length of the section does not vary along the span. For a wing of finite span (i.e., 3D), the high pressure air beneath the wing spills out around the wing tips toward the low pressure regions above the wing. As a consequence of the tendency of the pressure acting on the top surface near the tip of the wing to equalize with those on the bottom surface, the lift force per unit span decreases toward the tips. At the tip point no-lift occurs. The chordwise pressure distribution for different spanwise locations on a wing of finite span is illustrated in the Figure 2.1.

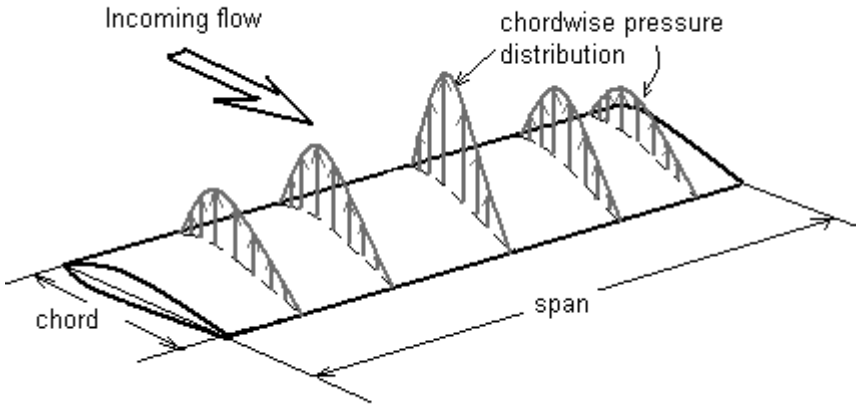

Figure 2.1 Pressure distributions on a wing.

The resultant lift force acting on a section (i.e., a unit span) is obtained by integrating the pressure distribution over the chord length.

As indicated in Figure 2.2 there is a spanwise variation in the resultant lift force.

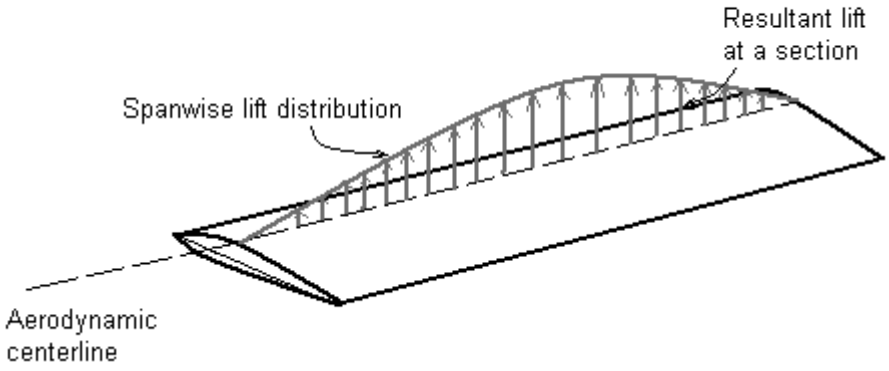

Figure 2.2 Spanwise lift distribution.

As a result of the spanwise variation, the air on the upper surface flows inboard toward the root. Similarly, on the lower surface, air will tend to flow outward toward the tips. The resultant flow around a wing of finite span is 3D, having both chordwise and spanwise velocity components.

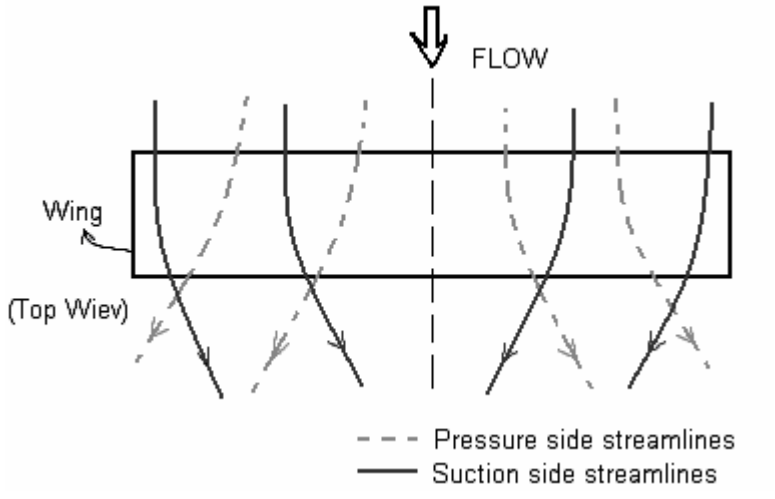

Figure 2.3 Streamline tendencies around the wing during the flow.

Where the flows from the upper surface and the lower surface join at the trailing edge, the difference in spanwise velocity components will cause the air to roll up into a number of streamwise vortices, distributed along the span. The small vortices roll up into large vortices just inboard of the wing tips. Very high velocities and low pressures exist at the core of the wing-tip vortices.

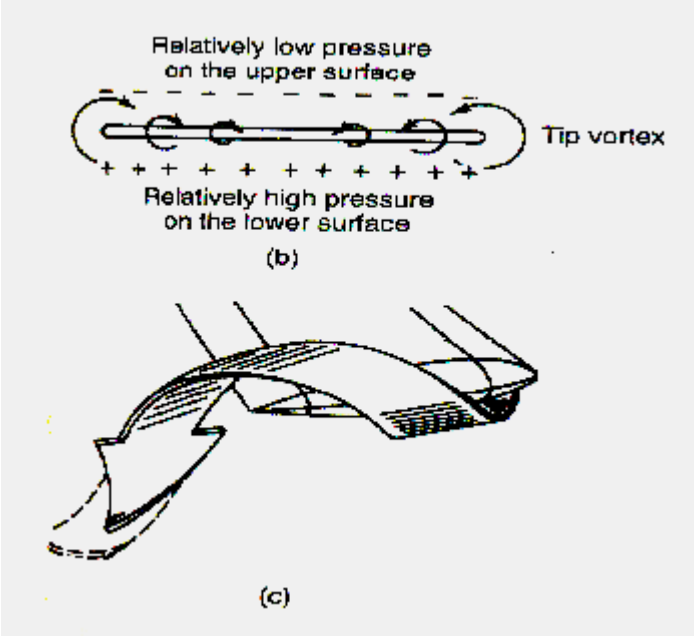

Figure 2.4 (b) Trailing vortices downstream of the wing
(c) The tip vortex. (Illustration from ref [6])

At this point, it is customary to assume the vortex wake, which is of finite thickness, may be replaced by an infinitesimal thin surface of discontinuity, designating the trailing vortex sheet, and the trailing vortex sheet remains flat as it extends downstream from the wing.

Since the lift force acting on the wing section at a given spanwise location is related to the strength of the circulation, there is a corresponding spanwise variation in circulation, such that the circulation at the wing tip is zero.

The vortex system consists of;

- The bound vortex system,
- The trailing vortex system,
- The starting vortex.

The idea allows a relation to be established between the physical load distribution for the wing and the trailing vortex system.

According to Helmholtz is that a vortex tube does not change strength between two sections unless a vortex filament equal in strength to the change joins or leaves the vortex tube. If $\Gamma(y)$ denotes the strength of the circulation along the y-axis, a semi-infinite vortex of strength $\Delta\Gamma$ trails from the segment Δy. The strength of the trailing vortex is given by,

$$\Delta\Gamma = \frac{d\Gamma}{dy}\Delta y \tag{2.1}$$

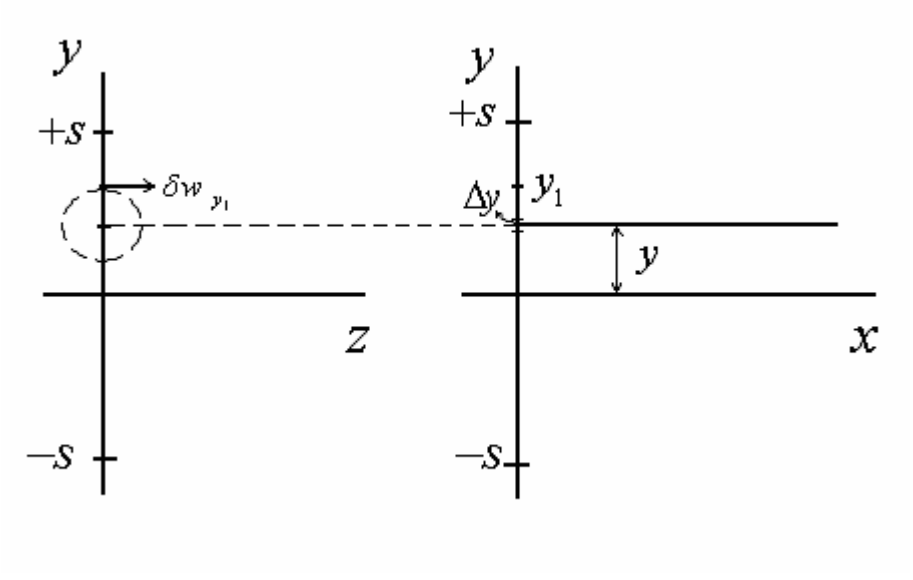

Figure 2.5 Induced velocity determination.

Velocity induced at y_1 due to the semi-infinite trailing vortex at y . (1/2 comes from the semi-infiniteness).

$$\delta w_{y_1} = \frac{1}{2}\left[+ \frac{d\Gamma}{dy} dy \frac{1}{2\pi(y - y_1)} \right] \tag{2.2}$$

Resultant induced velocity at any point y_1 due to the cumulative effect of all the trailing vortices one sets,

$$w_{y_1} = + \frac{1}{4\pi} \int_{-s}^{+s} \frac{d\Gamma / dy}{y - y_1} dy \tag{2.3}$$

Generally δw_{y_1} is negative (downwash).

The downwash angle, Λ , is,

$$\Lambda = Tan^{-1}\left(\frac{w_{y_1}}{U_\infty}\right) = -\frac{w_{y_1}}{U_\infty} \tag{2.4}$$

The downwash has the effect of "tilting" the undisturbed air, so the effective angle of attack at the aerodynamic center is,

$$\alpha = \alpha_G - \Lambda \tag{2.5}$$

Note that, if the wing has a geometric twist, both the angle of attack (geometric) and the downwash angle would be a function of the spanwise direction.

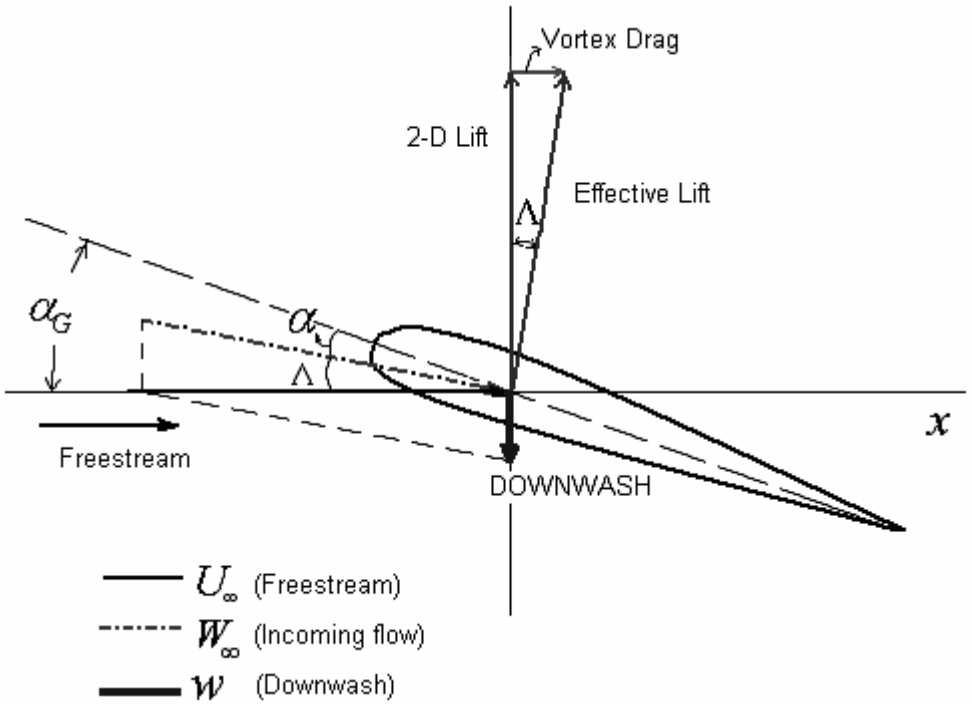

Figure 2.6 Three dimensional flow around a wing section.

Effective lift, due to 3D effects is perpendicular to the incoming flow. Induced drag (or vortex drag) is a drag component due to lift. One has now "form drag" (or pressure drag), "viscous drag", and "vortex drag".

The lift on an elemental airfoil section of the wing is,

$$l(y) = \rho_\infty U_\infty \Gamma(y) \tag{2.6}$$

from Kutta-Joukowski Theorem, while the vortex drag is,

$$d_v(y) = -\rho_\infty w(y)\Gamma(y) \tag{2.7}$$

The minus sign results because a downward (or negative) value of a downwash velocity produces a positive drag force. Integrating over the entire span of the wing, the total lift is given by,

$$L = \int_{-s}^{+s} \rho_\infty U_\infty \Gamma(y)dy \tag{2.8}$$

and the total induced (or vortex) drag is,

$$D_v = -\int_{-s}^{+s} \rho_\infty w(y)\Gamma(y)dy \tag{2.9}$$

In 2D flow airfoil circulation distribution along the span is constant (i.e., infinite span). No trailing vortices occur. No downwash velocities exist.

In 3D flow trailing vortices (change in bound vortices) creates downwash velocities.

Now one can consider the flow around an airfoil that making both translational and rotational motion (i.e., a wind turbine blade).

2.2 FLOWS AROUND WIND TURBINE BLADES AND WAKE STRUCTURE BEHIND THE ROTOR:

One makes an assumption that the flow is purely axial at the inlet of the wind turbine rotor (or turbine blades), so a one dimensional flow is considered at the entrance. In reality a modest whirl of air occurs at the entrance of the blade which is neglected. Across the blade section, due to interaction with the blade, this whirl velocity increases. Whirl velocity is opposite in direction to the blade rotational velocity. As a result, the fluid downstream of the rotor makes not only a translational but also a rotational motion. Whirl velocity changes along the blade and as a mean value, half of its value between the entrance and exit of the blade section is considered.

Due to the rotational motion of the blades, the wake ensuing from the rotor has a helicoidal shape. Since it resembles a screw, Glauert has given the name “Airscrew Theory” in the first half of the twentieth century, for this simplest model (ref [5]). At that time due to the lack of experimental techniques and availabilities helicoidal wake structure was not understood well, but nowadays with the help of such experimental devices it is very well understood.

The problem encountered today that there is not any available relation describing the structure of the wake behind the rotor for wind turbine operational condition. The best way to see its shape is to make experiments. For example, smoke test helps the scientists to understand its exact shape, but they can not make experiments every time because of financial problems. They are trying to find some models that are close to the natural behavior of the wake emanated due to the rotation of the rotor.

Figure 2.7 indicates an upwind three bladed HAWT. There are features of interest, these are, thrust on the rotor due to the aerodynamic loading and the trajectory of the tip vortex can be said. A conventional way to regulate the amount of thrust that a rotor sees is to pitch the blades along the pitch axis. The pitch axis runs radially outward along each blade. A tip vortex has been included for the blade that is located at an azimuthal angle of zero degrees. This tip vortex is a result of the pressure difference between the upwind and downwind side of the blade.

The air moving along the upwind side tends to be attracted to the low pressure region on the downwind side and rolls around the tip of the blade.

The tip vortex helix has a pitch and a radial variation associated with it. Depending on the wind speed and how fast the rotor is rotating, the pitch of the wake will vary. The total thrust on the rotor blades is a direct result of the pressure difference seen by each blade. With increasing thrust, one would expect the tip vortices to become more energetic and may cause the wake periphery to expand.

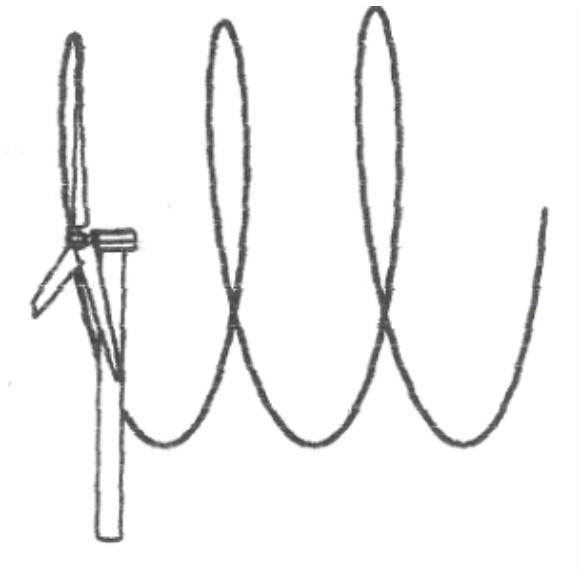

Figure 2.7 Tip vortex emanating from the tip of the blade.
(Illustration from ref [9])

All those tip vortices roll off the blades, the action of the pressure balance will rotate the vortices in a direction that will induce a velocity on the blades that is in the opposite direction of the wind.

Considering the three bladed rotor shown above, as the vortex is trailed by one blade, the following blade will feel the effect of this vortex and its induced velocity. The magnitude of this effect depends on the strength and location of the tip vortex.

In order to calculate the blade loading, the angle of attack and the incoming velocity along the blade must be calculated. By accurately locating the wake, its effect on the rotor can be similarly predicted.

In the prescribed wake approach, the geometry of the wake is established prior to the commencement of the solution. The strength of the vortex elements will vary according to the bound circulation on the blade. The geometry of the wake is fixed during the calculation cycle.

The solution is considered to be complete when the no-flow boundary conditions on the blade are satisfied.

The wind speed seen at the rotor disk of an operational wind turbine is typically 30 % slower than that measured far upstream. The exact amount of the retardation is determined by an exact accounting of the fluid dynamic structures which tend to cause it. Lifting line theory has provided the mathematical insight needed to recognize that the induced velocities are caused by trailing vortices in the wake. Although the theory was developed for airplanes, the extension to wind turbine rotors can be made. However, an additional complication results from the helical structure that is formed downstream. The implication with regard to aerodynamic modeling is that the wake structure must be known before an accurate analysis can be made.

The local static pressure between the upwind and downwind sides of the blades tends to vary radially.

Typically, a peak is found close to 80 % span of the blade. According to lifting line theory, air that is outboard of this peak will tend to roll up into a strong, concentrated tip vortex. The tip vortex shown in Figure 2.8 as the helical element that emanates from the blade tip. The air that is inboard of this peak will form a shear layer that consists of the inward moving air on the upwind side of the blade and the outward moving air on the downwind side. This layer is often called the inboard sheet.

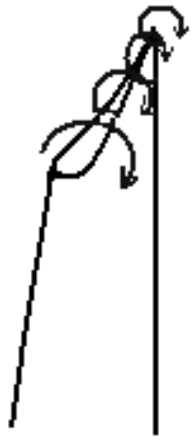

Figure 2.8 Tip vortex formation on a HAWT blade.

The tip vortices and inboard sheets that trail from wind turbine blades are vortical in nature and influence each other and fluid particles surrounding them. The integrated effect of the wake is felt by the blades. Accurately predicting the induced velocity that results is a key to improving performance prediction of a wind turbine rotor. To develop the models that can accomplish this, an understanding of the flow on a local level is required, but in this study some limitations will be made relating to the trace of the tip vortex and the shape of the wake structure. There is also a great effort to abolish these limitations by carrying out some experiments, since these experiments correlates the models found.

This theory can be considered as an advance one among the other basic theories developed. An analogy between Prandtl's lifting-line free vortex calculations and this theory can be found.

Most of the information was taken from the propellers because a HAWT blade and a propeller operates reversely, and some airplane wing sections (airfoils) were used for wind turbine blades (for ex. some NACA airfoils).

The analysis of HAWTs at off-design conditions is based on the vortex model as for the propellers, however the power is not prescribed and iteration is

needed to insure that the vortex system is consistent with the resulting power extracted from the air. This means that the extracted power amount is directly related to the shape of the vortex sheet. 2D data from experiments or viscous codes are used to correct for viscous effects. Comparisons indicate that the results are as correct as the results of other theories.

Vortex structure establishes as a result of the blade shedding. The rotational and translational motion develops a helicoidal free vortex structure downstream of the rotor. This shed vortex structure induces velocities on the blade sections in the axial and azimuthal directions which have a profound influence on the blade flow. These induced velocities are analogous with the induced velocities in the BEM Theory. They differ in magnitude but same in direction for both theories. Hence, the magnitude of the resultant induced velocity then differs in magnitude and direction in both theories. The main difference comes from 2D assumption used in BEM Theory that there is not any interaction between annular rings. A correction is made in BEM Theory by Prandtl's tip loss formula which includes tip losses. (More information can be found about these tip-losses in a report written by Sankar L. N., ref [15]).

For large Re, the phenomenon depends primarily on the advance ratio (inverse of TSR) and the power coefficient. The vortex sheet is a free surface and its location and strength depend on the conditions of the problem. The Euler and Navier-Stokes solvers cannot capture the vortex sheets beyond two or three turns, due to the dissipation properties of the numerical schemes. Therefore, most of the interaction is lost hence the flow can not be accurately predicted. In the present approach, the vortex structure is well represented and the interaction is allowed to take place. The influence coefficients from the multiple vortex sheets are computed using the Biot-Savart law. This is done in a very efficient and accurate way by treating the sheets as vortex lattices with variable discretization steps.

Now, at first the basic formulas of the ADT will be used so as to solve the problem. ADT and BEM Theory are used during the calculations of "Vortex Theory". If ADT is accepted as a "zeroth order" method, then BEM can be

considered as “first order” and Vortex Theory (or Helicoidal Vortex Theory) can be called as “second order”.

Recall from ADT that the convection speed of the flow at the rotor, in the axial direction is $U_\infty + u_a$. Here u_a is the induced velocity in the axial direction.

The total thrust and power on the rotor, according to ADT is,

$$P = 2\pi\rho_\infty R^2 (U_\infty + u_a)^2 u_a \tag{2.10}$$

$$T = -2\pi\rho_\infty R^2 (U_\infty + u_a) u_a \tag{2.11}$$

where u_a is equal to $-U_\infty a$.

If one chooses the positive x-direction towards right, then the absorbed power becomes negative, since u_a is negative (retardation). From equation (2.10) one concludes that, power has a negative value and from equation (2.11) thrust has a positive value. Figure 2.9 indicates this sign convention.

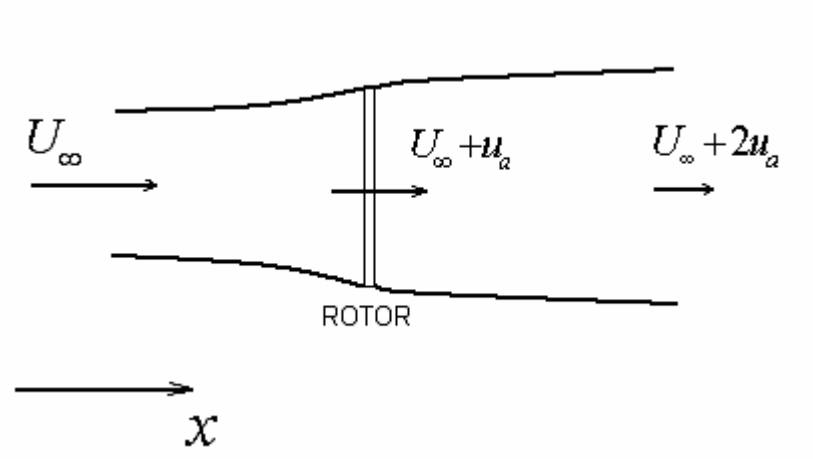

Figure 2.9 Axial velocities & sign convention relative to ADT.

The useful dimensionless parameters are introduced below as,

$$C_T = \frac{T}{0.5\rho_\infty U_\infty^2 R^2} \tag{2.12}$$

$$C_\tau = \frac{\tau}{0.5\rho_\infty U_\infty^2 R^3} = \mathrm{P}_\tau \lambda^2 \tag{2.13}$$

$$C_p = \frac{\mathrm{P}_\tau}{\pi} \lambda^3 \tag{2.14}$$

The coordinates, velocities, circulation and chord are made dimensionless as, $x = R\tilde{x}$, $y = R\tilde{y}$, $z = R\tilde{z}$, $u = U_\infty \tilde{u}$, $v = U_\infty \tilde{v}$, $w = U_\infty \tilde{w}$, $\Gamma = U_\infty R\tilde{\Gamma}$, $c = R\tilde{c}$.

The dimensionless variables will be used in the rest of the chapter for this theory and one will ignore the sign "tilde" for simplicity.

In the above equations "lambda" is the tip-speed-ratio, defined as,

$$\lambda = \Omega R / U_\infty \tag{2.15}$$

The analysis of blade flow, using BEM Theory, yields the moment (torque) and force (thrust) coefficients for one blade, respectively,

$$C_\tau = 2\int_{y_0}^{1} \Gamma(y)[1+u(y)].y.dy + \int_{y_0}^{1} q(y).[\lambda y + w(y)].C_d(y).c(y).y.dy \tag{2.16}$$

$$C_\mathrm{T} = -2\int_{y_0}^{1} \Gamma(y)[\lambda y + w(y)]dy + \int_{y_0}^{1} q(y)[1+u(y)]C_d(y).c(y).dy \tag{2.17}$$

Note again that the variables in the above equations are all non-dimensional.

$q(y)$ is the dimensionless incoming velocity in the y-constant plane. Recall that xyz frame of reference (Cartesian coordinate system) is attached to the blade (no relative motion with the rotor).

This mentioned incoming velocity is non-dimensionalized by using free-stream wind velocity and the following relationship is valid for it.

$$q(y) = \sqrt{[1+u(y)]^2 + [\lambda.y + w(y)]^2} \tag{2.18}$$

One can see the proof of this relation from Figure 2.10 as,

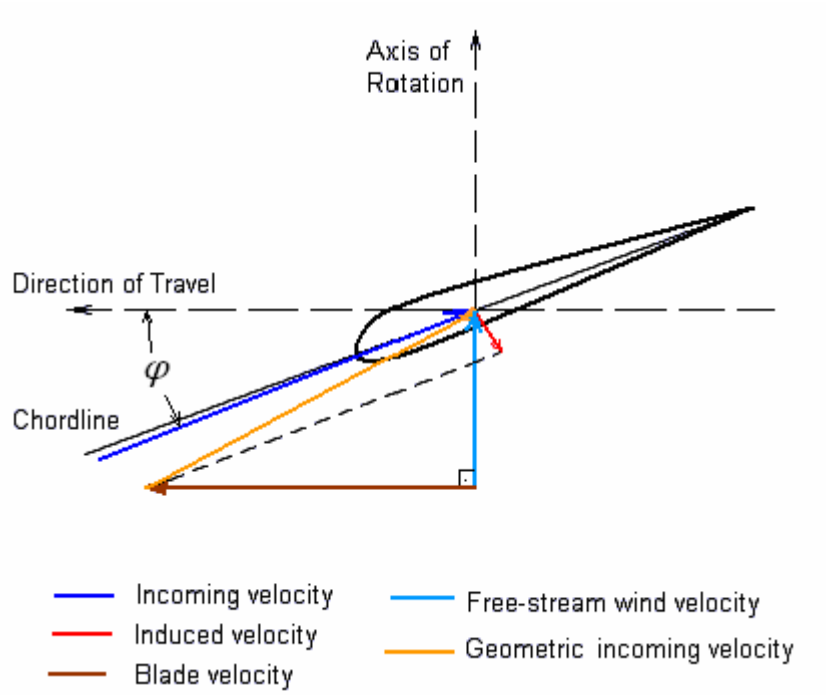

Figure 2.10 Entire velocity vectors on the blade section

The 2D viscous data (i.e., drag and lift coefficients) is obtained from experimental data or Xfoil (ref [16]).

Once the vortex structure is defined, the Biot-Savart law is used to obtain the influence coefficients relating the vortex strength $d\Gamma/dy$ to the induced axial (backwash) and azimuthal (downwash) velocities. The induced axial velocity is due to the winding of the sheet behind the rotor and goes to zero for a single wing in translation or for a very low tip-speed-ratio (or TSR).

The free-vortex structure downstream of the rotor, shed by one blade is shown in Figure 2.11, for a HAWT.

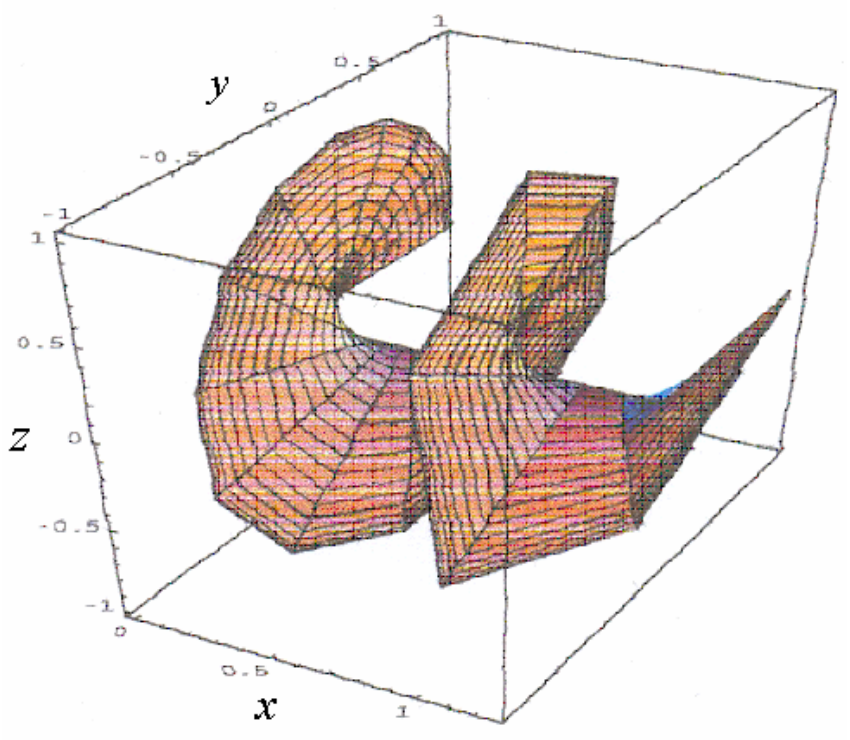

Figure 2.11 Wake structure behind the rotor shed by one blade (from ref [10]).

The assumptions that were considered in this theory are as follows,

- Non-expanding wake behind the rotor,
- Frozen vortex structure,
- Smooth vortex structure.

The above basic assumptions are made so as to simplify the problem. The first assumption is made in order to take the shape of the free vortex as a cylinder, the second one indicates the rigidity of the wake structure, this means, when the steady conditions are reached, vortex structure does not change its shape, and lastly, one considers a smooth vortex structure due to the low thrust coefficient, because for the turbines operating with high thrust coefficient values, the wake structure behind the rotor is in the turbulent wake state, i.e., no longer helicoidal in shape.

Before writing the equations for the induced velocities, it is worthwhile to remember the “Biot-Savart Formula” in electricity. Because one is going to carry out an analogy between electricity and fluid mechanics in order to adapt this formula to the present fluid problem.

Biot-Savart law in electricity says that, a current passing a wire causes magnetic field around it. Figure 2.12 illustrates this for a circular wire.

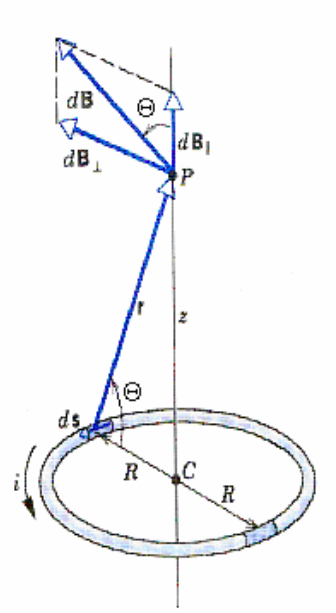

Figure 2.12 Current passing a wire induces magnetic field.

The induced magnetic field due to the electric current passing through a wire,

$$B = \frac{\mu_0 iR}{4\pi(R^2 + z^2)^{3/2}} \int ds$$

$$B = \frac{\mu_0 iR^2}{2(R^2 + z^2)^{3/2}}$$

according to Biot-Savart Law.

In fluid mechanics, a non-uniform bound circulation distribution around lifting surfaces causes velocity changes (induced velocities) on these surfaces. In Figure 2.13, the induced velocity at point C is desired to be calculated due to the vortex filament vector AB.

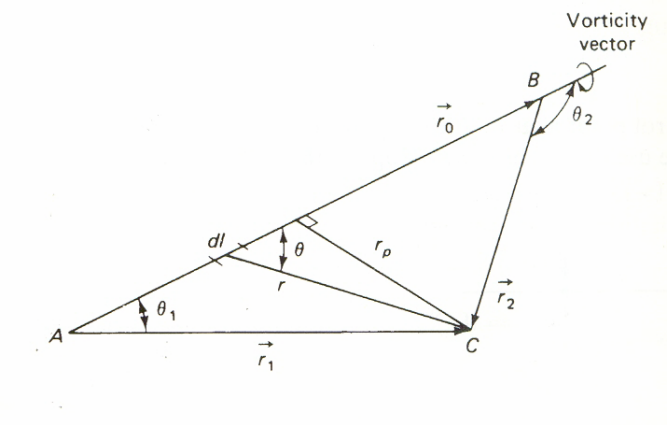

Figure 2.13 Vortex filament AB induces velocity at point C.

The following relation gives the induced velocity at point C both in magnitude and direction.

$$dV = \Gamma_n (dl \, xr) / 4\pi r^3 \tag{2.19}$$

The induced velocities around a wind turbine blade can be calculated with the same manner. One can consider the components of this velocity in the axial and tangential directions. The axial induction component exists due to the rotation of the blade, equation (2.20), differing from the wing that making only translational motion. This induced velocity component is known as “backwash” (This component corresponds to the axial induction factor which is discussed in Actuator Disc Theory). The backwash and downwash velocities are calculated, using Biot-Savart equations (2.20) and (2.21) respectively as,

$$u(y') = \int_{y_0}^{1} \int_{0}^{\infty} \frac{1}{4\pi} \frac{d\Gamma(y)}{dy} \frac{(y' - y_v)\frac{dz_v}{dx} + z_v \frac{dy_v}{dx}}{[x^2 + (y' - y_v)^2 + z_v^2]^{3/2}} dxdy \tag{2.20}$$

$$w(y') = -\int_{y_0}^{1} \int_{0}^{\infty} \frac{1}{4\pi} \frac{d\Gamma(y)}{dy} \frac{(y' - y_v) + x\frac{dy_v}{dx}}{[x^2 + (y' - y_v)^2 + z_v^2]^{3/2}} dxdy \tag{2.21}$$

where the equation of the vortex sheet is given by,

$$y_{vi,j} = y_j Cos(\lambda x_i)$$
$$z_{vi,j} = y_j Sin(\lambda x_i)$$

where $x \geq 0 \,\&\, y_0 \leq y \leq 1$

The above two equations represent a helicoidal, cylindrical sheet. The discrete formulation can be done by considering the vortex sheet as a vortex lattice. In the axial direction, a variable step allows for the clustering of points, due to a continuously retardation behind the rotor, near the blade where the integrand in the Biot-Savart formula is large. However, the stretching is limited to a point where there remains at least four points on a turn, until a sufficient distance L from the rotor is reached. This distance is typically taken as ten diameters downstream of the rotor (Trefftz Plane). In the y-direction, a cosine distribution of control points on the blades is used. For Prandtl's lifting-line problem the same cosine distribution is used.

The mesh system can be constructed by considering;

$$x_i = x_{i-1} + dx_i$$
$$dx_i = s dx_{i-1}$$
$$i = 1, \ldots\ldots\ldots, ix$$

and,

$$y_j = y_0 + \frac{1}{2}(1 - y_0)(1 - Cos\phi_j)$$

$$\phi_j = \frac{j-1}{jx-1}\pi$$

$$j = 1, ..., jx$$

Integration points are placed between the control points to avoid the singularity in the integrand, so,

$$y_k' = y_0 + \frac{1}{2}(1 - y_0)[1 - Cos(\phi_k + \frac{\Delta\phi}{2})]$$

$$\Delta\phi = \frac{\pi}{jx-1}$$

$$k = 1, ..., jx-1$$

Figure 2.14 indicates the control and integration points on the blades.

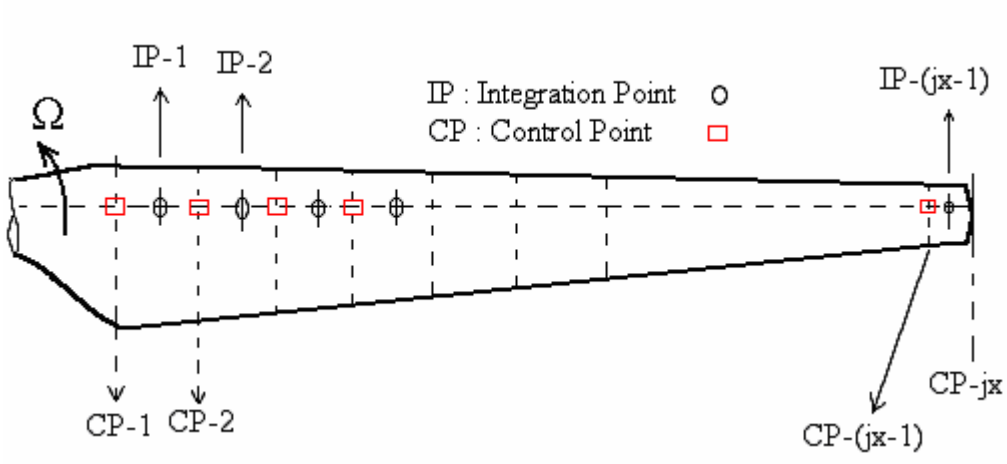

Figure 2.14 CP and IP distributions on the blade.

The axial discrete system can be shown in Figure 2.15 as,

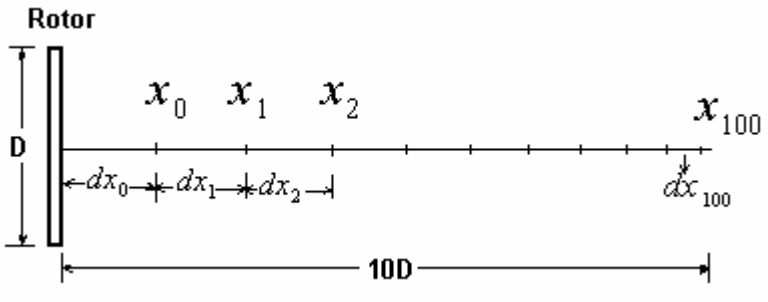

Figure 2.15 Axial discrete system.

The induced velocities are given in the discrete form as,

$$w_k = \sum_{j=1}^{jx-1} (\Gamma_{j+1} - \Gamma_j) a_{j,k} \tag{2.22}$$

$$u_k = \sum_{j=1}^{jx-1} (\Gamma_{j+1} - \Gamma_j) b_{j,k} \tag{2.23}$$

where,

$$a_{j,k} = -\frac{1}{4\pi} \sum_{i=2}^{ix} \frac{(y_k' - \bar{y}_{vi,j})(x_i - x_{i-1}) + \bar{x}_{i,j}(y_{vi,j} - y_{vi-1,j})}{[\bar{x}_{i,j}^2 + (y_k' - \bar{y}_{vi,j})^2 + \bar{z}_{vi,j}^2]^{3/2}} \tag{2.24}$$

$$b_{j,k} = \frac{1}{4\pi} \sum_{i=2}^{ix} \frac{(y_k' - \bar{y}_{vi,j})(z_{vi,j} - z_{vi,j}) + \bar{z}_{vi,j}(y_{vi,j} - y_{vi-1,j})}{[\bar{x}_{i,j}^2 + (y_k' - \bar{y}_{vi,j})^2 + \bar{z}_{vi,j}^2]^{3/2}} \tag{2.25}$$

where,

$$\bar{*}_{i,j} = \frac{*_{i-1,j} + *_{i,j}}{2}$$

Note that the sign " * " indicates any parameter and the bar upon it indicates the arithmetic average value of that mentioned parameter.

2.3 ANALYSIS OF HAWTs (Performance Prediction):

One can predict the performance of a HAWT in out of design conditions by using the vortex theory. When wind speed changes, increases or decreases; whatever, the machine operates at a different TSR, for a constant speed HAWT, rather than it was designed, so power coefficient value decreases.

Now the free vortex sheet behind the rotor need not to be a regular screw surface as mentioned in the design case, but for simplicity, especially when low thrust coefficient occurs, the surface of it will be taken as smooth in order to apply the previous helicoidal formulas. When the thrust coefficient amount increases this smoothness assumption gets away from reality and the amount of error increases as it is compared with the previous case. Hence the "smooth wake surface" assumption fails.

This increase of loading should be in the windmill state. If the wind speed is relatively high, then the rotor is in the windmill state. This time it becomes a heavily loaded wind turbine and one knows already that, for that situation a helicoidal vortex shape occurs downstream of the rotor. On the contrary, when the wind speed is relatively low, then turbulent wake occurs downstream of the blades (i.e., not helicoidal). Lightly loaded turbines exist in low winds. In the latter case the axial induction is at least 0.4 and thrust (i.e., loading) is relatively low, but the thrust coefficient becomes relatively high. Figure 2.16 indicates this situation. Glauert has developed an empirical relation regarding turbulent wake state conditions, since ADT is not valid in this state. The dashed curve illustrates ADT results.

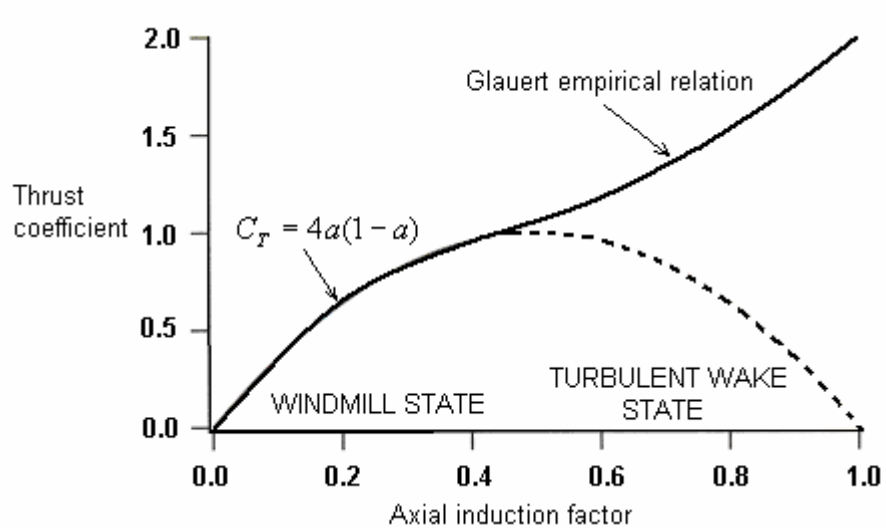

Figure 2.16 Thrust coefficient vs. axial induction factor.

The shape of the blades (chord and twist distributions), the tip angle, the radii, the angular speed and the blade number of the rotor are known. Since the free stream wind velocity is known, and then the TSR is also known. Now, from these data one can find the power production of the blades and the thrust force on the rotor in out of design conditions, but it should be again emphasized that the flow is still in the "windmill state".

In BEM Theory the bound circulation on the blades is assumed to be constant, but in reality this circulation changes along the blades as mentioned earlier in this chapter. The maximum circulation occurs nearly 80 % span of the blade, since the pressure difference between downstream and upstream of the blade has a maximum value approximately at that point, so it seems that the lift force on the blade has its maximum value at that region. As one moves towards the ends of the blades, circulation value decreases and becomes zero at both ends (i.e., tip and root), but there are still vortices rotating in the opposite direction of each other. Their magnitude is larger than the inboard vortices. Root vortex moves along the axial direction, however the tip vortex not only moves in the axial direction, but also moves in the radial direction due to the formation of the streamtube shape (for more

information about the tip vortex see ref. [12]). As it was said earlier one will neglect the radial component for simplicity. Tip vortex has a tangential velocity also, rotating in the opposite direction to the rotor due to the rotation of the blades.

Here, one aims to find the torque and thrust on each blade. In this case one has five unknowns which are the induced velocities in the axial and azimuthal (tangential) directions, circulation distribution, angle of attack and the lift coefficient at each section on the blades. Five equations are needed in order to solve the problem. In order to find the total lift and drag forces on the blades, the incoming velocity should be calculated at each section of the blade. Its direction helps the angle of attack to be found.

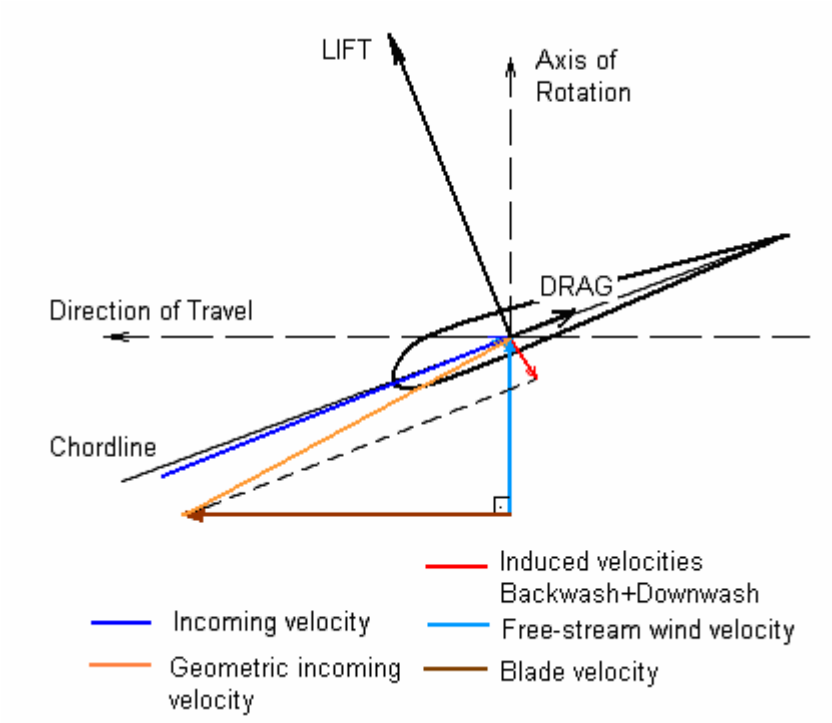

Figure 2.17 Full velocity pattern on a WT blade section

In Figure 2.17, the lift is perpendicular, and the drag is parallel to the incoming velocity. From the lift and drag coefficients we can define the lift and drag force acting on the section, and on the entire blade.

As it is seen in the above illustration and mentioned earlier, the tangential components of the lift and drag must be considered to determine the "torque", and their axial components must be considered to determine the "thrust" on the rotor.

In order to find the values of the five unknowns, five equations must be considered, for each blade section. The first equation comes from Kutta-Joukowski Theorem which relates circulation to the lift. The second one is 2D wind tunnel data that relates lift coefficient to the angle of attack. The third one is the compatibility condition that is used to check whether the angle of attack found from the lift coefficient, calculated by the Kutta-Joukowski formula, corresponds to the angle of attack which is found from the calculated incoming velocity value. If we obtain two more equations, then the problem can be solved. These two equations are provided using Biot-Savart Law applied to our fluid problem.

Here the main problem is to determine the shape of the wake. Because trailing vortices behind the rotor influences the incoming velocity acting on the blades. Correct determination of the incoming velocities requires correct determination of the position of the trailing vortices, i.e., shape of the wake.

2.3.1 ANALYSIS PROCEDURE:

Some coefficients that were defined before will be used again in the analysis procedure. The rotor power coefficient and the rotor torque coefficient are given as follows, respectively,

$$C_p = \frac{P}{0.5\rho_\infty U_\infty^3 A} \tag{2.26}$$

$$C_\tau = \frac{C_p \pi}{\lambda} \tag{2.27}$$

In order to find the power production of the rotor at a given wind speed different than the design wind speed, the way to be traced is as follows,

The known data are defined. These are the chord and twist distribution, tip angle, airfoil type, root location and radii of the blade, rotational speed, and free-stream wind velocity. From these, TSR can also be calculated.

The analysis procedure can be fulfilled considering the known data as follows, (the statements mentioned here are explained detailed in Appendix C).

i. Assume a rotor power output value for the measured wind velocity,

ii. Find a rotor power coefficient value from eqn. (2.26),

iii. Find the rotor torque coefficient from eqn. (2.27),

iv. Find an induced axial velocity w.r.t the ADT Theory.

v. Prescribe the wake geometry relative to this induced velocity. (Due to clustering of the vortex sheet).

vi. Calculate the influence coefficients.

vii. Guess a circulation distribution.

viii. Find the induced velocities in the axial and azimuthal directions w.r.t this circulation distribution.

ix. Find the incoming velocity at that section.

x. Find the angle of attack from subtracting settling angle from the angle of relative wind at the interested section (or element),

xi. Find the lift coefficient from Kutta-Joukowski equation,

xii. Check, whether the angle of attack and the lift coefficient values correspond to each other (for the same section) by using 2D airfoil wind tunnel data,

xiii. If they do not correspond to each other, then guess another circulation distribution (statement-vii) and continue the procedure. When convergence is reached, determine the new value of the torque coefficient corresponding to the

converged circulation distribution.

xiv. Check that value with statement-iii. If different, make iteration (i.e., guess another rotor output power value).

As it is seen, one tries to find the shape of the wake behind the rotor for that flow condition by changing the influence coefficients. When the corresponding shape is found, the assumed torque coefficient (statement-iii) and the newly found one (statement-xiii) becomes converged. The above analysis procedure can be made a little more advanced by increasing the number of control points on the blades, but at that time a computing time problem appears. In order to avoid this problem one can use some mathematical facilities, such as relaxation methods used in the design case. By doing so, selecting more control points (for example hundred points), one finds closer results.

One should remember that the power values found in the analysis corresponds to the rotor power production value, not the electrical output power value.

In order to find the electrical output power production, the mechanical efficiency must be included lastly. (recall Chapter 1)

2.3.2 DEFINING THE SHAPE OF THE WAKE:

One needs to define the free vortex sheet behind the rotor in order to find the values of the incoming velocities along the blades. Positions of the trailing vortices should be defined exactly, since they directly affect the magnitude and direction of the incoming flows, which are required to calculate the lift on the blades.

The convection speed of the fluid (or air) at the rotor can be defined from the ADT (or Rankine-Freud Theory). This velocity decreases up to a point at which is called “Trefftz Plane” that is ten diameters downstream of the rotor. At that point the air speed induction is considered to be two times the induction at the rotor plane. Both the upstream and the downstream velocities are thought to be constant

according to this theory. A linear deceleration occurs in the axial direction at the downstream of the rotor due to the formation of the enlarging streamtube. This deceleration replaces acceleration after ten diameter distance and the fluid particles start to accelerate and gains a magnitude equal to the freestream flow.

Figure 2.18 indicates the axial convection speed of the fluid particles vs. the time elapsed for them to move from the rotor to the Trefftz Plane. Lagrangian (or material) description is considered for the particles. At t = 0, the fluid particle is at the rotor.

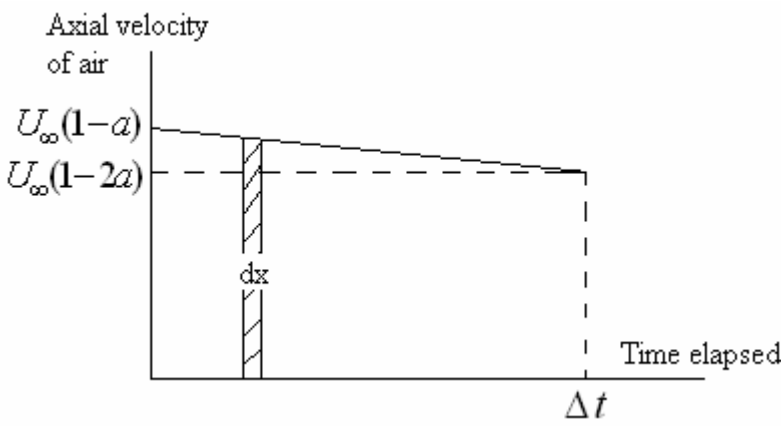

Figure 2.18 Deceleration process behind the rotor.

One should remember that the wake structure has a helicoidal cylinder shape. This resembles a screw so much, but the pitches of this screw are not the same for every inch due to the above mentioned deceleration. This effect is known as "clustering of the vortex sheet".

The clustering of the wake when forming a screw shape is sketched in Figure 2.19 as follows,

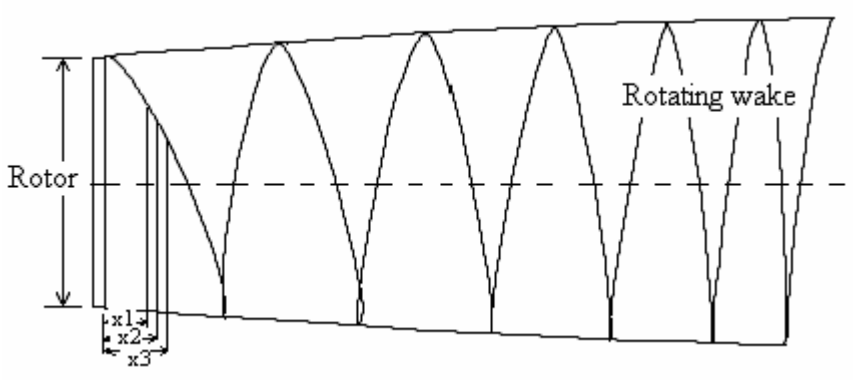

Figure 2.19 Variation of the pitches of the screw in the axial direction.

In Figure 2.19 $(x_2 - x_1) > (x_3 - x_2)$ due to the retardation of the air molecules. One benefits from ADT in order to make a close guess for the locations of the trailing vortices emanating from the rotor due to the non-uniform bound circulation distribution along the blades.

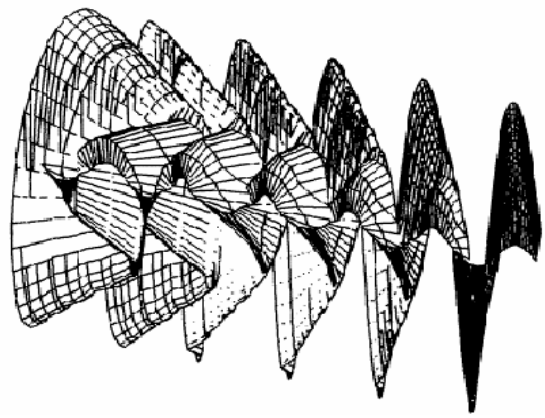

Figure 2.20 Typical wake shape behind the rotor.

2.3.3 PERFORMANCE PREDICTION PROGRAM:

A computer program “AEROPOWER”, written by using Visual Basic 6.0 and Excel combination, was developed to predict the output power production of a HAWT in out of design conditions (the term “off-design” is not appropriate here because, “off-design” is used generally for the extreme conditions, such as for turbulent wake state or propeller state etc…).

The conditions need to establish a helicoidal free vortex surface (or sheet) downstream of the rotor, as mentioned above, in order to make the program applicable.

A number of results were obtained by using this program, based on “Vortex Theory”, and some comments were carried out on those results. In the preceding sections this phenomenon will be discussed.

CHAPTER III

RESULTS & DISCUSSION

3.1 COMPARISON OF THE PROGRAM RESULTS WITH THE NREL TURBINE:

By using the performance prediction program AEROPOWER, one can find the power production of a HAWT in the limitations mentioned in Chapter 2.

National Renewable Energy Laboratory (NREL) has carried out (and still fulfilling) plenty of experiments on HAWTs. One of them is a 5.03 m radius, linear tapered, non-linear twisted two bladed rotor performance prediction experiment. This rotor produces 12.6 kW at 8.5 m/s wind speed (design wind speed) at 83 rpm (constant speed HAWT) and produces 28.60 kW as a rated rotor power. It should be noted that S809 airfoil type is used on the entire blade by NREL (ref [17]).

The NREL blade is shown in Figure 3.1 as,

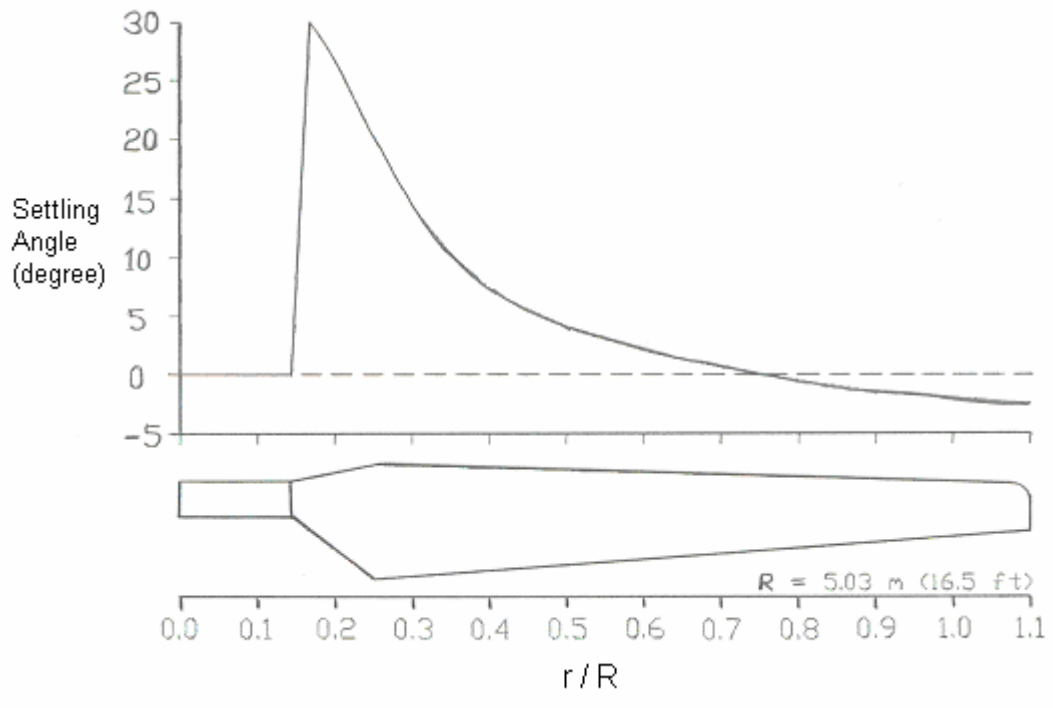

Figure 3.1 NREL Combined Experiment Rotor (CER) blade.

Keeping the rotor diameter, blade shape (twist distribution), settling angle, angular speed as constant, then one can obtain a power curve as illustrated in Figure3.2 as,

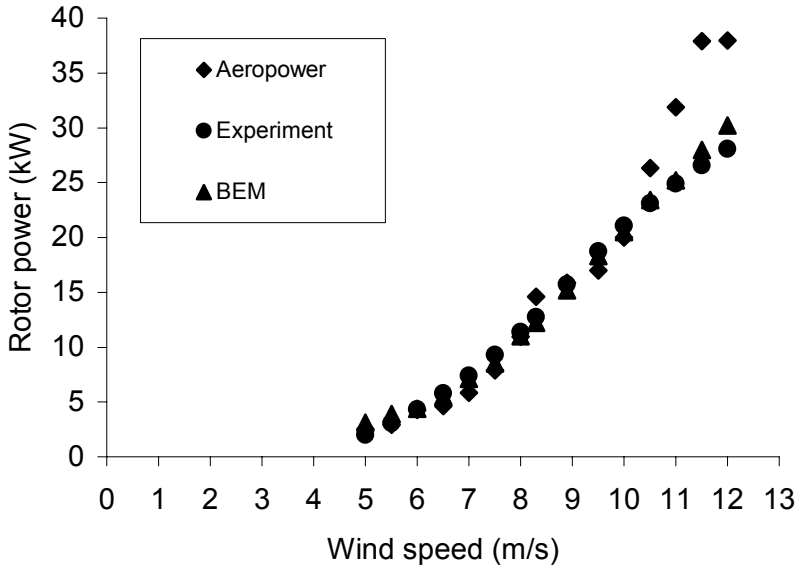

Figure 3.2 Comparison of performances.

The error existed from Figure 3.2 is,

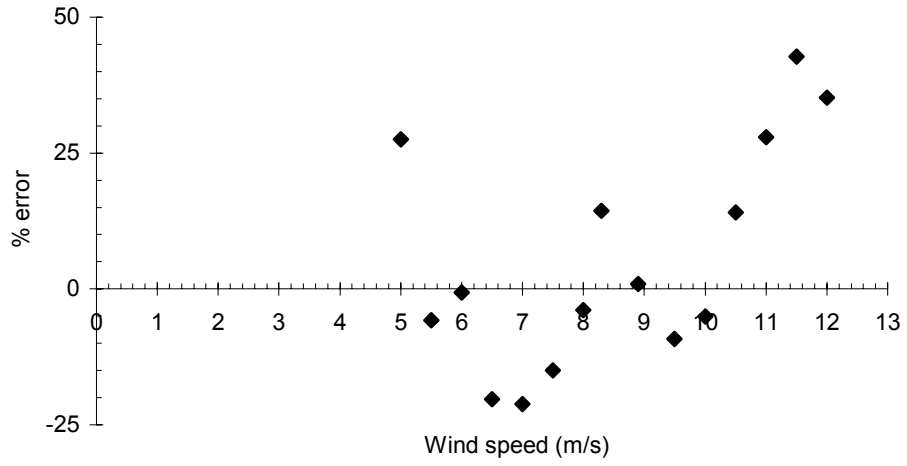

Figure 3.3 The amount of error between exp. and VT
(for 83 rpm and -3 degrees tip settling angle)

The comparison of Vortex Theory, using the program AEROPOWER, with the experimental results at 72 rpm for the same blade gives Figure 3.4.

It can be noticed that for relatively higher freestream wind speeds, the program over predicts the results due to the starting of the stall from the inner parts first, and influencing much portion of the blade as the wind speed increases.

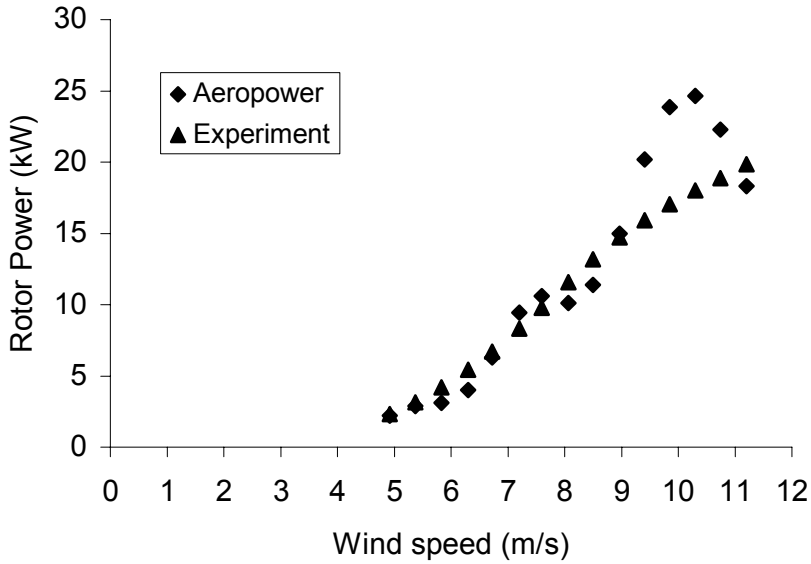

Figure 3.4 The rotor power production comparison for exp. and VT
(for 72 rpm and -3 degreed tip settling angle)

In the same manner, the error existed for this angular speed is,

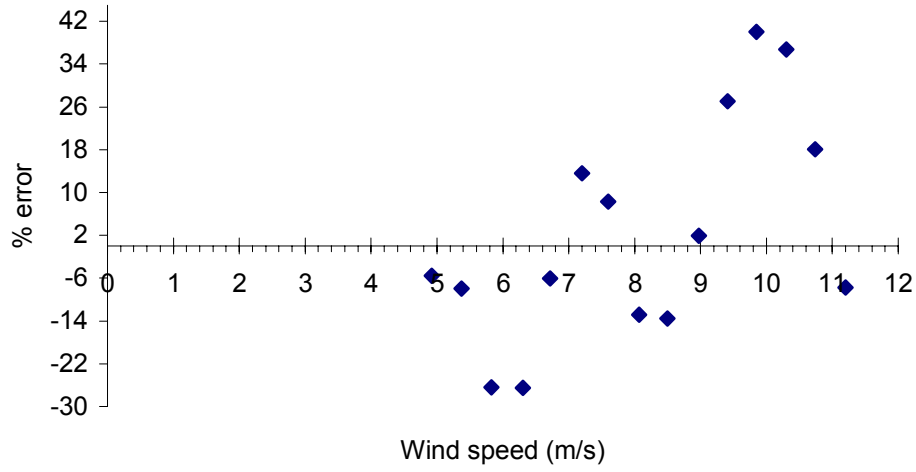

Figure 3.5 The amount of error between the exp. and VT
(for 72 rpm and -3 degrees tip settling angle)

The torque coefficient convergence values for both 83 rpm and 72 rpm are given in Figure 3.6 and in Figure 3.7, respectively as,

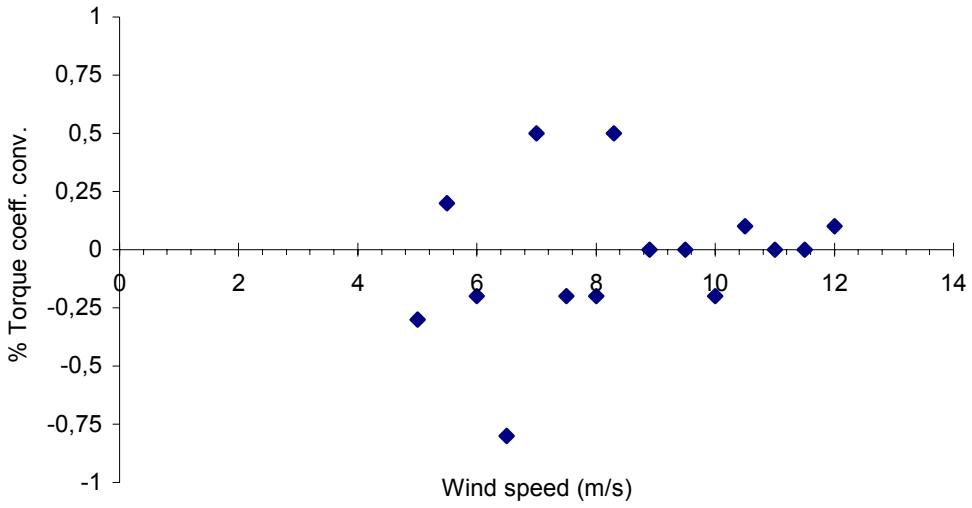

Figure 3.6 Torque coeff. Convergence
(for 83 rpm and -3 degrees tip settling angle)

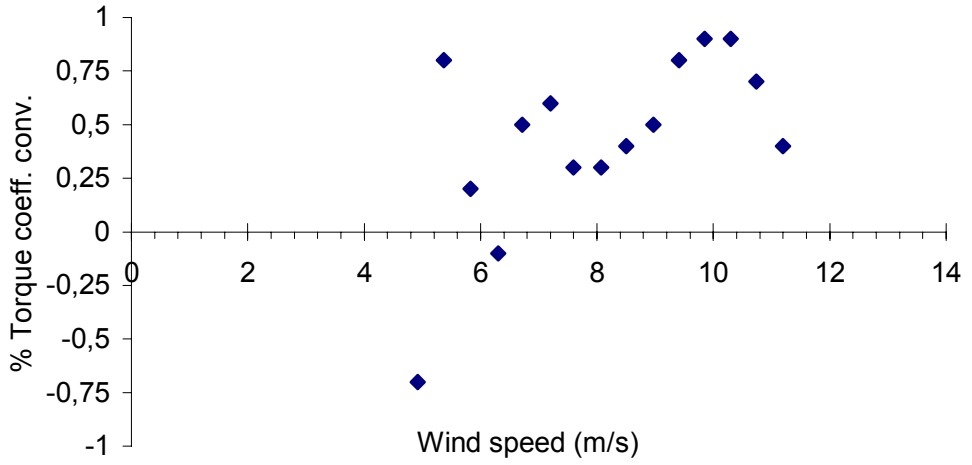

Figure 3.7 Torque coeff. convergence. (for 72 rpm and -3 degrees tip settling angle)

3.2 RESULTS FROM THE PROGRAM:

The variation of drag coefficients for the same blade, without changing the settling angles at each section and operating it at 83 rpm and 0.25 root location is as follows,

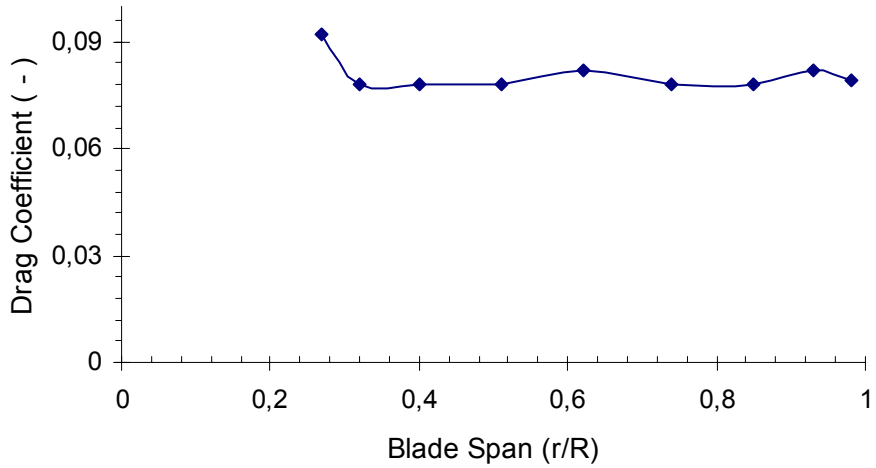

Figure 3.8 Drag coeff. distribution along the blade span.

The variation of the angle of the relative wind for the above mentioned conditions (83 rpm rotor angular speed, -3 degrees tip-settling angle) is illustrated in Figure 3.9, along the blade span (or radial direction).

It can be seen that the variation of the angle of the relative wind forming a curve, decreasing towards the tip due to the increase of the translational velocity of the blade in the radial direction towards the tip again. The material velocity (or translational velocity) of the blade is highly dominant at the tip regions.

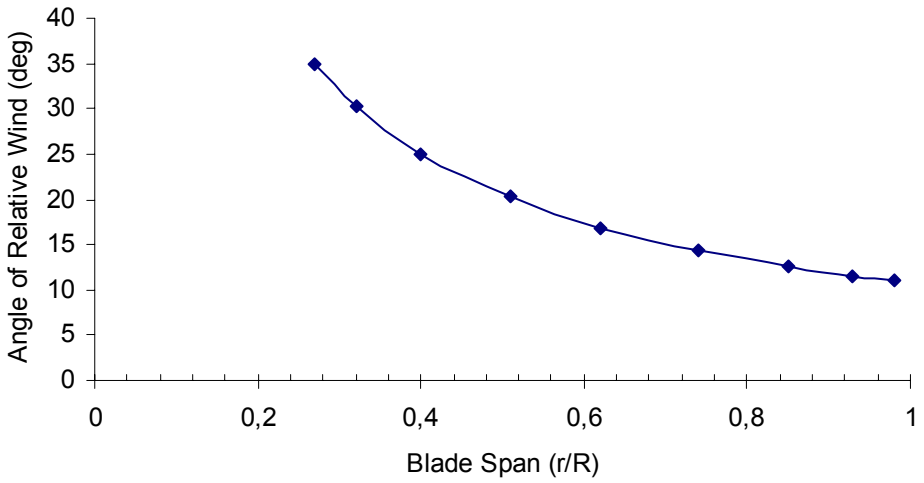

Figure 3.9 Angle of relative wind along the blade span.

Note that this is the angle between the direction of travel of the blade and the incoming velocity. The difference between the angle of the relative wind and the settling angle gives the angle of attack at the interested section.

The variation of angle of attacks along the blade span for different TSR values at 83 rpm rotor angular speed and -3 degrees tip-settling angle is shown in Figure 3.10, using AEROPOWER.

It can be easily seen from Figure 3.10 that at relatively lower tip-speed-ratio values the angle of attacks are decreasing along the blade span. On the contrary, at relatively higher tip-speed-ratio values, they are increasing along the span.

Angle of attacks have lower values at higher tip-speed-ratio values. At lower tip-speed-ratio values the wind speed is relatively high and causing the blade to become stall from the inner regions (or root regions). As a result, the angles of attacks at those regions are relatively higher.

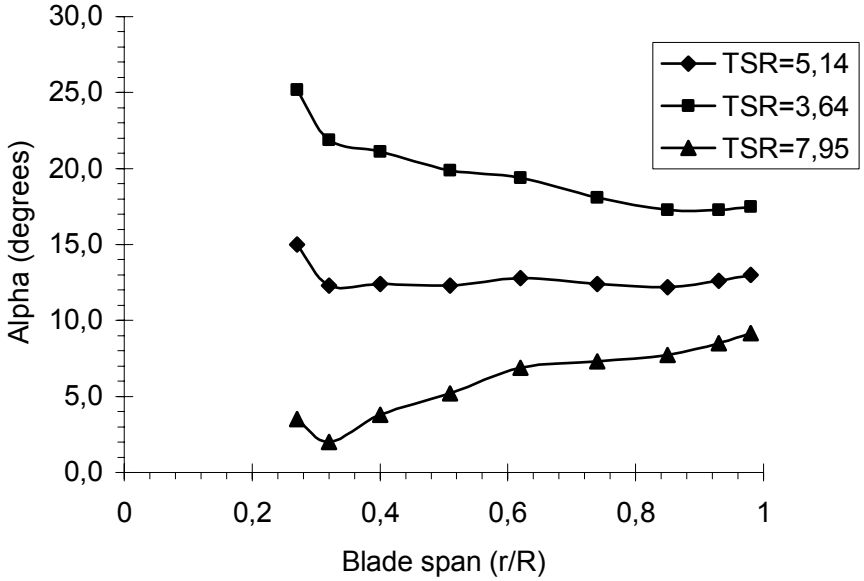

Figure 3.10 Variation of angle of attacks for different TSR values.
(83 rpm, -3 degrees tip settling angle)

The variation of incoming velocity along the blade span for different TSR values is shown in Figure 3.11.

As it can be seen from Figure 3.11 that the incoming velocities for all the three tip-speed-ratio values are almost linear due to the domination of the blade material velocity on the incoming velocity acting on the blade span.

The blade material velocity linearly increases in the radial direction. It is directly proportional with the blade radius, since the rotor angular speed is the same for all of the sections.

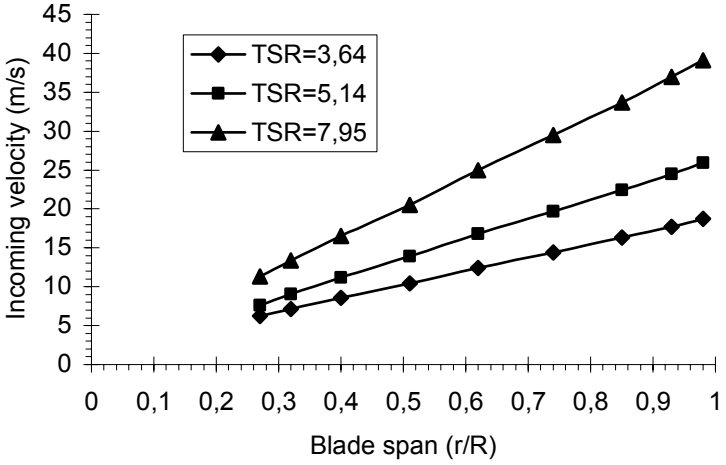

Figure 3.11 Variation of incoming velocities for different TSR values.
(83 rpm, -3 degrees tip settling angle)

Backwash and downwash components of the induced velocity for the same rpm are illustrated in Figure 3.12 and Figure 3.13 respectively as,

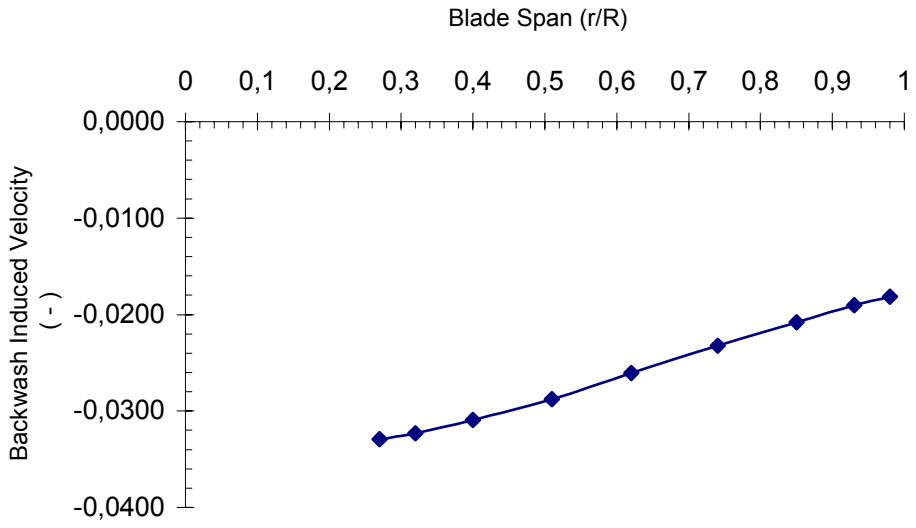

Figure 3.12 Backwash velocity distribution along the blade span.

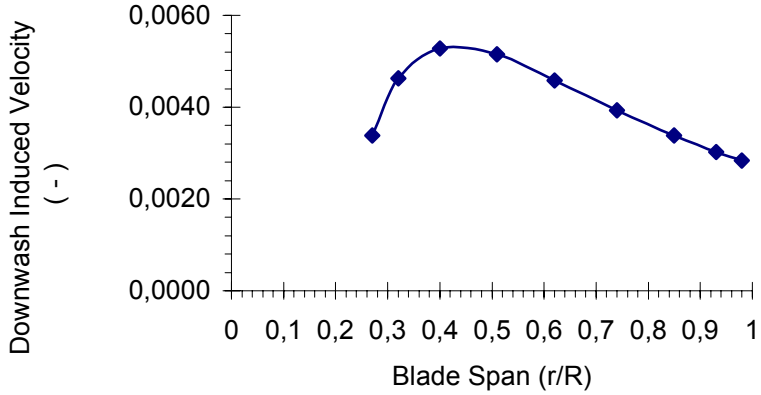

Figure 3.13 Downwash velocity distribution along the blade span.

The lift coefficient variation is,

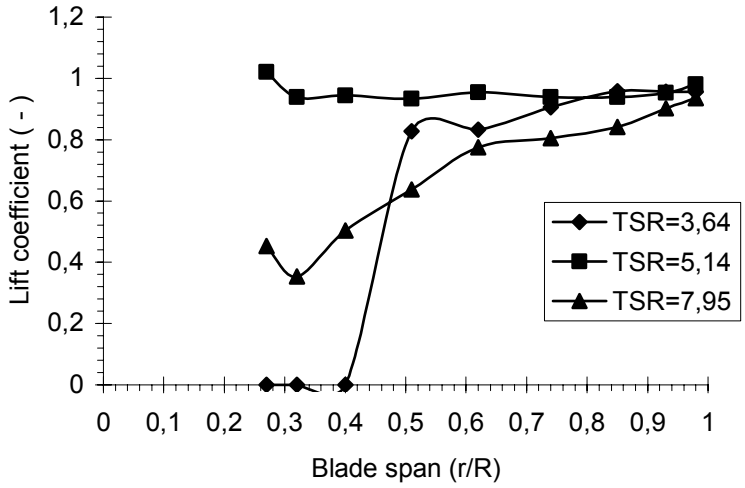

Figure 3.14 Variation of lift coefficients for different TSR values.
(83 rpm, -3 degrees tip settling angle)

The non-dimensional bound circulation distribution is,

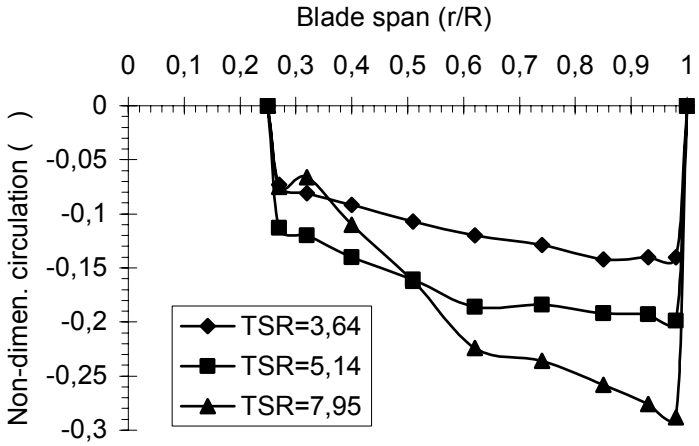

Figure 3.15 Variation of bound circulations for different TSR values.
(83 rpm, -3 degrees tip settling angle)

If one applies the same parameters for an angular speed of 72 rpm, the alpha and incoming velocity at each span are,

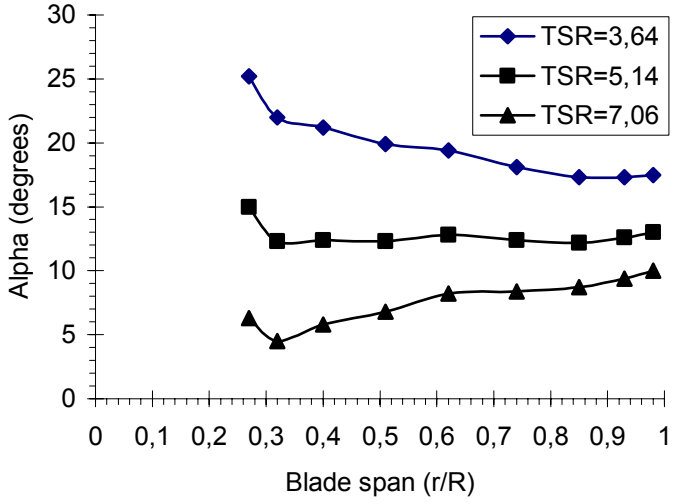

Figure 3.16 Variation of angle of attacks for different TSR values.
(72 rpm, -3 degrees tip settling angle)

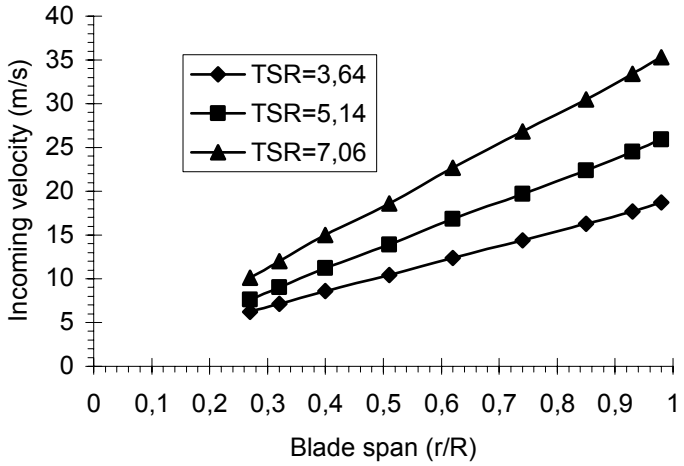

Figure 3.17 Variation of incoming velocities for different TSR values.
(72 rpm, -3 degrees tip settling angle)

The lift coefficient distribution along the blade span for 72 rpm, keeping the other parameters constant, gives,

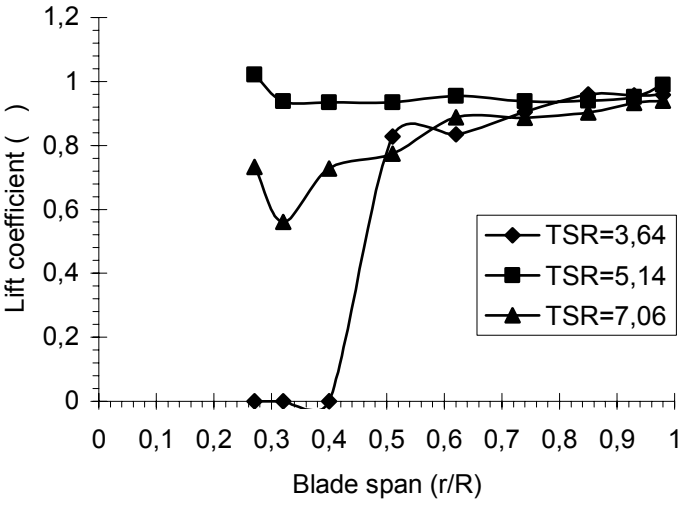

Figure 3.18 Variation of lift coefficients for different TSR values.
(72 rpm, -3 degrees tip settling angle)

At 72 rpm and -3 degrees tip-settling angle, the induced velocities, backwash and downwash, are illustrated in Figure 3.19 and 3.20 as follows,

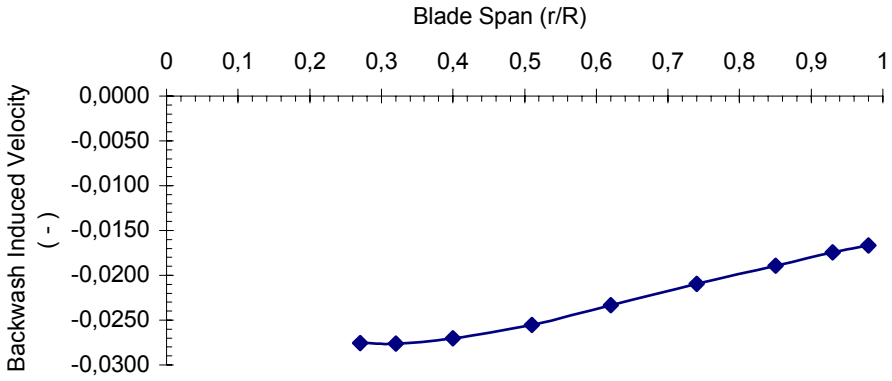

Figure 3.19 Backwash velocity along the blade span.

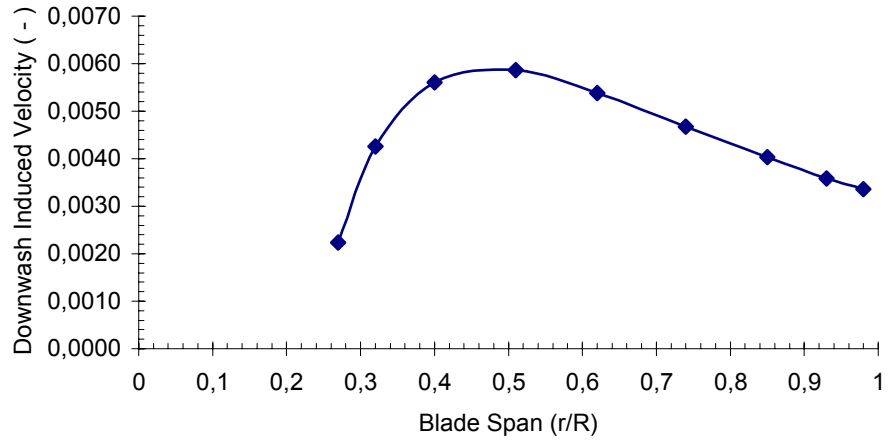

Figure 3.20 Downwash velocity along the blade span.

The bound circulation on the blade span at 72 rpm, keeping the other parameters constant gives,

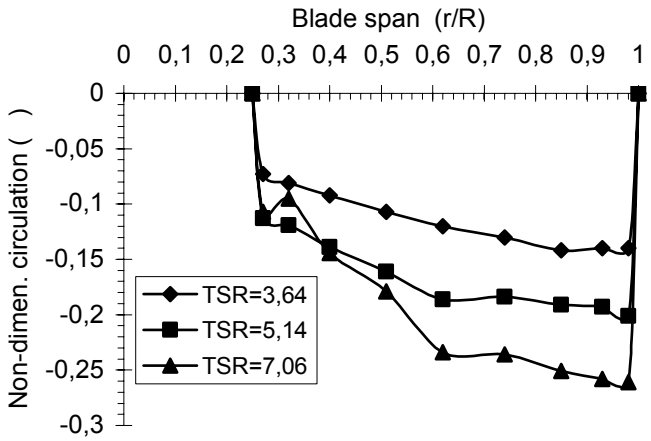

Figure 3.21 Variation of bound circulations for different TSR values.
(72 rpm, -3 degrees tip settling angle)

At 83 rpm, the variation of angle of attacks at TSR=4.37, for -3 degrees tip settling angle and 0.25 root location are,

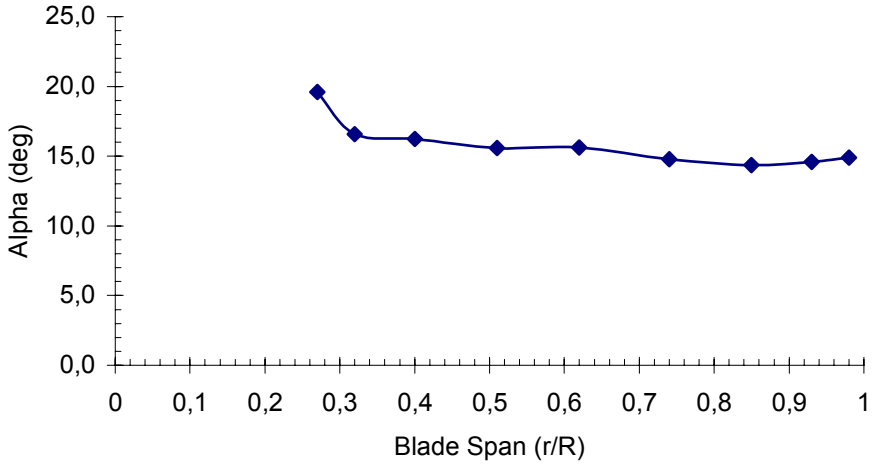

Figure 3.22 Angle of attack variation when TSR = 4.37

For different tip settling angles at 83 rpm, the angle of attack variation is obtained for different TSRs as illustrated in Figure 3.23,

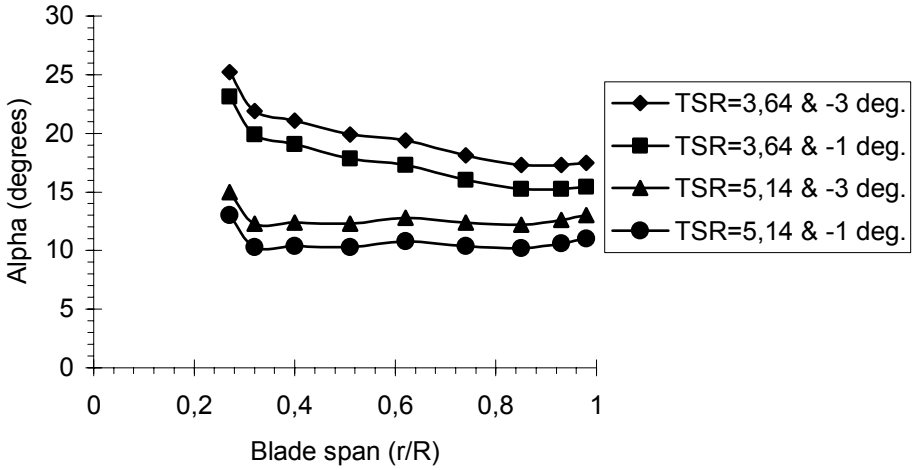

Figure 3.23 Variation of angle of attacks for different TSR values.

At 83 rpm, the variation of incoming velocities for different TSRs for -1 degrees and -3 degrees tip settling angle compared in Figure 3.24 as,

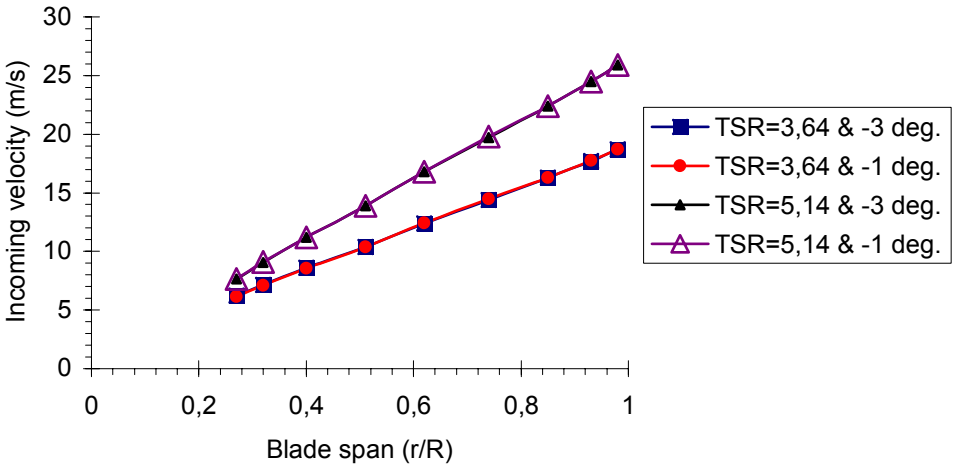

Figure 3.24 Variation of incoming velocities for different TSR values.

The variation of lift coefficient and bound circulation for the same rpm, but different tip settling angles give Figure 3.25 and Figure 3.26 respectively as,

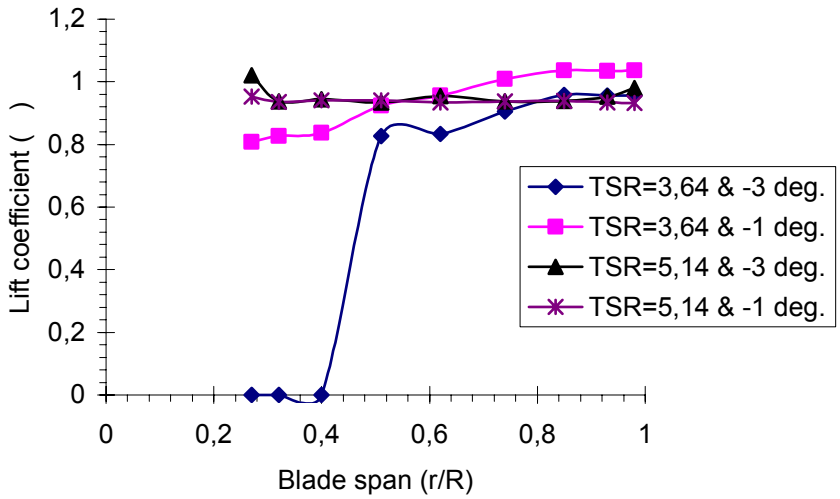

Figure 3.25 Variation of lift coefficients for different TSR values (83 rpm)

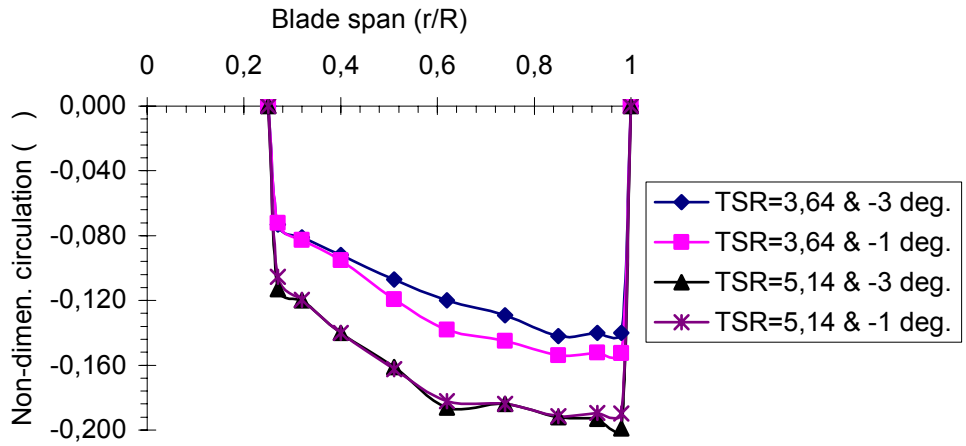

Figure 3.26 Variation of the bound circulations for different TSR values (at 83 rpm)

At 72 rpm, the alpha, incoming velocity and circulation distributions for -1 degrees settling angle for different TSR yields,

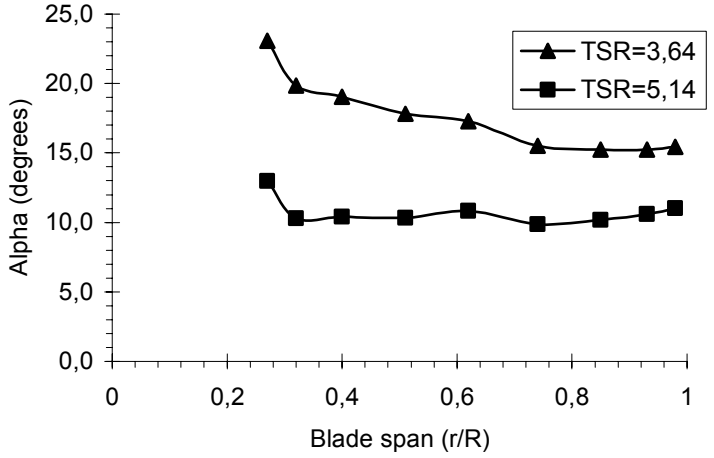

Figure 3.27 Variation of angle of attacks for different TSR values.
(72 rpm, -1 degrees tip settling angle)

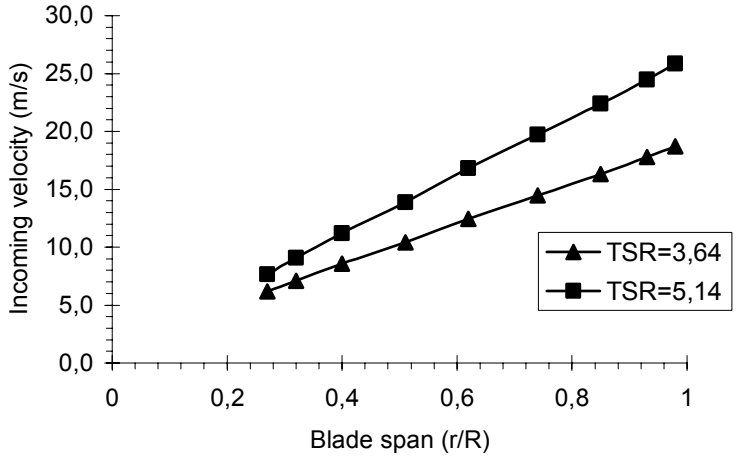

Figure 3.28 Variation of incoming velocities for different TSR values.
(72 rpm, -1 degrees tip settling angle)

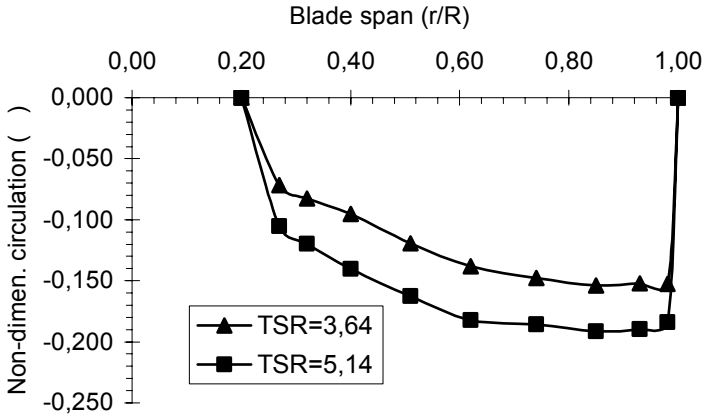

Figure 3.29 Variation of bound circulations for different TSR values.
(72 rpm, -1 degrees tip settling angle)

Up to now 0.25 root location is considered. Now let one observe how the root location affects the parameters, hence the rotor power production.

When the root location is changed from 0.25 to 0.20, the angle of attack and circulation distribution along the blade span for different TSR values become,

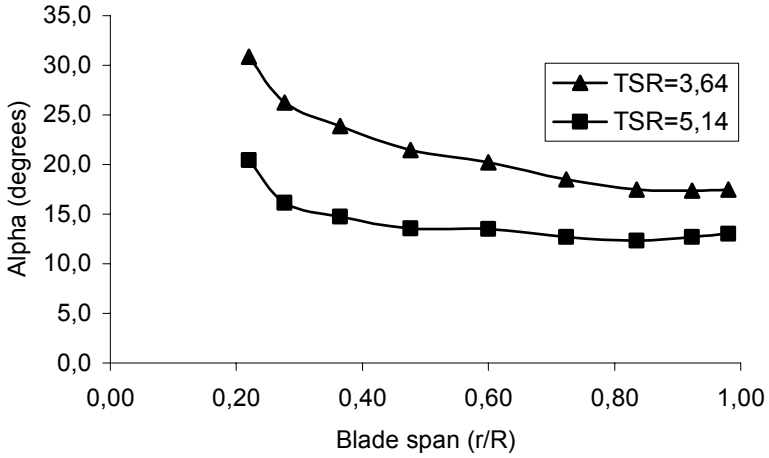

Figure 3.30 Variation of angle of attacks for different TSR values.
(83 rpm, -3 degrees tip settling angle)

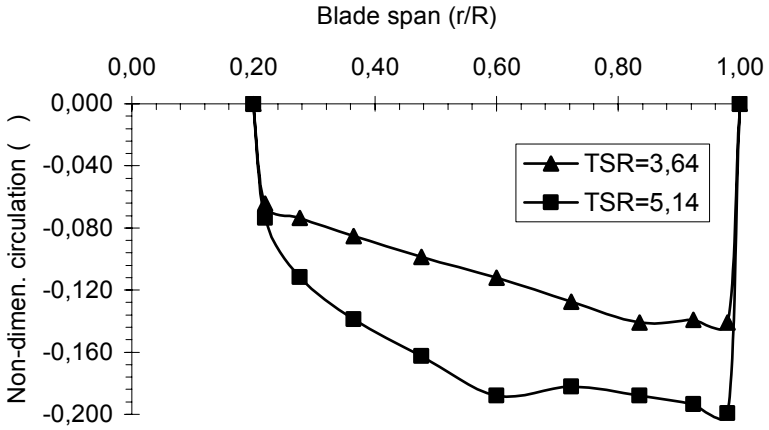

Figure 3.31 Variation of bound circulations for different TSR values.
(83 rpm, -3 degrees tip settling angle)

If one decreases the angular speed of the rotor to 60 rpm and keeping the tip-settling angle at -3 degrees and root location at 0.25 of the blade span, the incoming velocity distribution along the blade is as follows.

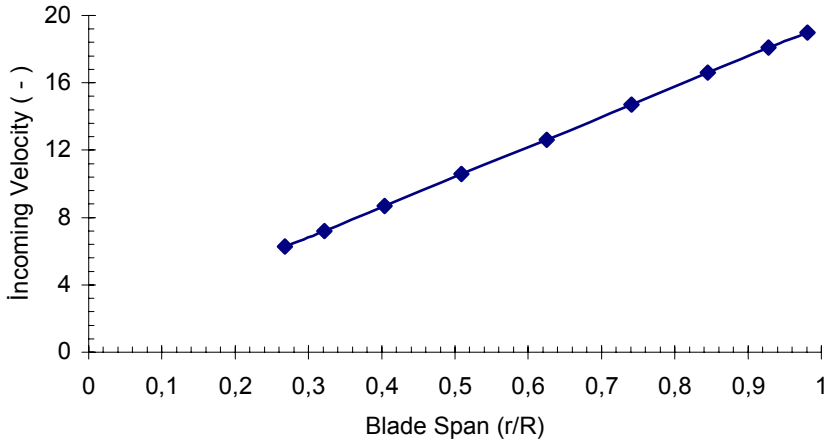

Figure 3.32 Incoming velocity distribution along the blade span.

The values of incoming velocities were obtained for a free-stream wind velocity of 8.5 m/s and tip-speed-ratio of 3.72. As it can be easily noticed that, the incoming velocity is heavily dependent on the translational velocity of the blades.

The drag coefficient distribution along the entire blade, for the conditions mentioned just above is,

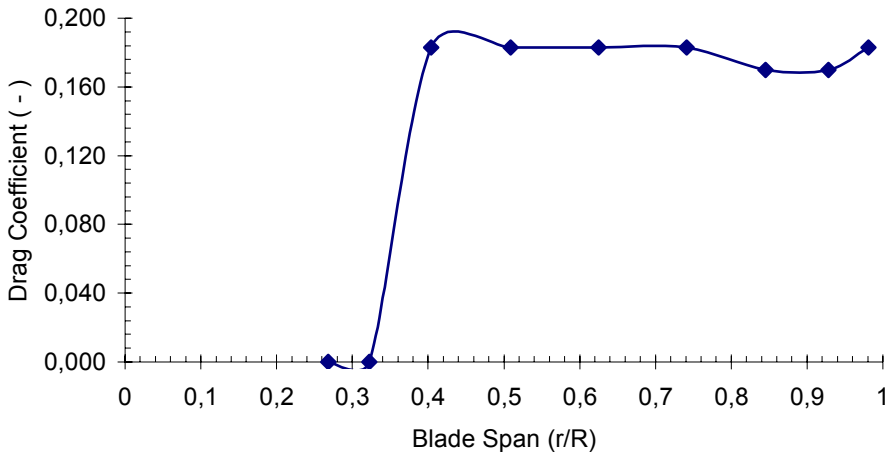

Figure 3.33 Drag coeff. distribution along the blade span.

In Figure3.33, the drag coefficient values between 25 % and 32% of the blade are obtained zero due to the acceptable tolerances used in the computer program. In fact they can't be zero.

The angle of the relative wind distribution (which is the angle between the incoming flow and the direction of travel) for the same conditions is illustrated in Figure 3.34 as,

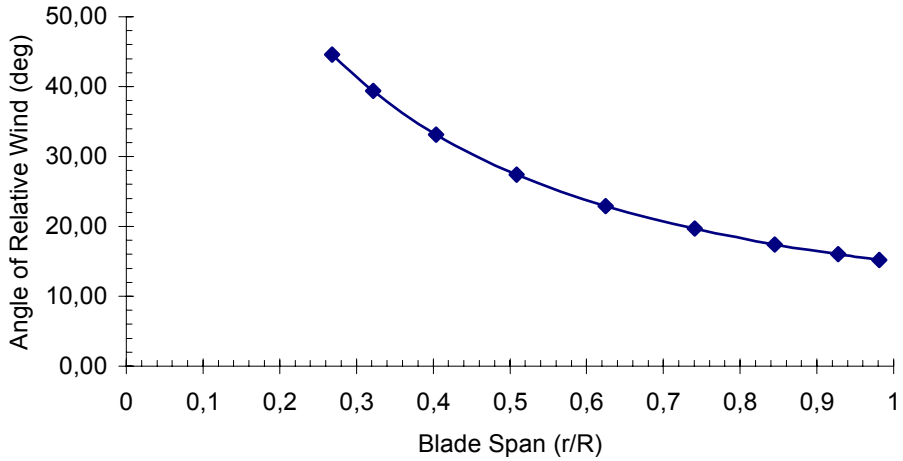

Figure 3.34 Angle of relative wind along the blade span.

As it can be seen in Figure 3.34, the maximum angle of the relative wind occurs at the root of the blade owing to the translational velocity of the blade has its lowest value there. This means that the freestream wind velocity has a magnitude closer to the translational (or material velocity) of the blade.

On the contrary the angle of the relative wind has the lowest value at the tip portion of the blade due to the material velocity of the blade has its maximum value at the tip section. As a result when one compares the freestream wind velocity and the material velocity, it is observed that the freestream is very much lower than the material velocity of the blade. This is why the turbine blades are given twist, in a shape that the chordline of the blade sections almost aligning with the direction of travel. At the tip sections the settling angles could have negative values in order to obtain the optimum angle of attack for the design conditions.

The lift coefficient distribution and the angle of attack distribution are given in Figure 3.35 and Figure 3.36, for 60 rpm rotor angular speed and -3 degrees tip-settling angle, respectively as,

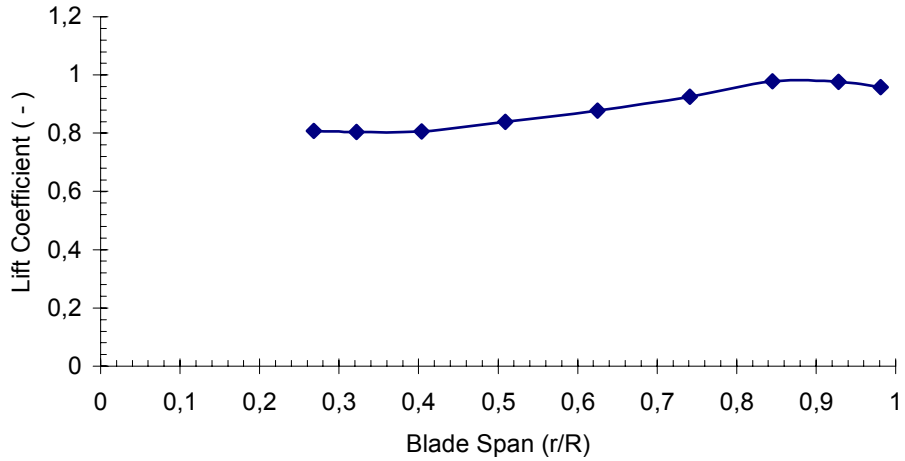

Figure 3.35 Lift coeff. distribution along the blade span

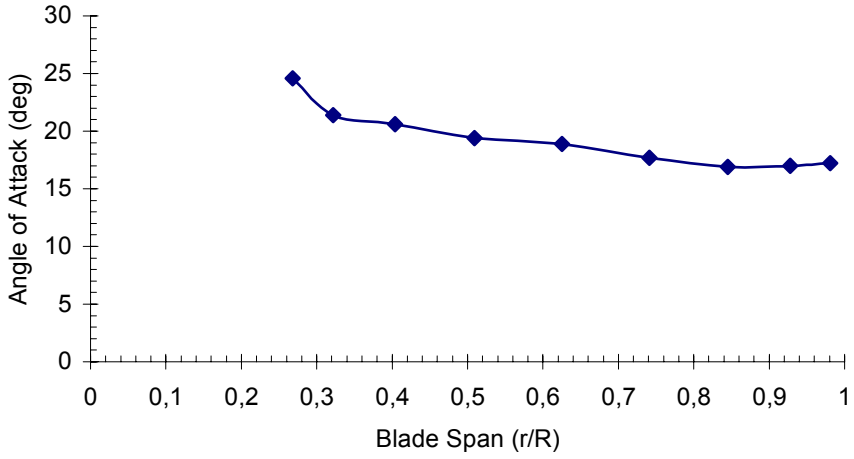

Figure 3.36 Angle of attack distribution along the blade span

The incoming velocities and the angle of attacks at the root and tip of the blades can not be calculated, since the bound circulation distribution at those points is considered as zero. Due to the zero circulation distribution, the lift coefficients at those points are taken as zero from the Kutta-Joukowski equation. As long as the angles of attacks are not known, the drag coefficients also cannot be determined for the implied two regions.

The power coefficient vs. TSR curve, for -3 degrees tip angle and 83 rpm is,

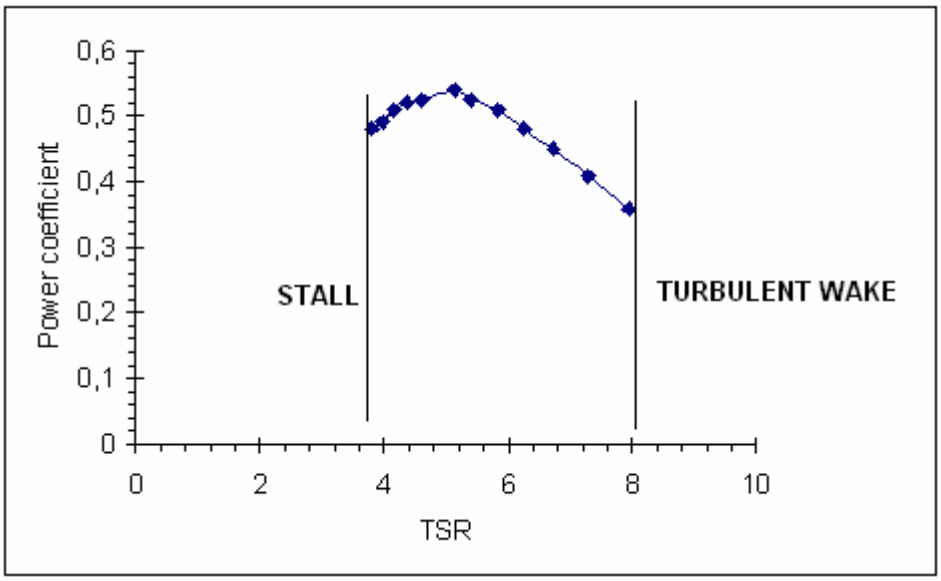

Figure 3.37 Power coefficient vs. TSR curve obtained by Vortex Theory.
(for 83 rpm,-3 degrees tip settling angle and 0.25 root location)

3.3 DISCUSSION ON RESULTS:

One tried to find the power production of a HAWT in out of design conditions. In off-design conditions one could not run the program due to the lack of a helicoidal free surface (or helicoidal vortex structure) downstream of the rotor. At relatively low wind speeds (w.r.t the design wind speed) there is not any relation giving the value of the axial induction factor, so one could not define the torque coefficient, both the assumed one (with the help of the power coefficient) and the lastly found one after the induced velocity relations. As a result it is impossible to make them converge to each other. At that wind speeds, program has only iterated the values and couldn't obtain any numerical solution.

At relatively high wind speeds the blades have started to become stall from root to tip. As the wind speed increases, the turbine blades experiencing stall, influencing much more portions of the blades. Hence even at one section becomes stalled; the inner part of the free wake structure loses its vortex (helicoidal) shape, so this disturbed region affects the other part of the blades. At that time one can not calculate the induced velocities due to that complex situation. This means that this program can not operate accurately in the stalled conditions.

At 83 rpm and -3 degrees tip settling angle, the amount of error changes w.r.t the experimental results, for different wind velocities they were observed numerically and shown in a graph. It was seen that the amount of errors are not low enough for our performance prediction program. Lower than 5.0 m/s, the program operates in the turbulent wake state at 83 rpm and since one has not ant empirical relation giving the direct value of the axial induction factor, one could not calculate the correct torque coefficient at, and below this velocity.

At 72 rpm and -3 degrees tip settling angle, the amount of error also observed and illustrated in a graph. It was seen that at that angular speed, the amount of error did not become smaller when compared to the 83 rpm case. On the contrary, between 7 and 9 m/s the amount of error has increased. At lower wind speeds, i.e., at higher TSR values, the system entered “Turbulent Wake State”. When tip settling angle changed from -3 to -1, it was seen that at 4.9 m/s the program works.

This means that for that settling angle, the free vortex structure downstream of the rotor is helicoidal. When operating, at 72 rpm and -3 degrees settling angle, due to the relatively lower tip-speed-ratio, the system is in the windmill state and gives results.

Wind speed at 11.0 m/s blade starts to be stalled up to 30 % portion of the radius and, as the wind speed increases, the stalled portion along the span increases as well. At 12.0 m/s, almost 45 % of the radius becomes stalled. Although stall starts, the incoming velocity increases. In spite of taking the torque coefficients “zero” for the stalled regions, up to a wind speed value 12 m/s, the rotor power production increases.

After that value it starts to decrease due to the domination of the stall. This amount of increase in the starting of stall may depend on two phenomenon; the first one is, when stall starts the inner part of the blade (root section) losses its helicoidal shape, but at that time program tries to find the influence coefficients for that section, but at the inner part there is a very complex air movement due to stall rather than a helicoidal shape. The trailing vortices mix together randomly, so the code cannot make so much for this region.

One has observed the effect of four parameter change on the rotor power production of a stall controlled, constant speed HAWT in this study. These changed four parameters are:

a) Wind speed,
b) Rotor angular speed,
c) Blade settling angle,
d) Root location.

Changing -3 degrees tip settling angle to -1 degrees did not give much difference in terms of the incoming velocities. For TSR=3.64 and TSR= 5.14 they give almost the same incoming velocity distribution along the blade span for the implied settling angles.

The same change in settling angle has given an almost 2 degrees reduction of the angle of attack along the blade span, due to that 2 degrees turning of the blade relative to the direction of travel. The reduction in the angle of attacks caused the lift force to decrease, since the lift force is directly proportional with the angle of attack for the non-stalled states.

At 83 rpm, for TSR=3.64 value the blade experienced stall almost its 45 % of the radius and lift coefficients have sharply dropped for -3 settling angle case when compared to the -1 degrees, since the higher angle of attack at the first three sections.

On the contrary for the TSR=5.14 value this situation has not been seen due to the closeness to the design conditions.

Root location in this study implies the starting point of the first power producing section. This means the first chord at that section. When changing its value, it directly influences the power production of a HAWT. Increasing this, drops the power, but decreasing the root location value increases the power production.

One has decreased it from 0.25 to 0.20 and observed the results. For example, for TSR=5.14 value, when the rotor rotating at 83 rpm and the tip settling angle position -3 degrees, setting 0.20 root location rather than 0.25, has given 5.2 % more rotor production.

The guess of the circulation distribution caused some instability. A preliminary circulation distribution is considered as a guess distribution. Then 1% increments are applied for each section. When the lift coefficients are calculated in an acceptable tolerance, the increase of the circulation distribution guess is stopped for the related section. For the sections where the lift coefficient is far from the 2D wind tunnel results the process continues for those ones.

The amount of increase in the power production when making guesses and the torque convergence should be in accordance. For much increase of power requires much convergence difference. One does not desire this situation, because the convergence amount directly measures the correction of the loop. If the difference is large, this means that one has calculated far results. The less power increments give better results due to it permits the convergence percentage to be lower.

In this program one considered the torque coefficient convergence to be maximum 1 % for each loop, but at some steps when calculating the rotor power production for different wind speeds, the approach of the calculated torque coefficient to the guessed ones may change direction. Upper and lower approaches can be seen. One of the reasons for those small deviations seen on the graph occurs due to the implied torque coefficient approach. The amount of convergence difference and their directions were observed in the previous sections graphically and at the appendix they can be found as tabled.

It should be noted that, during the calculations the boundary layers were assumed to be attached to the blades and during a certain wind speed it is considered

to have the same value on the entire blade. In reality Re number is constant for 70 % of the blade span for a constant wind speed.

When wind speed changes, the Re number also changes. This difference makes the 2D wind tunnel data deviate for different velocities, but here, due to a small deviation in 2D data, it is considered the same lift coefficient vs. angle of attack values (or curve) for different Re numbers.

The program AEROPOWER was developed for one and two-bladed, constant speed HAWTs. For three-bladed rotors this program can be correlated and only S809 airfoil data is found in this program. Other types of airfoils can be added for the desired rotor. Some HAWTs consist of different type of airfoils on their blades. When such a combined airfoil blade is encountered, this program should be modified relative to the mentioned blade.

CHAPTER IV

CONCLUSIONS

4.1 REVIEW OF THE STUDY:

In this chapter the whole study will be summarized and the final deduction will be done on the Vortex Theory.

At first it was said that the Vortex Theory is still being developed and there is still a lot of limitations made in order to make the calculations applicable for it. These limitations give further results when compared with the experimental ones. As the limitation level increases, one needs to correlate the calculations to obtain more realistic results.

Performance prediction of HAWTs in out of design and off-design conditions needs to be fulfilled to reduce the financial and time costs. Without making an experiment, to obtain a power curve of a HAWT is very important for this reason.

As it was mentioned earlier (Chapter 1), there are a lot of methods to obtain a power production of a HAWT using basically two methods; first "BEM Theory" and the second one is "Vortex Methods".

There are so many parameters that effect the power production of a HAWT. Every model can not consider those implied every parameter in their calculations. In our study also, one has neglected the effects of some parameters on the performances of the rotors.

For example one has assumed there was not any hub loss at the nose cone of a HAWT rotor and also neglected the coning angle or the teetering effects, if the turbine blades are teetering. Tilting nacelle may change the results a little as well.

In reality, the blades are flapping in the flapwise direction (downstream) of the nacelle and also in the edgewise direction (tangential). This may have an effect on the shape of the free wake surface downstream of the rotor. This could have a moderate effect on the predicted power value. For downstream turbines the effect of the tower should be considered as well. The cyclic loading on the blades could affect the value of many parameters.

Those were related to the structure of the turbine. There are also some aerodynamic parameters related to air. One considered that the air is entirely uniform at each section of the rotor, but in reality there is a wind shear due to the atmospheric boundary layer. No-slip condition on the ground makes the air stream non-uniform and rotating at the inlet of the blade sections. Viscosity and the density are also considered to be constant. Re number is also considered to be constant for the 70 % span of the blade from the axis of rotation, but one has taken the same Re number for the entire rotor to simplify the problem. In the program AEROPOWER, the lift and drag coefficients for 2D wind tunnel measurements are taken for a certain Re number at which the HAWTs most operates.

During the calculations the boundary layer is considered to be attached on the blades. When stall starts from the inlet parts, the results move further away from the real case.

Vortex Theory is applicable in the “Windmill State”. At low TSRs, this theory gives better results. At relatively lower wind speeds, the rotor is in the “Turbulent Wake State” and the helicoidal free wake sheet does not exist at the downstream of the rotor, so induced velocities (also angle of attack) can not be calculated due to the lack of the trailing vortices.

A “cylindrical wake” assumption is needed to obtain a geometric expression defining the shape of the wake behind the rotor. In reality this wake is hyperbolical, and there are some relations that can correlate this cylindrical assumption (ref [12]).

4.2 CONCLUSIONS ON POWER PREDICTION:

It takes almost one minute when operating a Pentium IV 2.4 GHz machine, for one entire iteration loop. The amount of increase of the power for each loop does not affect the time elapsed for the calculations. It affects the whole time of the performance prediction when starting from almost a zero power value to a power value desired. For large power producing HAWTs, this time becomes huge.

Almost 50 % of the time for one loop (one minute) is spent for prescribing the shape of the wake structure and the other part is used for the circulation distribution iteration which is an inner loop to catch the correct angle of attack and lift coefficient values.

For 50 W rotor power production increments, it takes 20 minutes to reach 1 kW (starting from zero). To reach 10 kW, it takes 200 minutes (3 hours 20 minutes) for the calculations when operating the same computer. Although the computer used is fast, the program written using Excel-Visual Basic 6.0 combination may operate slowly due to the Excel part.

The more control and integration points on the blade make the results closer to the exact values. The more mesh system points in the axial direction also better because the position of the trailing vortices affects the induced velocities both in magnitude and direction acting on the blades. As a result the induced velocity is affected. Direction is important, since it gives directly the angle of attack at each section.

By increasing the control points on each blade one can get better performance results. Also increasing the axial points in the downstream direction is beneficial for getting closer results. A rigid free wake structure behind the rotor and a cylindrical wake assumption are both needed here to solve the problem.

Applicability of the Vortex Theory is confined in an area between “stall” and “turbulent state”, so the performance prediction can be done in this implied narrow region in the power coefficient vs. TSR curve.

Constant speed HAWTs are generally stall controlled wind power machines. Stall controlled turbines does not have any pitch mechanism to change the settling angle of the blade in order to catch the best performance production. In stall controlled machines due to the lack of the pitch mechanism, the turbine power output is heavily dependent on the freestream wind velocity. Angle of attack changes very frequently. When wind speed drops below the cut-in wind speed of the turbine, it does not produce any electricity (cut-in wind speed is defined as a wind speed at which the wind turbine starts to produce electricity). When the wind speed is extremely high, the blade experiences stall starting from the inner boards towards the outer boards and tip sections, so the lift decreases to almost zero, due to the high angle of attack values. As a result the turbine is protected from gusts.

Consequently, a HAWT performance prediction is not an easy task since so many parameters participate in the calculations. There is not any linearity between the parameters changed. In today's technology there are some amounts of limitations done in order to solve the problem by this theory as well.

REFERENCES

[1] Manwell J. F. et.al "Wind Energy Explained", John Wiley & Sons Ltd., England, 2002

[2] Spera, D. "Wind Turbine Technology", ASME Press, 1994

[3] Buhl, M. L., Jr. "WT_PERF User's Guide", NREL, Colorado, 2004

[4] Scheck, S. "HAWT Aerodynamics and Models from Wind Tunnel Measurements, NREL, Colorado, 2002

[5] Glauert, H. "The Elements of Aerofoil and Airscrew Theory", University Press, Cambrige, 1959

[6] Bertin, J. J. and Smith, M. L. "Aerodynamics for Engineers", Third Edition, Prentice Hall, New Jersey, 1998

[7] Katz J, Plotkin J. "Low Speed Aerodynamics", McGraw- Hill Inc., New York, 1991

[8] Reissner, H. "A Generalized Vortex Theory of The Screw Propeller & It's Application", Armour Institute of Technology, Washington, February 1940

[9] Fisichella, C. J. "An Improved Prescribed Wake Analysis for Wind Turbine Rotors", University of Illinois at Urbana Campaign, 1993

[10] Chattot, J. J. "Design and Analysis of Wind Turbines Using Helicoidal Vortex Model," CFD Journal, Vol. 11, No. 1, 2002

[11] Jeng, D.R., Keith, T.G., Aliakbarkhanafjeh, A., "Aerodynamic Analysis of a Horizontal Axis Wind Turbine by Use of Helical Vortex Theory, Volume I: Theory," NASA CR-168054, December 1982

[12] Vermeer, N. J. "A Review of Wind Turbine Wake Research at Tudelft", AIAA Journal, The Netherlands, 2001

[13] Van Garrel, A., "Development of a Wind Turbine Aerodynamics Simulation Module", NOVEM, The Netherlands, 2003

[14] Eraydın, E. , "Application of a Generalized Vortex Lattice", Ankara, 1989

[15] Sankar, L. N. "Computational Studies of Horizontal Axis Wind Turbines", NREL, Colorado, June 2001

[16] Drela, M. "XFOIL : An Analysis & Design System for Low Reynolds Number Airfoils", conference on Low Re number Aerodynamics,1989

[17] Giguere, P. & Selig M.S. "Design of a Tapered and Twisted Blade for the NREL Combined Experiment Rotor", NREL, April 1999

[18] Tangler J. L. "The Nebulous art of Using Wind-Tunnel Airfoil Data for Predicting Rotor Performance", NREL Journal, Colorado, 2002

[19] Sorensen, N. N. et. al. "Airfoil Characteristics for Wind Turbines", Riso National Laboratory, Roskilde, Denmark, March 1999

APPENDIX A

TABLED RESULTS OF SOME PARAMETERS UNDER DIFFERENT CONDITIONS

Wind speed (m/s)	Rotor power by AEROPOWER (kW)	Rotor power Experimental (kW)	Error (%)	Torque coeff. Convergence (%)
5.0	2.55	2.00	27.5	-0.3
5.5	2.90	3.08	-5.8	0.2
6.0	4.30	4.33	-0.7	-0.2
6.5	4.60	5.77	-20.3	-0.8
7.0	5.85	7.42	-21.2	0.5
7.5	7.90	9.29	-15	-0.2
8.0	10.95	11.39	-3.9	-0.2
8.5	16.15	13.74	14.4	0.5
9.0	16.25	15.71	0.9	0.0
9.5	16.30	18.73	-9.2	0.0
10.0	20.00	21.07	-5.1	-0.2
10.5	26.35	23.10	14.1	0.1
11.0	31.85	24.91	27.9	0.0
11.5	37.90	26.56	42.7	0.0
12.0	37.95	28.06	35.2	0.1

Table 1 Results obtained from the program at 83 rpm and -3 degrees tip angle.

Table 2 Results obtained from the program at 72 rpm rotor speed and -3 degrees tip-settling angle.

Wind speed (m/s)	Rotor power by AEROPOWER (kW)	Rotor power Experimental (kW)	Error (%)	Torque coeff. Convergence (%)
3.58	Turbulent	0.30	---	---
4.03	Turbulent	0.86	---	---
4.48	Turbulent	1.52		
5.0	2.20	2.33	-5.58	-0.7
5.37	2.90	3.15	-7.94	0.8
5.83	3.10	4.21	-26.37	0.2
6.3	4.00	5.44	-26.47	-0.1
6.72	6.30	6.71	-6.11	0.5
7.2	9.45	8.32	13.58	0.6
7.6	10.60	9.79	8.27	0.3
8.07	10.10	11.59	-12.86	0.3
8.5	11.40	13.18	-13.51	0.4
8.97	15.00	14.72	1.90	0.5
9.41	20.20	15.9	27.04	0.8
9.85	23.85	17.03	40.05	0.9
10.3	24.65	18.03	36.72	0.9
10.74	22.30	18.88	18.11	0.7
11.2	18.30	19.84	-7.76	0.4

Table 3 Results obtained from the program at 83 rpm, -3 degrees tip-settling angle When TSR=3.64

Blade span (r/R)	Incoming velocity (m/s)	Angle of attack (degrees)	Lift coeff. ( )	Circulation ( )
0.25	undetermined	undetermined	undetermined	0.000
0.27	6.25	25.2	0.000	-0.073
0.32	7.16	21.9	0.000	-0.081
0.40	8.59	21.1	0.000	-0.092
0.51	10.4	19.9	0.827	-0.107
0.62	12.4	19.4	0.833	-0.120
0.74	14.4	18.1	0.905	-0.129
0.85	16.3	17.3	0.958	-0.142
0.93	17.7	17.3	0.957	-0.140
0.98	18.7	17.5	0.957	-0.140
1.00	undetermined	undetermined	undetermined	0.000

Table 4 Results obtained from the program at 83 rpm, -3 degrees tip-settling angle When TSR=5.14

Blade span (r/R)	Incoming velocity (m/s)	Angleof attack (degrees)	Lift coeff. ( )	Circulation ( )
0.25	undetermined	undetermined	undetermined	0.000
0.27	7.63	15.0	1.021	-0.113
0.32	9.05	12.3	0.938	-0.120
0.40	11.2	12.4	0.944	-0.140
0.51	13.9	12.3	0.934	-0.161
0.62	16.8	12.8	0.955	-0.186
0.74	19.7	12.4	0.938	-0.184
0.85	22.4	12.2	0.939	-0.192
0.93	24.5	12.6	0.953	-0.193
0.98	25.9	13.0	0.980	-0.199
1.00	undetermined	undetermined	undetermined	0.000

Table 5 Results obtained from the program at 83 rpm, -3 degrees tip-settling angle when TSR=7.95

Blade span (r/R)	Incoming velocity (m/s)	Angleof attack (degrees)	Lift coeff. ( )	Circulation ( )
0.25	undetermined	undetermined	undetermined	0.000
0.27	11.3	3.5	0.453	-0.075
0.32	13.4	2.0	0.353	-0.066
0.40	16.5	3.8	0.503	-0.110
0.51	20.5	5.2	0.637	-0.162
0.62	25.0	6.9	0.775	-0.224
0.74	29.5	7.3	0.804	-0.236
0.85	33.7	7.7	0.841	-0.258
0.93	37.0	8.5	0.903	-0.276
0.98	39.1	9.2	0.936	-0.288
1.00	undetermined	undetermined	undetermined	0.000

Table 6 Results obtained from the program at 72 rpm, -3 degrees tip-settling angle when TSR=3.64

Blade span (r/R)	Incoming velocity (m/s)	Angleof attack (degrees)	Lift coeff. ( )	Circulation ( )
0.25	undetermined	undetermined	undetermined	0.000
0.27	6.24	25.2	0.000	-0.073
0.32	7.15	22.0	0.000	-0.081
0.40	8.58	21.2	0.000	-0.092
0.51	10.4	19.9	0.828	-0.107
0.62	12.4	19.4	0.834	-0.120
0.74	14.4	18.1	0.905	-0.130
0.85	16.3	17.3	0.959	-0.142
0.93	17.7	17.3	0.957	-0.140
0.98	18.7	17.5	0.958	-0.140
1.00	undetermined	undetermined	undetermined	0.000

Table 7 Results obtained from the program at 72 rpm, -3 degrees tip-settling angle When TSR=5.14

Blade span (r/R)	Incoming velocity (m/s)	Angleof attack (degrees)	Lift coeff. ( )	Circulation ( )
0.25	undetermined	undetermined	undetermined	0.000
0.27	7.64	15.0	1.021	-0.113
0.32	9.05	12.3	0.938	-0.119
0.40	11.2	12.4	0.935	-0.139
0.51	13.9	12.3	0.934	-0.161
0.62	16.8	12.8	0.954	-0.186
0.74	19.7	12.4	0.938	-0.184
0.85	22.4	12.2	0.939	-0.191
0.93	24.5	12.6	0.952	-0.193
0.98	25.9	13.0	0.990	-0.201
1.00	undetermined	undetermined	undetermined	0.000

Table 8 Results obtained from the program at 72 rpm, -3 degrees tip-settling angle When TSR=7.06

Blade span (r/R)	Incoming velocity (m/s)	Angleof attack (degrees)	Lift coeff. ( )	Circulation ( )
0.25	undetermined	undetermined	undetermined	0.000
0.27	10.1	6.3	0.732	-0.107
0.32	12.0	4.5	0.561	-0.095
0.40	15.0	5.8	0.728	-0.144
0.51	18.6	6.8	0.775	-0.179
0.62	22.7	8.2	0.888	-0.234
0.74	26.8	8.4	0.887	-0.236
0.85	30.5	8.7	0.903	-0.251
0.93	33.4	9.4	0.933	-0.258
0.98	35.3	10.0	0.940	-0.261
1.00	undetermined	undetermined	undetermined	0.000

Table 9 Results obtained from the program at 83 rpm, -1 degrees tip-settling angle When TSR=3.64

Blade span (r/R)	Incoming velocity (m/s)	Angleof attack (degrees)	Lift coeff. ( )	Circulation ( )
0.25	undetermined	undetermined	undetermined	0.000
0.27	6.17	23.1	0.000	-0.072
0.32	7.10	19.9	0.827	-0.083
0.40	8.56	19.1	0.837	-0.095
0.51	10.40	17.8	0.923	-0.119
0.62	12.43	17.3	0.957	-0.138
0.74	14.46	16.0	1.008	-0.145
0.85	16.29	15.2	1.035	-0.154
0.93	17.76	15.3	1.036	-0.152
0.98	18.71	15.4	1.037	-0.152
1.00	undetermined	undetermined	undetermined	0.000

Table 10 Results obtained from the program at 83 rpm, -1 degrees tip-settling angle When TSR=5.14

Blade span (r/R)	Incoming velocity (m/s)	Angleof attack (degrees)	Lift coeff. ( )	Circulation ( )
0.25	undetermined	undetermined	undetermined	0.000
0.27	7.64	13.0	0.952	-0.105
0.32	9.10	10.3	0.936	-0.120
0.40	11.2	10.4	0.941	-0.140
0.51	13.9	10.3	0.940	-0.162
0.62	16.8	10.8	0.934	-0.182
0.74	19.8	10.4	0.937	-0.184
0.85	22.4	10.2	0.939	-0.192
0.93	24.5	10.6	0.934	-0.189
0.98	25.9	11.0	0.933	-0.190
1.00	undetermined	undetermined	undetermined	0.000

Table 11 Results obtained from the program at 72 rpm, -1 degrees tip-settling angle When TSR=3.64

Blade span (r/R)	Incoming velocity (m/s)	Angleof attack (degrees)	Lift coeff. ( )	Circulation ( )
0.25	undetermined	undetermined	undetermined	0.000
0.27	6.2	23.1	0.000	-0.072
0.32	7.1	19.9	0.827	-0.083
0.40	8.6	19.0	0.836	-0.095
0.51	10.4	17.8	0.923	-0.119
0.62	12.4	17.3	0.957	-0.138
0.74	14.5	15.5	1.038	-0.148
0.85	16.3	15.2	1.035	-0.154
0.93	17.8	15.2	1.035	-0.152
0.98	18.7	15.4	1.037	-0.152
1.00	undetermined	undetermined	undetermined	0.000

Table 12 Results obtained from the program at 72 rpm, -1 degrees tip-settling angle When TSR=5.14

Blade span (r/R)	Incoming velocity (m/s)	Angleof attack (degrees)	Lift coeff. ( )	Circulation ( )
0.25	undetermined	undetermined	undetermined	0.000
0.27	7.6	13.0	0.952	-0.105
0.32	9.1	10.3	0.936	-0.120
0.40	11.2	10.4	0.941	-0.140
0.51	13.9	10.3	0.940	-0.162
0.62	16.8	10.8	0.934	-0.182
0.74	19.7	9.9	0.925	-0.186
0.85	22.7	10.2	0.939	-0.192
0.93	24.5	10.6	0.934	-0.189
0.98	25.8	11.0	0.933	-0.184
1.00	undetermined	undetermined	undetermined	0.000

Table 13 Results obtained from the program at 60 rpm, -3 degrees tip-settling angle When TSR=3.72

Blade span (r/R)	Incoming velocity (m/s)	Angleof attack (deg)	Lift coeff. ( )	Ang. of relative wind (deg)
0.25	undetermined	undetermined	undetermined	undetermined
0.27	6.2	24.6	0.808	44.60
0.32	7.2	21.4	0.805	39.40
0.40	8.7	20.6	0.807	33.10
0.51	10.6	19.4	0.839	27.40
0.62	12.6	18.9	0.878	22.90
0.74	14.7	17.7	0.925	19.70
0.85	16.6	16.9	0.979	17.40
0.93	18.1	17	0.977	16.00
0.98	19	17.2	0.959	15.20
1.00	undetermined	undetermined	undetermined	undetermined

Table 14 Results obtained from the program at 83 rpm, -3 degrees tip-settling angle

Blade span (r/R)	Drag coeff. ( )	Angle of relative wind (deg)	Downwash Velocity (m/s)	Backwash Velocity (m/s)
0.25	undetermined	undetermined	undetermined	undetermined
0.27	0.092	35	0.0034	-0.0329
0.32	0.078	30.3	0.0046	-0.0323
0.40	0.078	24.9	0.0053	-0.0309
0.51	0.078	20.3	0.0052	-0.0288
0.62	0.082	16.8	0.0046	-0.0261
0.74	0.078	14.4	0.0039	-0.0232
0.85	0.078	12.7	0.0034	-0.0208
0.93	0.082	11.6	0.0030	-0.0191
0.98	0.079	11	0.0028	-0.0182
1.00	undetermined	undetermined	undetermined	undetermined

Table 15 Results obtained from the program at 72 rpm, -3 degrees tip-settling angle

Blade span (r/R)	Drag coeff. ( )	Angle of relative wind (deg)	Downwash Velocity (m/s)	Backwash Velocity (m/s)
0.25	undetermined	undetermined	undetermined	undetermined
0.27	0.092	35	0.0034	-0.0329
0.32	0.078	30.3	0.0046	-0.0323
0.40	0.078	24.9	0.0053	-0.0309
0.51	0.078	20.3	0.0052	-0.0288
0.62	0.082	16.8	0.0046	-0.0261
0.74	0.078	14.4	0.0039	-0.0232
0.85	0.078	12.7	0.0034	-0.0208
0.93	0.082	11.6	0.0030	-0.0191
0.98	0.079	11	0.0028	-0.0182
1.00	undetermined	undetermined	undetermined	undetermined

Table 16 Chord and settling angle distribution of the NREL blade

Blade span (r/R)	Non-dimensional chord distribution	Settling angle distribution (deg)
0.25	0.108	20
0.27	0.105	18
0.32	0.102	12.5
0.40	0.096	8.0
0.51	0.090	4.0
0.62	0.084	2.0
0.74	0.072	0.5
0.85	0.066	-1.0
0.93	0.060	-2.0
0.98	0.057	-2.5
1.00	0.048	-3.0

APPENDIX B

DATA OF THE NREL ROTOR:

Number of Blades: 2

Configuration: Upwind

Speed Control: Stall Controlled

Rotor Speed: Constant Speed

Rotor Radii: 5.03 m

Maximum Chord Length: 755 mm

Minimum Chord Length: 335 mm

Linear Chord Distribution (see Appendix A)

Non-Linear Twist Distribution (see Appendix A)

S809 Airfoil is used along the entire blade span

2D wind tunnel data of S809 airfoil (from ref [18]) is,

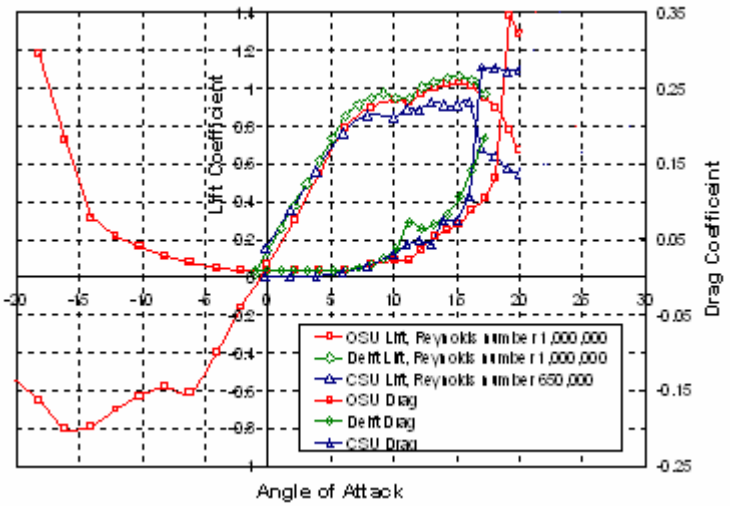

Figure B.1 2D Wind Tunnel Data for S809 Airfoil

APPENDIX C

PERFORMANCE PREDICTION PROCEDURE:

The following procedure is explained here in order to make the reader to understand the statements in Chapter 2, (2.3.1 Analysis Procedure Section).

i. “Assume a rotor power output value for the measured wind velocity” statement says that one needs to assume a preliminary rotor output value (i.e., P) in order to start the calculations. The amount of the power value would better to be started from a very low kilowatt (say 0.05 kW).

ii. “Find a rotor power coefficient value”, leads the reader to calculate the rotor power coefficient from the equation,

$$C_p = \frac{P}{0.5\rho_\infty U_\infty^3 A}$$

In the above equation the denominator indicates the power in the bunch of streamlines that the wind turbine is exposed to. Air density and freestream wind velocity are known parameters. The area is the rotor swept area, defined by,

$$A = \pi . R^2$$

Note that the radius in the above equation is defined the distance between the hub center and the blade tip point. (Radius is also known from the manufacturer).

iii. “Find the rotor torque coefficient value”, says that one needs to calculate the rotor torque coefficient to compare this value with the lastly found one. The guessed value is calculated from the equation,

$$C_\tau = \frac{C_p \pi}{\lambda}$$

In the above equation the denominator is the tip-speed-ratio and defined as the ratio of the blade tip speed to the freestream wind speed,

$$\lambda = \Omega R / U_{\infty}$$

The rotational speed of the blade is known from the design (or manufacture) considerations. This speed is constant, since one is dealing with a constant wind turbine in this study.

iv. "Find an induced axial velocity w.r.t the Actuator Disc Theory" says one needs to calculate an induced axial velocity in order to find a closer shape of the free vortex sheet. The induced velocity directly locates the pitches of the wake surface approximately downstream of the rotor. From the equation,

$$\mathrm{P} = -2\pi\rho_{\infty} R^2 (U_{\infty} + u_a)^2 u_a$$

one can find the induced velocity $u_a = - U_{\infty} a$, since the other parameters are known.

v. "Prescribe the wake geometry relative to this induced velocity", it is expected to find the preliminary shape of the wake structure. (In Chapter 2, section 2.3.2 this procedure is illustrated graphically).

The axial mesh system (Figure 2.15) can be constructed by the axial mesh points in the downstream direction of the rotor,

$$x_i = x_{i-1} + dx_i$$
$$dx_i = s dx_{i-1}$$
$$i = 1, \ldots\ldots\ldots, ix$$

Every "x" value indicates a mesh point in the axial direction. The spacing between "x" values is changing due to the clustering of the wake (retardation of the air molecules downstream of the rotor). The parameter "s" is the stretching parameter, can be calculated from Figure 2.18. The total area in that figure indicates the distance to the Trefftz Plane (ten diameters from the rotor). The ratio of the two consecutive differential areas in Figure 2.18 is the mentioned stretching parameter. One can obtain the relation from that figure as,

$$s = \frac{2 - 0.3a}{2 - 0.1a}$$

since the total time Δt is dropped in the calculations. (i.e., one does not need to know the time elapsed for one molecules travel from the rotor to the Trefftz Plane).

vi. "Calculate the influence coefficients", statement says one has to calculate the effectiveness of each trailing vortices, forming the wake structure, downstream of the rotor. Their magnitudes are important due to they are used to calculate the induced velocities at ach section of the blades. These induced velocities give the magnitude and direction of the incoming velocity. From the equations,

$$a_{j,k} = -\frac{1}{4\pi}\sum_{i=2}^{ix}\frac{(y_k^{'} - \bar{y}_{vi,j})(x_i - x_{i-1}) + \bar{x}_{i,j}(y_{vi,j} - y_{vi-1,j})}{[\bar{x}_{i,j}^2 + (y_k^{'} - \bar{y}_{vi,j})^2 + \bar{z}_{vi,j}^2]^{3/2}}$$

$$b_{j,k} = \frac{1}{4\pi}\sum_{i=2}^{ix}\frac{(y_k^{'} - \bar{y}_{vi,j})(z_{vi,j} - z_{vi,j}) + \bar{z}_{vi,j}(y_{vi,j} - y_{vi-1,j})}{[\bar{x}_{i,j}^2 + (y_k^{'} - \bar{y}_{vi,j})^2 + \bar{z}_{vi,j}^2]^{3/2}}$$

A discretized form of the Biot-Savart integrals is used due to the complexity of the integrals to handle. The axial discretization steps "x" are known from the above calculations. The values in the above equations can be found from,

$$y_j = y_0 + \frac{1}{2}(1 - y_0)(1 - Cos\phi_j)$$

$$\phi_j = \frac{j-1}{jx-1}\pi$$

$$j = 1, ..., jx$$

Since the root location of the blade is known. The number of the control points (jx) on the blades depends on our preference (note that jx is a number, not a multiplication). The term "j" is an index and constructs the discrete system (control points) on the blades. The integration points "k" are also along the blades shifted an amount to avoid the singularity in the integrals. It is also an index between the control points, "j".

The integration points y_k' is,

$$y_k' = y_0 + \frac{1}{2}(1 - y_0)[1 - Cos(\phi_k + \frac{\Delta\phi}{2})]$$

$$\Delta\phi = \frac{\pi}{jx - 1}$$

$$k = 1, ..., jx - 1$$

One should define the points on the helicoidal cylinder from the geometric equations of the helicoidal cylinder,

$$y_{vi,j} = y_j Cos(\lambda x_i)$$

$$z_{vi,j} = y_j Sin(\lambda x_i)$$

All parameters on the right hand side of the above two equations are known. ("Lambda" is the tip-speed-ratio, defined above).

The sign "bar" on some parameters in the influence coefficient formulas indicates the arithmetic average of the consecutive two meshes in the both axial and tangential directions.

$$\overline{*}_{i,j} = \frac{*_{i-1,j} + *_{i,j}}{2}$$

vii. "Guess a circulation distribution" is needed due to find the values of the induced velocities from,

$$w_k = \sum_{j=1}^{jx-1} (\Gamma_{j+1} - \Gamma_j) a_{j,k}$$

$$u_k = \sum_{j=1}^{jx-1} (\Gamma_{j+1} - \Gamma_j) b_{j,k}$$

The values of the influence coefficients are known now, and one needs to calculate the induced velocities at each section. Circulation values can be predicted from a known data first, and then by making iterations their values are found.

viii. “Find the induced velocities in the axial and azimuthal directions w.r.t this circulation distribution”, from the above two equations their values are found, but for one section of the blade. When the index “k” is changed, the induced velocities at the other parts of the blade sections can be found.

ix. “Find the incoming velocity at that section”, says one should find the incoming velocity acting on the blade section in order to find the lift acting on it. The magnitude and its direction can be found from eqn. (2.18) and Figure 2.10, respectively, since one knows the induced velocities mentioned in eqn. (2.18). The discretized form of eqn. (2.18) is,

$$q_j = \sqrt{(1+u_j)^2 + (\lambda.y_j + w_j)^2}$$

This gives the induced velocities at the control points of the blade.

x. “Find the angle of attack from subtracting settling angle from the angle of relative wind at the interested section (or element)”, says the angle of attack now can be defined, since the direction of the incoming velocity is known.

xi. “Find the lift coefficient from Kutta-Joukowski equation”, one can write,

$$l = \rho_\infty . U_\infty . \Gamma$$

$$C_l = \frac{l}{0.5 \rho_\infty U_\infty c}$$

these two equations reduces to,

$$C_l = \frac{2\Gamma}{qc}$$

in the discretized form,

$$C_{l\,j} = \frac{2\Gamma_j}{q_j c_j}$$

The chord (c) is known from the beginning and the circulation and the incoming velocity is known from above, but they are both guessed values.

xii. “Check, whether the angle of attack and the lift coefficient values correspond to each other (for the same section) by using 2D airfoil wind tunnel data”,

Now, one should compare the angle of attacks calculated in statement-x with the 2D S809 airfoil data whether they correspond to the same lift coefficient value. Because both the angle of attacks and the lift coefficients in the 2D data and the values found in the statements must correspond to each other.

xiii. “If they do not correspond to each other, then guess another circulation distribution (statement-vii) and continue the procedure. When convergence is reached, determine the new value of the torque coefficient corresponding to the converged circulation distribution”. The new value of the torque coefficient is calculated from the equation in terms of circulations according to BEM theory,

$$C_\tau = 2\int_{y_0}^{1} \Gamma(y)[1+u(y)].y.dy + \int_{y_0}^{1} q(y).[\lambda y + w(y)].C_d(y).c(y).y.dy$$

in discretized form,

$$C_\tau = 2B\sum_{k=2}^{jx-1} \Gamma_k(1+u_k)y_k^{'}.(y_k - y_{k-1}) + B\sum_{k=2}^{jx-1} q_k(\lambda y_k^{'} + w_k)c_{d_k}c_k y_k^{'}(y_k - y_{k-1})$$

This statement says that if the calculated values of the lift coefficients and angle of attacks do not correspond to the 2D wind tunnel data (S809 here), then continue to guess a new values for circulation at each section of the blade, for instance increasing their amount by a certain percentage.

When convergence is reached with the 2D data, then one reads the value of the incoming velocity for that converged situation.

xiv. “Check that value with statement-iii. If different, make iteration (i.e., guess another rotor output power value)”, leads the reader to compare the torque coefficient value found from equation,

$$C_\tau = \frac{C_p \pi}{\lambda} \quad \text{(Statement-iii)}$$

and equation,

$$C_\tau = 2B\sum_{k=2}^{jx-1}\Gamma_k(1+u_k)y_k'.(y_k - y_{k-1}) + B\sum_{k=2}^{jx-1}q_k(\lambda y_k' + w_k)c_{d_k}c_k y_k'(y_k - y_{k-1})$$

where B is the number of blades.

DETAILED FORMULATIONS FOR PERFORMANCE PREDICTION:

The following formulations explain the performance prediction of a stall controlled, constant speed, rigid hubed HAWT using "Vortex Theory".

Known Data:

Design wind speed: 8.5 m/s

Design Rotor Power Output: 12.5 kW

It is desired to predict the rotor power production at 10 m/s,

$U_\infty = 10m/s$

$\rho_\infty = 1.225kg/m^3$

$R = 5.03m$

$\Omega = 83rpm$

$r_0 = 1.2575m$

Chord and settling angle distribution are indicated in Appendix A.

Assume that this rotor produces P=19 kW at 10 m/s, and then the performance prediction procedure could be done as follows,

The rotor swept area is,

$$A = \pi R^2 = 79.485m^2$$

Power coefficient,

$$C_p = \frac{P}{0.5\rho_\infty U_\infty^3 A} = \frac{19{,}000W}{0.5(1.225)(1000)(79.485)} = 0.39$$

Tip-speed-ratio is,

$$\lambda = (\Omega R/U_\infty) = (8.69)(5.03)/10 = 4.37$$

Torque coefficient,

$$C_\tau = \frac{C_p\pi}{\lambda} = 0.281$$

The axial induction factor is,

$$\mathrm{P} = 2\pi\rho_{\infty}U_{\infty}^{3}R^{2}a(1-a)^{2}$$
$$(19{,}000W) = 2\pi(1.225)a(1-a)^{2}$$
$$a = 0.128$$

The stretching parameter is,

$$s = \frac{2 - 0.3a}{2-0.1a} = \frac{2 - 0.3(0.128)}{2-0.1(0.128)} = 0.9985$$

Number of mesh points in the axial direction is selected ix=100, then the axial discrete system,

$$dx_i = sdx_{i-1}$$
$$x_i = x_{i-1} + dx_i$$
$$i = 1,.....100$$

$x_0 = 0$
$dx_0 = 0.216$ are the initial conditions.

dx_0 is the differential distance starting from the aerodynamic centerline of the blade sections. Its value is selected by the program such that the distribution of the axial mesh points properly fit the distance between the rotor and the Trefftz Plane (or ten diameters downstream of the rotor). x_0 is the zeroth axial mesh point at where the trailing vortices gain shape and induces velocities on the blades.

The control point distribution on the blade,

$$y_0 = \frac{r_0}{R} = 0.25$$

$$y_j = y_0 + \frac{1}{2}(1-y_0)(1-Cos\phi_j)$$
$$\phi_j = \frac{j-1}{jx-1}\pi$$
$$j = 1,....., jx$$

In this study jx =11

The integration point distribution is,

$$\Delta\phi = \frac{\pi}{jx-1} = \frac{\pi}{10}$$

$$y_k' = y_0 + \frac{1}{2}(1-y_0)[1-Cos(\phi_k + \frac{\pi}{20})$$

$$k = 1,.....10$$

The points on the helicoidal cylinder,

$$y_{vi,j} = y_j Cos(\lambda x_i)$$

$$z_{vi,j} = y_j Sin(\lambda x_i)$$

For i =1 and j =1,

$$y_{v1,1} = y_1 Cos(\lambda x_1)$$

$$z_{v1,1} = y_1 Sin(\lambda x_1)$$

For i =1 and j =2,

$$y_{v1,2} = y_2 Cos(\lambda x_1)$$

$$z_{v1,2} = y_2 Sin(\lambda x_1)$$

For i =2 and j =1

$$y_{v2,1} = y_1 Cos(\lambda x_2)$$

$$z_{v2,1} = y_1 Sin(\lambda x_2)$$

For i =2 and j =2,

$$y_{v2,2} = y_2 Cos(\lambda x_2)$$

$$z_{v2,2} = y_2 Sin(\lambda x_2)$$

This makes a (i x j) = (100x11) matrix in this study.

The influence coefficients can be calculated as follows,

The arithmetic average value of any parameter can be found for this mesh system as defined before,

$$\bar{*}_{i,j} = \frac{*_{i-1,j} + *_{i,j}}{2}$$

$$a_{j,k} = -\frac{1}{4\pi}\sum_{i=2}^{ix} \frac{(y_k' - \bar{y}_{vi,j})(x_i - x_{i-1}) + \bar{x}_{i,j}(y_{vi,j} - y_{vi-1,j})}{[\bar{x}_{i,j}^2 + (y_k' - \bar{y}_{vi,j})^2 + \bar{z}_{vi,j}^2]^{3/2}}$$

$$b_{j,k} = \frac{1}{4\pi}\sum_{i=2}^{ix} \frac{(y_k' - \bar{y}_{vi,j})(z_{vi,j} - z_{vi,j}) + \bar{z}_{vi,j}(y_{vi,j} - y_{vi-1,j})}{[\bar{x}_{i,j}^2 + (y_k' - \bar{y}_{vi,j})^2 + \bar{z}_{vi,j}^2]^{3/2}}$$

For j =1 and k =1

$$a_{1,1} = -\frac{1}{4\pi}\sum_{i=2}^{100}\frac{(y_1^{'} - \bar{y}_{vi,1})(x_i - x_{i-1}) + \bar{x}_{i,1}(y_{vi,1} - y_{vi-1,1})}{[\bar{x}_{i,1}^2 + (y_1^{'} - \bar{y}_{vi,1})^2 + \bar{z}_{vi,1}^2]^{3/2}}$$

$$\bar{x}_{i,1} = \frac{x_{i-1,1} + x_{i,1}}{2}\ ,\ \bar{y}_{vi,1} = \frac{y_{vi-1,1} + y_{vi,1}}{2},\ \bar{z}_{vi,1} = \frac{z_{vi-1,1} + z_{vi,1}}{2}$$

$$a_{1,1} = -\frac{1}{4\pi}\left[\frac{(y_1^{'} - \bar{y}_{v2,1})(x_2 - x_1) + \bar{x}_{2,1}(y_{v2,1} - y_{v1,1})}{\left(\bar{x}^2{}_{2,1} + (y_1^{'} - \bar{y}_{v2,1})^2 + \bar{z}_{v2,1}{}^2\right)^{3/2}} + \frac{(y_1^{'} - \bar{y}_{v3,1})(x_3 - x_2) + \bar{x}_{3,1}(y_{v3,1} - y_{v2,1}}{\left(\bar{x}^2{}_{3,1} + (y_1^{'} - \bar{y}_{v3,1} + \bar{z}_{v3,1}{}^2\right)^{3/2}}\right.$$

$$\left. + \ldots\ldots\ldots\ldots\ldots\ldots + \frac{(y_1^{'} - \bar{y}_{v100,1})(x_{100} - x_{99}) + \bar{x}_{100,1}(y_{v100,1} - y_{v99,1})}{\left(\bar{x}^2{}_{100,1} + (y_1^{'} - \bar{y}_{v100,1})^2 + \bar{z}^2{}_{v100,1}\right)^{3/2}}\right]$$

$a_{1,2}, a_{2,2}, b_{1,1}, b_{1,2}$..... can be written in the same manner. At the end (j, k) = (11x10) matrix is obtained for both of the two influence coefficients every of them containing hundred axial discrete points.

The induced velocities are,

$$w_k = \sum_{j=1}^{jx-1}(\Gamma_{j+1} - \Gamma_j)a_{j,k}$$

$$u_k = \sum_{j=1}^{jx-1}(\Gamma_{j+1} - \Gamma_j)b_{j,k}$$

There is two unknowns in the induced velocity relations. Circulation (gamma) distribution can be guessed by looking at the previous results of different studies on this subject. There is almost an elliptical bound circulation distribution occurs on the blades. A sample distribution is illustrated,

Γ1	0	0
Γ2	-0,08905	-0,015
Γ3	-0,11962	-0,03
Γ4	-0,14295	-0,04
Γ5	-0,16735	-0,045
Γ6	-0,18781	-0,05
Γ7	-0,1877	-0,052
Γ8	-0,1935	-0,05
Γ9	-0,1933	-0,048
Γ10	-0,19356	-0,039
Γ11	0	0

In the second column the first guessed values of the circulations are shown, in the first column the circulation distributions corresponding to the converged lift coefficients (as will be explained below) are written.

A sample circulation distribution along the blade is,

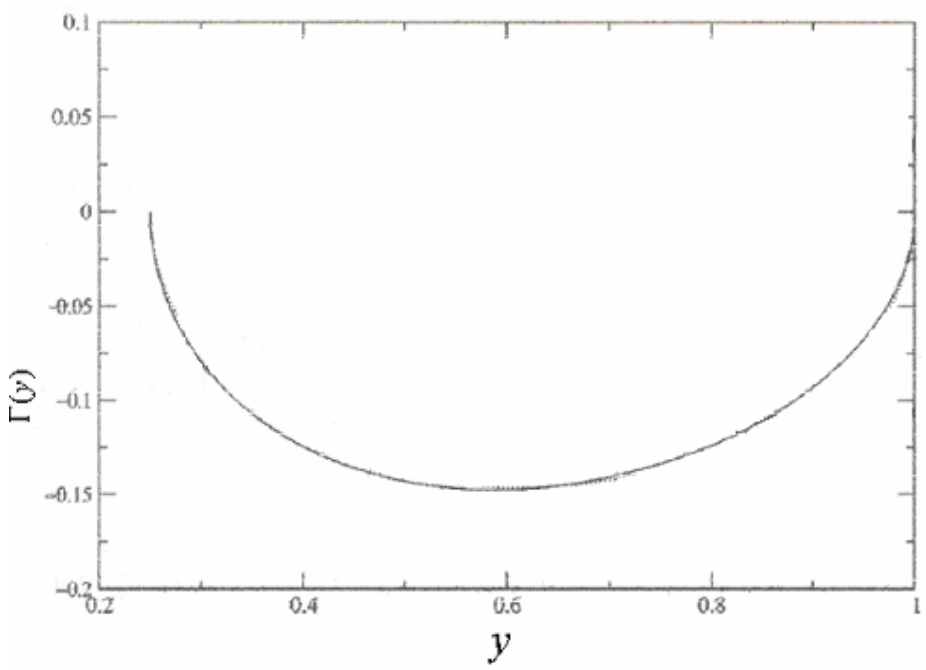

Figure C.1 Circulation distribution for a HAWT (Illustration from ref [10])

The circulations at the root and the tip point are taken as zero, since it is thought that they correspond to the tip points on either side. The parameters can be

defined among the first and the eleventh points.

The incoming velocities,

$$q_j = \sqrt{(1+u_j)^2 + (\lambda.y_j + w_j)^2}$$

$q_2 = 1.33$
$q_3 = 1.58$

$q_{10} = 4.41$

Please note that the incoming velocities above are all non-dimensional. In order to find their dimensional values, they have to be multiplied by the freestream wind velocity.

The lift coefficient,

$$C_{l\,j} = \frac{2\Gamma_j}{q_j c_j}$$

$$C_{l2} = \frac{2\Gamma_2}{q_2 c_2} = 0.915 \quad C_{l3} = \frac{2\Gamma_3}{q_3 c_3} = 1.070 \,,\ldots\ldots\ldots, C_{l10} = \frac{2\Gamma_{10}}{q_{10} c_{10}} = 1.110$$

The corresponding angle of attacks is obtained (see Figure 2.10) since the settling angles (or blade section positions known from design considerations),

$\alpha_2 = 19.6$, $\alpha_3 = 16.6$,……, $\alpha_{10} = 14.9$

since the incoming velocities are known both in magnitude and direction by the help of the induced velocities.

The 2D data for this angle of attacks obtained, gives the lift coefficients (or S809 experiments) as,

$C_{l2} = 0.920$, $C_{l3} = 1.070$,……, $C_{l10} = 1.120$

Since the differences between the lift coefficients found (after a circulation guess) do not converge to the values of the 2D data for the same angle of attacks. This means

that the circulation distribution must be reassumed (in the program at each section, for each cycle this increase is taken as 1%). When the convergence is reached to a sufficient amount for the lift coefficients, then the torque coefficient can be found from the formula (from BEM Theory),

$$C_\tau = 4\sum_{k=2}^{10} \Gamma_k (1+u_k) y_k^{'} .(y_k - y_{k-1}) + 2\sum_{k=2}^{10} q_k (\lambda y_k^{'} + w_k) c_{d_k} c_k y_k^{'} (y_k - y_{k-1})$$

$$C_\tau = 0.298$$

but the first value for the torque coefficient was obtained at the beginning as,

$$C_\tau = \frac{C_p \pi}{\lambda} = 0.281$$

Since the difference can not be acceptable for the torque coefficients, iteration is needed. This is done by selecting another rotor power production value. In the program 50W increments are used for the rotor power production. At 20.05 kW the torque coefficients converge to a value 0.8 % for the guessed and found one. This value is considered to be acceptable.

A guess for the circulations helps the reader to find the induced velocities, but these velocities are not the exact values due to the circulation guess. One needs to check the values of the lift coefficients found in the calculations (or Kutta-Joukowski equation) with the values of the 2D S809 airfoil data. The lift coefficients should match each other at the same angle of attacks. The values of the angle of attacks can be found by subtracting the angle of the relative wind from the settling angle at each section of the blades.

If the lift coefficients are in an unacceptable tolerance, then another guess of circulation is needed, and the procedure should be repeated from the “circulation guess” part.

APPENDIX D

SOME USEFUL WIND TURBINE TERMS:

- **AC**--See Alternating Current
- **Airfoil**--The cross section profile of the leeward side of a wind generator blade. Designed to give low drag and good lift. Also found on an airplane wing.
- **Air Gap**--In a permanent magnet alternator, the distance between the magnets and the laminates.
- **Alternating Current**--Electricity that changes direction periodically. The period is measured in Cycles per Second (Hertz, Hz).
- **Alternator**--A device that produces Alternating Current from the rotation of a shaft.
- **Anemometer**--A device that measures wind speed.
- **Angle of Attack**--The angle of relative air flow to the blade chord.
- **Armature**--The moving part of an alternator, generator or motor. In many PM alternator designs, it carries the magnets and is attached to the blades and hub. Also called a Rotor.
- **Axial Alternator**--An alternator design where a flat disc carrying magnets on the face (the Armature) rotates near a flat disc carrying coils (the Stator).
- **Axis**--The centerline of a rotating object's movement.
- **Battery**--An electrochemical device for storing energy.
- **Betz Coefficient**--59.3 percent. This is the theoretical maximum efficiency at which a wind generator can operate, by slowing the wind down. If the wind generator slows the wind down too much, air piles up in front of the blades and is not used for extracting energy.
- **Blade**--The part of a wind generator rotor that catches the wind.

- **Brake-drum Windmill**--A home-built wind generator design by Hugh Piggott of Scotland.
- **Braking System**--A device to slow a wind turbine's shaft speed down to safe levels electrically or mechanically.
- **Brushes**--Devices for transferring power to or from a rotating object. Usually made of carbon-graphite.
- **Chord**--The width of a wind turbine blade at a given location along the length.
- **Cowling**--See Nacelle.
- **Cut-In**--The rotational speed at which an alternator or generator starts pushing electricity hard enough (has a high enough voltage) to make electricity flow in a circuit.
- **Darrieus**--A Vertical Axis Wind Turbine design from the 1920s and 1930s by F.M. Darrieus, a French wind turbine designer.
- **DC**--See Direct Current
- **Downwind**--Refers to a Horizontal Axis Wind Turbine in which the hub and blades point away from the wind direction, the opposite of an Upwind turbine.
- **Drag**--In a wind generator, the force exerted on an object by moving air. Also refers to a type of wind generator or anemometer design that uses cups instead of blades with airfoils.
- **Dump Load**--A device to which wind generator power flows when the system batteries are too full to accept more power, usually an electric heating element. This diversion is performed by a Shunt Regulator, and allows a Load to be kept on the Alternator or Generator.
- **Dynamo**--A device that produces Direct Current from a rotating shaft. See Generator.

- **Eddy Currents**--Currents that flow in a substance from variations in magnetic induction. See also Lenz Effect. Laminates are used to prevent eddy currents, which cause physical and electrical resistance in an alternator or transformer, therefore wasting power.
- **Efficiency**--The ratio of energy output to energy input in a device.
- **Fiberglas® Resin**--Another 2-part adhesive system, NOT compatible with Epoxy. Often used for making castings, since it is much cheaper than Epoxy.
- **Furling**--The act of a wind generator Yawing out of the wind either horizontally or vertically to protect itself from high wind speeds.
- **Furling Tail**--A wind generator protection mechanism where the rotor shaft axis is offset horizontally from the yaw axis, and the tail boom is both offset horizontally and hinged diagonally, thus allowing the tail to fold up and in during high winds. This causes the blades to turn out of the wind, protecting the machine.
- **Gearing**--Using a mechanical system of gears or belts and pulleys to increase or decrease shaft speed. Power losses from friction are inherent in any gearing system.
- **Generator**--A device that produces Direct Current from a rotating shaft.
- **Guy Anchor**--Attaches tower guy wires securely to the earth.
- **Guy Radius**--The distance between a wind turbine tower and the guy anchors.
- **Guy Wire**--Attaches a tower to a Guy Anchor and the ground.
- **H-Rotor**--A Vertical Axis Wind Turbine design.
- **Hub**--The center of a wind generator rotor, which holds the blades in place and attaches to the shaft.
- **Induction**--The production of a magnetic field by the proximity of a electric charge or the production of a magnetic field by proximity of an electric charge.

- **Induction Motor**--An AC motor in which the rotating armature has no electrical connections to it (ie no slip rings), and consists of alternating plates of aluminum and steel.
- **Leading Edge**--The edge of a blade that faces toward the direction of rotation.
- **Leeward**--Away from the direction from which the wind blows.
- **Lift**--The force exerted by moving air on asymmetrically-shaped wind generator blades at right angles to the direction of relative movement. Ideally, wind generator blades should produce high Lift and low Drag.
- **Losses**--Power that is harvested by a wind generator but is not transferred to a usable form. Losses can be from friction, electrical resistance, or other causes.
- **Magnetic Field**--Magnetic fields are historically described in terms of their effect on electric charges. A moving electric charge, such as an electron, will accelerate in the presence of a magnetic field, causing it to change velocity and its direction of travel. An electrically charged particle moving in a magnetic field will experience a force (known as the Lorentz force) pushing it in a direction perpendicular to the magnetic field and the direction of motion. Also called magnetic flux.
- **Maximum Energy Product**--Determines how good a magnet that different materials can make. Technically, the amount of energy that a material can supply to an external magnetic circuit when operating within its demagnetization curve.
- **Nacelle**--The protective covering over a generator or motor.
- **Permanent Magnet**--A material that retains its magnetic properties after an external magnetic field is removed.
- **Permanent Magnet Alternator**--An Alternator that uses moving permanent magnets instead of Electromagnets to induce current in coils of wire.
- **Propeller**--The spinning thing that makes an airplane move forward. Often incorrectly used (by Otherpower.com also!) to describe a wind turbine Rotor.

- **Rated Power Output**--Used by wind generator manufacturers to provide a baseline for measuring performance. Rated output may vary by manufacturer. For example, one manufacturer's 1500 watt turbine may produce that amount of power at a 30 mph windspeed, while another brand of 1500 watt turbine may not make 1500 Watts until it gets a 40 mph windspeed! So read manufacturer's ratings statements very carefully.
- **Root**--The area of a blade nearest to the hub. Generally the thickest and widest part of the blade.
- **Rotor**--1) The blade and hub assembly of a wind generator. 2) The disc part of a vehicle disc brake. 3) The armature of a permanent magnet alternator, which spins and contains permanent magnets.
- **RPM**--Revolutions Per Minute. The number of times a shaft completes a full revolution in one minute.
- **Savonius**--A vertical-axis wind turbine design by S.J. Savonius of Finland from the 1920s and 30s. Shaped like a barrel split from end to end and offset along the cut. They are drag machines, and thus give very low rpm but lots of torque.
- **Settling Angle**--The angle between the blade Chord and the plane of the blade's rotation. Also called Pitch or blade angle. A blade carved with a Twist has a different setting angle at the Tip than at the Root.
- **Shaft**--The rotating part in the center of a wind generator or motor that transfers power.
- **Slip Ring**--Devices used to transfer electricity to or from rotating parts. Used in wound-field alternators, motors, and in some wind generator yaw assemblies.
- **Start-Up**--The windspeed at which a wind turbine rotor starts to rotate. It does not necessarily produce any power until it reaches cut-in speed.
- **Thrust**--In a wind generator, wind forces pushing back against the rotor. Wind generator bearings must be designed to handle thrust or else they will fail.

- **Thrust Bearing**--A bearing that is designed to handle axial forces along the centerline of the shaft--in a wind generator, this is the force of the wind pushing back against the blades.
- **Tilt-Up**--A tower that is hinged at the base and tilted up into position using a gin pole and winch or vehicle. Wind turbines on tilt-up towers can be serviced on the ground, with no climbing required.
- **Tip**--The end of a wind generator blade farthest from the hub.
- **Tip Speed Ratio**--The ratio of how much faster than the windspeed that the blade tips are moving. Abbreviation TSR.
- **Torque**--Turning force, equal to force times radius. See also Moment.
- **Tower**--A structure that supports a wind generator, usually high in the air.
- **Trailing Edge**--The edge of a blade that faces away from the direction of rotation.
- **TSR**--See Tip Speed Ratio.
- **Twist**--In a wind generator blade, the difference in Pitch between the blade root and the blade tip. Generally, the twist allows more Pitch at the blade root
- for easier Startup, and less Pitch at the tip for better high-speed performance.
- **Vane**--A large, flat piece of material used to align a wind turbine rotor correctly into the wind. Usually mounted vertically on the tail boom. Sometimes called a Tail.
- **Variable Pitch**--A type of wind turbine rotor where the attack angle of the blades can be adjusted either automatically or manually.
- **Windmill**--A device that uses wind power to mill grain into flour. But informally used as a synonym for wind generator or wind turbine, and to describe machines that pump water with wind power.
- **Windward**--Toward the direction from which the wind blows.
- **Yaw**--Rotation parallel to the ground. A wind generator Yaws to face winds coming from different directions.
- **Yaw Axis**--Vertical axis through the center of gravity.